NASA TECHNICAL MEMORANDUM

FLUTTER OF LAMINATED PLATES

IN SUPERSONIC FLOW

BY

JAMES WAYNE SAWYER
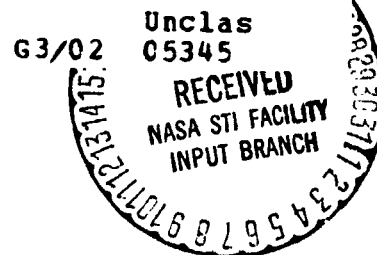
This informal documentation medium is used to provide accelerated or special release of technical information to selected users. The contents may not meet NASA formal editing and publication standards, may be revised, or may be incorporated in another publication.

NATIONAL AERONAUTICS AND SPACE ADMINISTRATION

LANGLEY RESEARCH CENTER, HAMPTON, VIRGINIA 23665

1. Report No.	2. Government Accession No.	3. Recipient's Catalog No.
NASA TM X-72800		

4. Title and Subtitle	5. Report Date
Flutter of Laminated Plates in Supersonic Flow	Nov. 1975
	6. Performing Organization Code

7. Author(s)	8. Performing Organization Report No.
James Wayne Sawyer	

9. Performing Organization Name and Address	10. Work Unit No.
NASA Langley Research Center	506-17-22-01
Hampton, VA 23665	11. Contract or Grant No.

12. Sponsoring Agency Name and Address	13. Type of Report and Period Covered
National Aeronautics and Space Administration	Technical Memorandum
Washington, DC 20546	14. Sponsoring Agency Code

15. Supplementary Notes

16. Abstract

A solution procedure has been developed using linear small deflection theory
for the flutter of simply supported laminated plates. For such plates, the
bending and extensional governing equations are coupled and have cross-
stiffness terms which do not appear in classical plate theory. An extended
Galerkin method is used to obtain approximate solutions to the governing
equations, and the aerodynamic pressure loading used in the analysis is that
given by linear piston theory with flow at arbitrary cross-flow angle. A
limited parametric study has been conducted for typical laminated composite
plates. The calculations show that both the bending-extensional coupling and
the cross-stiffness terms have a large destabilizing effect on flutter.
Since classical plate theory does not consider bending-extensional coupling
and cross stiffness terms, it usually gives inaccurate and nonconservative
flutter boundaries for laminated plates.

17. Key Words (Suggested by Author(s)) (STAR category underlined)	18. Distribution Statement
STRUCTURAL MECHANICS Panel Flutter Composite Plates Laminated Plates	Unclassified - Unlimited

19. Security Classif. (of this report)	20. Security Classif. (of this page)	21. No. of Pages	22. Price*
Unclassified	Unclassified	119	$5.25

NOTATION

A_{ij}	matrix of elastic areas defined by equation (2.18)
A^*_{ij}	matrix defined by equation (2.23)
a_{mnrs}	coefficient matrix (See equation (3.18).)
a, b	plate dimensions along x and y axis, respectively
B_{ij}	matrix of elastic statical moment defined by equation (2.18)
B^*_{ij}	matrix defined by equation (2.23)
b_{mnrs}	coefficient matrix (See equation (3.18).)
C_{mn}, C_{rs}	Fourier series coefficients
c_{ij}	coefficient matrix (See equation 3.18.)
D_{ij}	matrix of elastic moments of inertia defined by equation (2.18)
D^*_{ij}	matrix defined by equation (2.23)
$\bar{D}_{ij}$	matrix of D_{ij} with $\theta=0$.
D_{ij}	matrix of D_{ij} with $\theta=0$ and $\theta'=0$
E_{11}, E_{22}	Principal Young's moduli in 1 and 2 directions, respectively
F	Airy stress function, defined by equation (2.31)
G_{12}	shear modulus in 1-2 planes
h	total plate thickness
h_k	distance from plate midplane to the lamina boundary as shown in figure 3.
H_{mn}, H_{rs}	Fourier series coefficients
i, j	integers
K	number of layers in plate
$\bar{K}_x, \bar{K}_y$	nondimension inplane normal loads, $-\dfrac{\bar{N}_x a^2}{\bar{D}_{11} \pi^2}$, $-\dfrac{\bar{N}_y a^2}{\bar{D}_{11} \pi^2}$

iv

$\overline{K}_{xy}$ nondimensional inplane shear load, $-\dfrac{\overline{N}_{xy} a^2}{\overline{D}_{11} \pi^2}$

M_{∞} Mach number

M,N total number of terms in x and y direction, respectively

M_x, M_y bending moment resultants as defined by equation (2.9)

M_{xy} twisting moment resultant as defined by equation (2.9)

m,n integers

$\overline{N}_x, \overline{N}_y$ inplane normal loads per unit length in x and y directions, respectively

N'_{xy} induced inplane shearing loads

$\overline{N}_{xy}$ inplane shearing loads per unit length

N'_x, N'_y induced inplane normal loads

N_x, N_y inplane normal resultant as defined by equation (2.8)

N_{xy} inplane shear resultant as defined by equation (2.8)

p intensity of transverse load

Q_{ij} constitutive coefficient matrix for specially orthotropic lamina

$\overline{Q}_{ij}$ constitutive coefficient matrix for generally orthotropic lamina

q dynamic pressure of airstream

r,s integers

u^o, v^o midplane displacements in x and y direction, respectively

w normal displacements

x,y,z cartesian coordinates

β compressibility factor, $\sqrt{M_\infty^2 - 1}$

γ plate mass per unit area

$\gamma_{xy}, \gamma_{yz}, \gamma_{xz}$ shearing strain components

δ lamina thickness (See figure 14.)

$\varepsilon_x, \varepsilon_y$ normal strains in x, and y directions, respectively

$\varepsilon^o_x, \varepsilon^o_y$ normal midplane strains in x and y directions, respectively

θ rotation angle of the fibers with respect to the plate axis

θ' rotation angle of the fibers in the inner laminas with respect to plate axis (See figures 14 and 15.)

$\kappa_x, \kappa_y, \kappa_{xy}$ plate curvature as defined by equation (2.5)

Λ cross-flow angle

λ flutter parameter defined by equation (3.16)

ν_{12} poisson's ratio for orthotropic lamina defined by $- E_2/E_1$

$\sigma_x, \sigma_y, \sigma_z$ normal stress components in x, y, and z directions, respectively

$\tau_{xy}, \tau_{xz}, \tau_{yz}$ shearing stress components

ω natural frequency

ω_r fundamental frequency of simply supported beam as given by equation (3.17)

LIST OF TABLES

LIST OF FIGURES

FIGURE   PAGE

Chapter 1

INTRODUCTION

Laminated composite materials have been in use for many centuries. Pieces of laminated wood have been found which date back to about 1500 B.C. Some excellent swords were made in the 15th century by laminating several layers of steel to provide an extremely hard and keen cutting edge with a softer tough body. Although some of the advantages of using composite materials have been known for some time, only in recent years have determined efforts been made to fully develop composite materials. The advent of high performance aircraft and spacecraft has brought about the need for more efficient use of materials. Recent energy shortages have emphasized in even a greater way the importance of developing composite materials for everyday usage.

In recent years, composite materials have been the subject of a large number of experimental and analytical investigations and have been developed to the point where structural components are now being used in actual applications. Previously, most of the composite applications have been structural components built to replace existing conventional components. However, new designs are emerging which have considered composite materials in the total design. As new applications are considered for composite designs, a better understanding of the behavior of structural components under various load conditions is needed.

One structural component that is used extensively in a wide variety of applications is the flat plate. Plates fabricated from composite

materials usually consist of individual lamina bonded together. Each
lamina usually consists of a number of high strength filaments aligned in
the same direction and held in place by a plastic matrix material.
The lamina may be highly orthotropic, and since the principal material direc-
tion or the angle the fibers make with the plate axis may differ for each
lamina, the resulting anisotropic plate is more complex to analyze than
an orthotropic plate.

This study is being conducted to obtain a better understanding of
the flutter characteristics of laminated composite flat plates. However,
the following discussion will include a general review of previous studies
of laminated composite plates. Most previous studies of laminated plates
have been concerned only with deflection, vibration, and buckling char-
acteristics. The development and solution of the governing equations
for plates under various conditions will be reviewed and a proposed area
of investigation identified. Solution techniques and possible problem
areas will also be discussed.

1.1 Review of Literature

Numerous theoretical analyses of composite laminated plates have been
made and are discussed in references 1-23. These references represent
work that cover the spectrum from classical small deflection theory and
approximate solutions to non-linear theory and exact solutions. Much of
the early analytical work for composite plates was conducted using classi-
cal small deflection theory, and solutions were obtained only for special
classes of plates which resulted in considerable simplification of the

analysis. Recent studies have obtained solutions to more general plate problems with transverse shear and rotary inertia effects.

In addition to the reports and articles, some excellent books have considered laminated composite plates. Diet (24) in 1969 published a good review of much of the early analytical work in laminated composites and gave a thorough listing of references. Ashton, Halpin, and Petit (25) in 1969 published an excellent primer for those new in the field. They give a good development and discussion of the governing equations. Ashton and Whitney (26) in 1970 published a good review of the progress in laminated plate theory and the various solutions and solution techniques.

1.1.1 Formulation of Equations

Two early investigators, Reissner and Stavsky (1), analyzed a plate composed of two orthotropic laminas of equal thickness aligned so that the principal material axes of the two laminas are rotated at an angle of +θ and -θ with the plate axes (later referred to as angle-ply plates). They found that even for a small deflection theory analysis, there exists a coupling between the transverse bending and inplane stretching equations that does not exist for orthotropic plates. They showed that the coupling effect exists in the boundary conditions as well as in the governing equations.

Reissner and Stavsky (1) formulated the governing equations as two 4th order partial differential equations in terms of the Airy stress function and the transverse displacement. Due to the coupling of the two equations, they must be solved simultaneously, and inplane, as well as

transverse boundary conditions, must be specified at each boundary to obtain a particular plate solution. Stavsky (2) formulated the governing equations as an eighth order partial differential equation in terms of the Airy stress function and later (3) in the form of three simultaneous partial differential equations in the displacements u, v, and w. Although each of the formulations have advantages in certain problems, they present about the same order of difficulty in obtaining a solution.

Later contributions to the laminated plate formulations have been made by several authors. Tsai and Azzi (4) added thermal stresses to the formulation of laminated plate equations. Whitney and Leissa (5), and Yang, Norris, and Stavsky (6) included rotary inertia terms in the formulation and the latter authors also included transverse shear which becomes important for thick plates. The formulation by Yang, Norris, and Stavsky results in five coupled partial differential equations in terms of the displacements u, v, and w and two rotations of the normals to the midplane.

1.1.2 Solutions for Symmetric Plates

Although available formulations of the governing equations and boundary conditions are applicable for general laminated plates, most of the solutions have been obtained for special classes of plates which result in considerable simplification to the governing equations. Stavsky (2) in his early work showed that for laminated plates symmetric about the geometric midplane both in properties and fiber orientation, the transverse bending and inplane stretching equations and the boundary

conditions become uncoupled and can be solved independently. However,
he showed that even for symmetric laminated plates, the governing equations
and boundary conditions still contain some   ɔss-stiffness terms due to
the laminas which result in the governing equations being different
from those of an orthotropic analysis. He further showed that only for
very special kinds of symmetric plates do the cross-stiffness terms vanish
and the governing equations become identical with the orthotropic equa-
tions. As a result of these simplifications, symmetric plates have been
studied extensively in the literature.

The Rayleigh-Ritz method of solution with beam mode shape functions
has been used effectively by several investigators to obtain deflection,
vibration, and buckling solutions. Ashton and Waddoups (7) investigated
symmetric laminated plates and presented analytical results for uniaxially
loaded plates with the loaded edges clamped and the unloaded edges free.
They also presented calculated frequencies and mode shapes for canti-
levered plates which showed good agreement with experiment. Ashton (8)
extended the analysis to include nonuniform cross section and material
properties and presented results for tapered plates under unaxial
lo ⌐ing with simple supported and clamped boundary conditions. Ashton
(9) further extended the analysis to include elastically restrained
boundary conditions and presented some deflection results with re-
strained boundary conditions.

Later Srinivas and Rao (10) obtained closed form solutions for the
free vibration and buckling of simply supported symmetric laminated

thick plates using linear small deflection theory. They compared their results with thin plate theory and showed that the error associated with thin plate theory increases with plate thickness and the modular ratio between the lamina. A similar analysis by Whitney (11) showed the same trends. Thus the definition of "thin" for laminated plates must take into account modular ratio as well as plate thickness.

1.1.3 Solutions for Angle-ply and Cross-ply Plates

Angle-ply plates are unsymmetric and consist of an even number of layers having the same thickness and elastic properties, and the ortho-tropic axes of symmetry for each ply are alternately oriented at angles of $+\theta$ and $-\theta$ to the plate axes (See fig. 1.). Cross-ply plates are un-symmetric and consist of an even number of layers all of the same thick-ness and elastic properties with the orthotropic axes of symmetry in each ply alternately oriented at 0 degrees and 90 degrees to the plate axes (See fig. 2.). Whitney and Leissa (5) showed that for angle-ply plates and cross-ply plates, the governing equations and boundary condi-tions are considerably simplified but are still coupled and must be solved simultaneously. As a result of the simplifications, angle-ply and cross-ply laminated plates have been studied by several investigators to deter-mine the effects of bending-extensional coupling.

Several solution procedures have been developed which are effective in solving the coupled governing equations and boundary conditions. Whitney and Leissa (5) and Whitney (12) used a Fourier series technique to obtain solutions for deflection, free vibration, and buckling of both

angle-ply and cross-ply plates for simply supported boundary conditions which allow inplane displacements normal and tangent to the boundary for cross-ply and angle-ply plates respectively. Bert and Mayberry (13) used a Rayleigh-Ritz approach with beam mode shape functions to obtain free vibration results for cross-ply and angle-ply plates with clamped boundary conditions. Whitney (14) used a Galerkin procedure to obtain solutions for the shear buckling of cross-ply plates with simply supported boundary conditions.

In all cases cited, the bending-extensional coupling significantly affected the results. Bending-extensional coupling has the overall effect of reducing the plate stiffness and thus increasing the static deflection and reducing the natural frequencies and buckling loads. The effect of coupling is increased as the number of laminas are decreased and as the degree of anisotropy between lamina is increased.

Fortier (15) used a Rayleigh-Ritz solution procedure to investigate the effects that various types of inplane boundary restraints have on the behavior of angle-ply and cross-ply plates with small initial curvature. He also considered the effects of transverse shear and inplane loads on the natural frequencies. He found that inplane boundary conditions, initial curvature, transverse shear, and inplane loads all have a significant effect on the behavior of unsymmetric plates. However, Whitney (16) considered transverse shear for cylindrical bending of symmetric and cross-ply plates and showed that transverse shear has less effect on the deflection of cross-ply plates than symmetric plates.

1.3 4 Approximate Solutions

Due to the difficulty of obtaining general plate solutions, approximate solutions have emerged also. A "reduced bending stiffness" method was proposed by Ashton (20) in which the bending-extensional coupling is accounted for in an approximate way. Approximate solutions were obtained by reducing the bending stiffness of the plate by an amount determined by the coupling terms and then neglecting the coupling effect. Ashton used the method to compare maximum deflections of a cross-ply and an angle-ply plate with measured results and obtained good agreement. Whitney (21) also used the method to compare results with those calculated using the Fourier series technique and showed good agreement for both angle-ply and cross-ply plates for simply supported boundary conditions, but for lamped boundary conditions, relatively poor agreement was obtained for certain angle-ply cases.

A more refined analysis was presented by Srinivas (22) which considers transverse shear deformations and rotary inertia effects. By assuming piecewise linear variations of the displacements u and v and constant values of w across the plate thickness, the problem becomes two dimensional. Trigonometric series solutions were obtained for the approximate two dimensional problem for plates with simply supported boundary conditions, and the results showed good agreement with exact theory.

1.1.5 Dynamic Stability

A limi.ed number of investigators have considered the dynamic stability of laminated plates. Smirnov (17) considered the flutter of an infinite sandwich plate subjected to cylindrical bending in a gas stream and obtained an exact solution. He later extended the analysis (18) to include semi-infinite sandwich plates with various boundary conditions. He used linear piston theory aerodynamics and obtained solutions for both clamped and simply supported semi-infinite plates.

Librescu and Badoiu (19) and Ramkumar (23) analyzed the flutter of flat, symmetrically laminated, simply supported plates with inplane normal loads. They used linear piston theory dynamics with aerodynamic damping and the Rayleigh-Ritz solution procedure with beam mode shape functions. Flutter boundaries are presented as a function of the orientation of the principal axis of the lamina for various inplane loads and aerodynamic damping coefficients. However, it should be noted that all the flutter boundaries presented in reference 19 were obtained using only two terms in both the streamwise and cross-stream direction and the results presented in reference 23 were obtained using ten terms in the streamwise direction but only two terms in the cross-stream direction. Thus, in both cases, the results presented may not have been completely converged.

1.2 Statement of Problem

Although much work has been done in the analysis of composite laminated plates, as discussed in the literature survey, panel flutter

stands out as having received very little attention. Panel flutter has long been recognized as a problem for the design of conventional panels subjected to supersonic flow. This is evident by the large number of reported panel flutter investigations some of which are listed in references 27-42. The panel flutter work that has been done for laminated plates is so limited that it is of little value to the designer. It is evident that to design efficient laminated composite panels for supersonic application, a better understanding of their flutter characteristics is needed.

Another area that has received little attention is the solution of general laminated plate problems where the plates may have any number of layers stacked in an arbitrary sequence with the fibers in each layer rotated at an arbitrary angle to the plate axis. For general laminated plates, the complete bending and extensional governing equations and boundary conditions are coupled and must be solved simultaneously to obtain plate solutions. Considerable difficulty is encountered in solving the coupled equations and boundary conditions. Thus, although the governing equations and boundary conditions have been formulated for general laminated plates, no general solutions were found in the literature survey. All the solutions presented were for specially laminated (symmetric, angle-ply, or cross-ply) plates whose special geometry results in simplifications to the governing equations and boundary conditions which make it considerably easier to obtain solutions. However, since in the design of laminated plates it is not always practical or desirable to use specially laminated plates, an analysis is needed which

obtains solutions for general laminated plates.

The purpose of this investigation is to obtain the flutter characteristics of flat, general laminated plates using approximate methods. The analysis will be based upon small deflection theory but will consider the general coupled governing equations and boundary conditions for simply supported plates. Thus, an approximate solution procedure will be developed for completely general plates which may have any number of layers stacked in an arbitrary sequence and with the fibers in each lamina rotated at an arbitrary angle to the plate axes. The plate may be subjected to uniform inplane normal and shear loads.

An extended Galerkin method will be used to obtain approximate solutions to the governing equations and boundary conditions. The extended Galerkin method will be used since it provides a straightforward solution procedure for nonconservative problems (See ref. 42) using simple series to describe the displacements. The aerodynamic loading on the panel will be assumed to be given by linear piston theory and the flow may be at an arbitrary cross-flow angle. Piston theory aerodynamics will be used because it gives simple expressions for the aerodynamic loading and has been shown to be applicable for Mach numbers greater than 1.6 (See ref. 28 and 29).

Since symmetric and angle-ply plates have been the subject of many investigations, approximate solutions will be obtained for typical laminated plates from each class, and a limited parametric study will be conducted to determine the effects on the flutter boundaries. The parameters to be studied will include the number and orientation of the plies,

length-width ratio, inplane shear and normal loads, and cross-flow angles. The flutter boundaries from this analysis will be compared with those calculated using classical orthotropic plate theory and the reduced bending stiffness method.

Since general laminated plates have not been investigated prior to this time, approximate solutions of their governing equations will be of special interest. Thus, flutter boundaries will be calculated for some typical general laminated plates and the results will be compared with those obtained for specially constructed symmetric and angle-ply plates. Flutter boundaries will also be calculated for some composite stiffened aluminum plates that do not have a symmetric or angle-ply construction.

Although the approximate procedure will be developed for the purpose of obtaining flutter solutions, the analysis will also have the capability of giving natural vibration frequencies, and inplane normal and shear static buckling loads. Since no numerical results are available in the literature for general laminated plates, a significant contribution to the literature could be made by using the natural vibration and static buckling capabilities of the analysis. However, only a limited number of natural frequency calculations will be made to compare with published results to verify the solution procedure.

Chapter 2

DEVELOPMENT OF GOVERNING EQUATIONS

In order to develop the governing equations for this investigation, several assumptions are made as follows:

1. The plate is constructed of flat, uniform thickness layers of orthotropic sheets bonded together. The direction of principal stiffness of the individual layers do not in general coincide with the plate edges.

2. The plate is thin; i.e., the thickness is much smaller than the other physical dimensions.

3. The displacements are small compared to the thickness.

4. Each lamina obeys Hooke's law.

5. The Kirchhoff hypothesis is used; i.e., normals to the midplane of the undeformed plate remain straight and normal to the midplane during deformation.

6. Transverse shear and normal strains are negligible.

7. Body and rotary inertia forces are negligible.

8. The plate is of constant thickness.

These assumptions give rise to the conclusions that γ_{xz}, γ_{yz}, τ_{xz}, τ_{yz}, and σ_z are negligible which is the case for an approximate state of plane stress.

The coordinate system used to identify the plate and lamina geometry is shown in figure 3. The distances to the individual laminas are measured from the geometrical midplane of the plate. The positive directions for stresses are shown in figure 4.

13

2.1 Lamina Stress-Strain Equations

From elementary strength of materials, Hooke's law for an orthotropic lamina in a state of plane stress is given as follows (See ref. 25.)

$$
\begin{bmatrix} \sigma_1 \\ \sigma_2 \\ \tau_{12} \end{bmatrix}_\ell
=
\begin{bmatrix} Q_{11} & Q_{12} & 0 \\ Q_{12} & Q_{22} & 0 \\ 0 & 0 & Q_{66} \end{bmatrix}_\ell
\begin{bmatrix} \varepsilon_1 \\ \varepsilon_2 \\ \gamma_{12} \end{bmatrix}_\ell
\qquad (2.1)
$$

where the stresses $\sigma_1, \sigma_2, \tau_{12}$, and strains $\varepsilon_1, \varepsilon_2$, and γ_{12} are referred to the direction of principal stiffness and the subscript ℓ refers to a particular lamina. This relationship, written for another (x-y-z) system of axes (See figure 5.) where the x-y axes are rotated at an angle θ with respect to the 1-2 axes, is given as follows:

$$
\begin{bmatrix} \sigma_x \\ \sigma_y \\ \tau_{xy} \end{bmatrix}_\ell
=
\begin{bmatrix} \overline{Q}_{11} & \overline{Q}_{12} & \overline{Q}_{16} \\ \overline{Q}_{12} & \overline{Q}_{22} & \overline{Q}_{26} \\ \overline{Q}_{16} & \overline{Q}_{26} & \overline{Q}_{66} \end{bmatrix}_\ell
\begin{bmatrix} \varepsilon_x \\ \varepsilon_y \\ \gamma_{xy} \end{bmatrix}_\ell
\qquad (2.2)
$$

where the $\overline{Q}_{ij}$ matrix is a transformed matrix with the elastic properties along the principal axes of the lamina rotated to the x-y-z (plate) axes system. The $\overline{Q}_{ij}$ matrix has non-zero values for all terms when the principal axes of the lamina do not coincide with the plate axes system (for example, a fibrous composite with the fibers rotated at an angle with the plate axes).

From elementary strength of materials considerations, the strain at any point in a lamina undergoing deformation can be expressed in terms of the deformation of the geometrical midplane of the lamina. For small deflections and a state of plane stress, the strain at any point in a lamina z distance from the midplane is given in terms of the midplane strain and curvature as follows:

$$\begin{bmatrix} \epsilon_x \\ \epsilon_y \\ \gamma_{xy} \end{bmatrix}_\ell = \begin{bmatrix} \epsilon_x^o \\ \epsilon_y^o \\ \gamma_{xy}^o \end{bmatrix}_\ell + z \begin{bmatrix} \kappa_x \\ \kappa_y \\ \kappa_{xy} \end{bmatrix}_\ell \tag{2.3}$$

where ϵ_x^o, ϵ_y^o, and γ_{xy}^o are the midplane strains and κ_x, κ_y, and κ_{xy} are the midplane curvatures. The midplane strains and curvatures defined in terms of the displacements are needed in the later development of the equations and are given as follows:

$$\epsilon_x^o = \frac{\partial u^o}{\partial x} \qquad \text{(a)}$$

$$\epsilon_y^o = \frac{\partial v^o}{\partial y} \qquad \text{(b)} \qquad\qquad (2.4)$$

$$\gamma_{xy}^o = \frac{\partial u^o}{\partial y} + \frac{\partial v^o}{\partial x} \qquad \text{(c)}$$

$$\kappa_x = \frac{-\partial^2 w}{\partial x^2} \qquad \text{(a)}$$

$$\kappa_y = \frac{-\partial^2 w}{\partial y^2} \qquad \text{(b)} \qquad\qquad (2.5)$$

$$\kappa_{xy} = \frac{-2 \, \partial^2 w}{\partial x \partial y} \qquad (c)$$

Using equations (2.2) and (2.3), the stress state at any point in a lamina may be written in terms of the midplane strain and curvature as:

$$
\begin{bmatrix} \sigma_x \\ \sigma_y \\ \tau_{xy} \end{bmatrix}_\ell =
\begin{bmatrix} \bar{Q}_{11} & \bar{Q}_{12} & \bar{Q}_{16} \\ \bar{Q}_{12} & \bar{Q}_{22} & \bar{Q}_{26} \\ \bar{Q}_{16} & \bar{Q}_{26} & \bar{Q}_{66} \end{bmatrix}_\ell
\begin{bmatrix} \epsilon^0_x \\ \epsilon^0_y \\ \gamma^0_{xy} \end{bmatrix}_\ell +
z \begin{bmatrix} \bar{Q}_{11} & \bar{Q}_{12} & \bar{Q}_{16} \\ \bar{Q}_{12} & \bar{Q}_{22} & \bar{Q}_{26} \\ \bar{Q}_{16} & \bar{Q}_{26} & \bar{Q}_{66} \end{bmatrix}_\ell
\begin{bmatrix} \kappa_x \\ \kappa_y \\ \kappa_{xy} \end{bmatrix}_\ell \qquad (2.6)
$$

or

$$[\sigma]_\ell = [\bar{Q}]_\ell \, [\epsilon^0]_\ell + z \, [\bar{Q}]_\ell \, [\kappa]_\ell \qquad (2.7)$$

where z is the distance from the midplane to the point.

2.2 Lamina and Plate Constitutive Equations

Since for a plate composed of several laminas, the stresses, strains, and displacements will be different for each lamina, it is convenient to define some equivalent system of forces and moments which will be considered to be applied to the midplane of the plate. Within the plane stress assumption, such a system will be defined for a lamina in terms of three stress and three moment resultants. The stress and moment resultants for a lamina are defined as:

$$N_x = \int_{h_{k-1}}^{h_k} \sigma_x \, dz \qquad (a) \qquad\qquad (2.8)$$

$$N_y = \int_{h_{k-1}}^{h_k} \sigma_y \, dz \qquad \text{(b)}$$

$$N_{xy} = \int_{h_{k-1}}^{h_k} \tau_{xy} \, dz \qquad \text{(c)}$$

$$M_x = \int_{h_{k-1}}^{h_k} z \, \sigma_x \, dz \qquad \text{(a)}$$

$$M_y = \int_{h_{k-1}}^{h_k} z \, \sigma_y \, dz \qquad \text{(b)} \qquad\qquad\qquad (2.9)$$

$$M_{xy} = \int_{h_{k-1}}^{h_k} z \, \tau_{xy} \, dz \qquad \text{(c)}$$

and are statically equivalent to the actual stresses on the lamina and may be considered to be applied at the midplane of the lamina. The positive directions for the stress and moment resultants on the plate are shown in figure 6. Using equations (2.6), (2.8) and (2.9) the stress and moment resultants can be related to the strain and curvature of the midplane. The resulting relations are known as the lamina constitutive equations and are given as follows:

$$\begin{bmatrix} N_x \\ N_y \\ N_{xy} \end{bmatrix}_\ell = \int_{h_{k-1}}^{h_k} \begin{bmatrix} \sigma_x \\ \sigma_y \\ \tau_{xy} \end{bmatrix}_\ell dz = \int_{h_{k-1}}^{h_k} \begin{bmatrix} \bar{Q}_{11} & \bar{Q}_{12} & \bar{Q}_{16} \\ \bar{Q}_{12} & \bar{Q}_{22} & \bar{Q}_{26} \\ \bar{Q}_{16} & \bar{Q}_{26} & \bar{Q}_{66} \end{bmatrix}_\ell \begin{bmatrix} \varepsilon_x^o \\ \varepsilon_y^o \\ \gamma_{xy}^o \end{bmatrix}_\ell dz + \int_{h_{k-1}}^{h_k} z \begin{bmatrix} \bar{Q}_{11} & \bar{Q}_{12} & \bar{Q}_{16} \\ \bar{Q}_{12} & \bar{Q}_{22} & \bar{Q}_{26} \\ \bar{Q}_{16} & \bar{Q}_{26} & \bar{Q}_{66} \end{bmatrix}_\ell \begin{bmatrix} \kappa_x \\ \kappa_y \\ \kappa_{xy} \end{bmatrix}_\ell dz$$

$$\text{(2.10)}$$

$$\begin{bmatrix} M_x \\ M_y \\ M_{xy} \end{bmatrix}_\ell = \int_{h_{k-1}}^{h_k} z \begin{bmatrix} \sigma_x \\ \sigma_y \\ \tau_{xy} \end{bmatrix}_\ell dz = \int_{n_{k-1}}^{h_k} z \begin{bmatrix} \bar{Q}_{11} & \bar{Q}_{12} & \bar{Q}_{16} \\ \bar{Q}_{12} & \bar{Q}_{22} & \bar{Q}_{26} \\ \bar{Q}_{16} & \bar{Q}_{26} & \bar{Q}_{66} \end{bmatrix}_\ell \begin{bmatrix} \varepsilon_x^o \\ \varepsilon_y^o \\ \gamma_{xy}^o \end{bmatrix}_\ell dz + \int_{h_{k-1}}^{h_k} z^2 \begin{bmatrix} \bar{Q}_{11} & \bar{Q}_{12} & \bar{Q}_{16} \\ \bar{Q}_{12} & \bar{Q}_{22} & \bar{Q}_{26} \\ \bar{Q}_{16} & \bar{Q}_{26} & \bar{Q}_{66} \end{bmatrix}_\ell \begin{bmatrix} \kappa_x \\ \kappa_y \\ \kappa_{xy} \end{bmatrix}_\ell dz$$

$$\text{(2.11)}$$

The plate constitutive equations will be developed from equations (2.10) and (2.11) by summing up the individual terms for each lamina. Thus,

$$\begin{bmatrix} N_x \\ N_y \\ N_{xy} \end{bmatrix}_\ell = \sum_{k=1}^{K} \int_{h_{k-1}}^{h_k} \begin{bmatrix} \sigma_x \\ \sigma_y \\ \tau_{xy} \end{bmatrix}_\ell dz = \sum_{k=1}^{K} \int_{h_{k-1}}^{h_k} \begin{bmatrix} \bar{Q}_{11} & \bar{Q}_{12} & \bar{Q}_{16} \\ \bar{Q}_{12} & \bar{Q}_{22} & \bar{Q}_{26} \\ \bar{Q}_{16} & \bar{Q}_{26} & \bar{Q}_{66} \end{bmatrix}_\ell \begin{bmatrix} \varepsilon_x^o \\ \varepsilon_y^o \\ \gamma_{xy}^o \end{bmatrix}_\ell dz + \sum_{k=1}^{K} \int_{h_{k-1}}^{h_k} z \begin{bmatrix} \bar{Q}_{11} & \bar{Q}_{12} & \bar{Q}_{16} \\ \bar{Q}_{12} & \bar{Q}_{22} & \bar{Q}_{26} \\ \bar{Q}_{16} & \bar{Q}_{26} & \bar{Q}_{66} \end{bmatrix}_\ell \begin{bmatrix} \kappa_x \\ \kappa_y \\ \kappa_{xy} \end{bmatrix}_\ell dz$$

$$\text{(2.12)}$$

and

$$\begin{bmatrix} M_x \\ M_y \\ M_{xy} \end{bmatrix}_\ell = \sum_{k=1}^{K} \int_{h_{k-1}}^{h_k} z \begin{bmatrix} \sigma_x \\ \sigma_y \\ \tau_{xy} \end{bmatrix}_\ell dz = \sum_{k=1}^{K} \int_{h_{k-1}}^{h_k} z \begin{bmatrix} \bar{Q}_{11} & \bar{Q}_{12} & \bar{Q}_{16} \\ \bar{Q}_{12} & \bar{Q}_{22} & \bar{Q}_{26} \\ \bar{Q}_{16} & \bar{Q}_{26} & \bar{Q}_{66} \end{bmatrix}_\ell \begin{bmatrix} \varepsilon_x^o \\ \varepsilon_y^o \\ \gamma_{xy}^o \end{bmatrix}_\ell dz + \sum_{k=1}^{K} \int_{h_{k-1}}^{h_k} z^2 \begin{bmatrix} \bar{Q}_{11} & \bar{Q}_{12} & \bar{Q}_{16} \\ \bar{Q}_{12} & \bar{Q}_{22} & \bar{Q}_{26} \\ \bar{Q}_{16} & \bar{Q}_{26} & \bar{Q}_{66} \end{bmatrix}_\ell \begin{bmatrix} \kappa_x \\ \kappa_y \\ \kappa_{xy} \end{bmatrix}_\ell dz$$

$$\text{(2.13)}$$

Since ε^o and κ are functions of x and y only and $\overline{Q}$ is a function of lamina properties, they can be taken outside the integral. Thus,

$$
\begin{bmatrix} N_x \\ N_y \\ N_{xy} \end{bmatrix} = \sum_{k=1}^{K} \begin{bmatrix} \overline{Q}_{11} & \overline{Q}_{12} & \overline{Q}_{16} \\ \overline{Q}_{12} & \overline{Q}_{22} & \overline{Q}_{26} \\ \overline{Q}_{16} & \overline{Q}_{26} & \overline{Q}_{66} \end{bmatrix}_\ell \begin{bmatrix} \varepsilon_x^o \\ \varepsilon_y^o \\ \gamma_{xy}^o \end{bmatrix}_\ell \int_{h_{k-1}}^{h_k} dz + \sum_{k=1}^{K} \begin{bmatrix} \overline{Q}_{11} & \overline{Q}_{12} & \overline{Q}_{16} \\ \overline{Q}_{12} & \overline{Q}_{22} & \overline{Q}_{26} \\ \overline{Q}_{16} & \overline{Q}_{26} & \overline{Q}_{66} \end{bmatrix}_\ell \begin{bmatrix} \kappa_x \\ \kappa_y \\ \kappa_{xy} \end{bmatrix}_\ell \int_{h_{k-1}}^{h_k} z\, dz
$$

and

(2.14)

$$
\begin{bmatrix} M_x \\ M_y \\ M_{xy} \end{bmatrix} = \sum_{k=1}^{K} \begin{bmatrix} \overline{Q}_{11} & \overline{Q}_{12} & \overline{Q}_{16} \\ \overline{Q}_{12} & \overline{Q}_{22} & \overline{Q}_{26} \\ \overline{Q}_{16} & \overline{Q}_{26} & \overline{Q}_{66} \end{bmatrix}_\ell \begin{bmatrix} \varepsilon_x^o \\ \varepsilon_y^o \\ \gamma_{xy}^o \end{bmatrix}_\ell \int_{h_{k-1}}^{h_k} z\, dz + \sum_{k=1}^{K} \begin{bmatrix} \overline{Q}_{11} & \overline{Q}_{12} & \overline{Q}_{16} \\ \overline{Q}_{12} & \overline{Q}_{22} & \overline{Q}_{26} \\ \overline{Q}_{16} & \overline{Q}_{26} & \overline{Q}_{66} \end{bmatrix}_\ell \begin{bmatrix} \kappa_x \\ \kappa_y \\ \kappa_{xy} \end{bmatrix}_\ell \int_{h_{k-1}}^{h_k} z^2\, dz
$$

(2.15)

or after integrating these may be written as:

$$
\begin{bmatrix} N_x \\ N_y \\ N_{xy} \end{bmatrix} = \begin{bmatrix} A_{11} & A_{12} & A_{16} \\ A_{12} & A_{22} & A_{26} \\ A_{16} & A_{26} & A_{66} \end{bmatrix} \begin{bmatrix} \varepsilon_x^o \\ \varepsilon_y^o \\ \gamma_{xy}^o \end{bmatrix} + \begin{bmatrix} B_{11} & B_{12} & B_{16} \\ B_{12} & B_{22} & B_{26} \\ B_{16} & B_{26} & B_{66} \end{bmatrix} \begin{bmatrix} \kappa_x \\ \kappa_y \\ \kappa_{xy} \end{bmatrix}
$$

(2.16)

$$
\begin{bmatrix} M_x \\ M_y \\ M_{xy} \end{bmatrix} = \begin{bmatrix} B_{11} & B_{12} & B_{16} \\ B_{12} & B_{22} & B_{26} \\ B_{16} & B_{26} & B_{66} \end{bmatrix} \begin{bmatrix} \varepsilon_x^o \\ \varepsilon_y^o \\ \varepsilon_{xy}^o \end{bmatrix} + \begin{bmatrix} D_{11} & D_{12} & D_{16} \\ D_{12} & D_{22} & D_{26} \\ D_{16} & D_{26} & D_{66} \end{bmatrix} \begin{bmatrix} \kappa_x \\ \kappa_y \\ \kappa_{xy} \end{bmatrix}
$$

(2.17)

where

$$A_{ij} = \sum_{k=1}^{K} (\overline{Q}_{ij})_k \ (h_k - h_{k-1}) \qquad \text{(a)}$$

$$B_{ij} = \sum_{k=1}^{K} (\overline{Q}_{ij})_k \ \frac{1}{2} (h_k^2 - h_{k-1}^2) \qquad \text{(b)} \qquad\qquad (2.18)$$

$$D_{ij} = \sum_{k=1}^{K} (\overline{Q}_{ij})_k \ \frac{1}{3} (h_k^3 - h_{k-1}^3) \qquad \text{(c)}$$

Writing the constitutive equations for laminated plates in matrix notation, they become:

$$[N] = [A] [\epsilon^\circ] + [B] [\kappa] \qquad\qquad (2.19)$$

$$[M] = [B] [\epsilon^\circ] + [D] [\kappa] \qquad\qquad (2.20)$$

These equations indicate that for a general laminated plate either stress or moment resultants produce both strains and curvatures. Thus there is a coupling between the stress and moment resultants through the matrix $[B]$. Since $[B]$ is an even function of h (See eq. $(2.18)_b$), it is zero and hence the equations are uncoupled for classical orthotropic plates and for laminated plates that are symmetric about the plate midplane.

Equations (2.19) and (2.20) will be rewritten in a more useful form for the following development by solving equation (2.19) for the midplane strains, and rewriting equation (2.20) in terms of the stress resultants. Equations (2.19) and (2.20) become:

$$[\varepsilon^{\circ}] = [A^*] \, [N] + [B^*] \, [\kappa] \tag{2.21}$$

$$[M] = [-B^{*^T}] \, [N] + [D^*] \, [\kappa] \tag{2.22}$$

where

$$[A^*] = [A^{-1}]$$

$$[B^*] = -[A^{-1}] \, [B]$$

$$[D^*] = [D] - [B] \, [A^{-1}] \, [B] \tag{2.23}$$

2.3 Plate Governing Equations

Due to the coupling between moment and stress resultants noted in equations (2.19) and (2.20), two differential equations are required to describe the behavior of the plate under various load conditions. The first equation will be developed using plate equations of motion and the second equation will be developed from the compatibility conditions that must be satisfiea between the strains.

2.3.1 Equations of Motion

The equations of motion for a thin laminated plate are identical to those of homogenous plate theory. For a plate subjected to inplane normal and shear loads and loads perpendicular to the plate surface, the equations of motion are given as follows (See ref. 26.) where the inertia terms in the x and y directions are considered to be negligible.

$$\frac{\partial N_x}{\partial x} + \frac{\partial N_{xy}}{\partial y} = 0 \tag{2.24}$$

$$\frac{\partial N_y}{\partial y} + \frac{\partial N_{xy}}{\partial x} = 0 \qquad (2.25)$$

$$\frac{\partial^2 M_x}{\partial x^2} + \frac{\partial^2 M_y}{\partial y^2} + 2 \frac{\partial^2 M_{xy}}{\partial x \partial y} = -p - N_x \frac{\partial^2 w}{\partial x^2}$$

$$- N_y \frac{\partial^2 w}{\partial y^2} - 2 N_{xy} \frac{\partial^2 w}{\partial x \partial y} + \gamma \frac{\partial^2 w}{\partial t^2} \qquad (2.26)$$

The inplane loads N_x, N_y, and N_{xy} may be separated into the uniform externally applied loads and the loads induced by the plate deflections as follows:

$$N_x = \overline{N}_x + N'_x \qquad \text{(a)}$$

$$N_y = \overline{N}_y + N'_y \qquad \text{(b)}$$

$$N_{xy} = \overline{N}_{xy} + N'_{xy} \qquad \text{(c)} \qquad (2.27)$$

Substituting the expressions for N_x, N_y, and N_{xy} given by equation (2.27) into equations (2.24), (2.25), and (2.26) results in the following equations of motion:

$$\frac{\partial N'_x}{\partial x} + \frac{\partial N'_{xy}}{\partial y} = 0 \qquad (2.28)$$

$$\frac{\partial N'_y}{\partial y} + \frac{\partial N'_{xy}}{\partial x} = 0 \qquad (2.29)$$

$$\frac{\partial^2 M_x}{\partial x^2} + \frac{\partial^2 M_y}{\partial y^2} + 2 \frac{\partial^2 M_{xy}}{\partial x \partial y} = -p - \bar{N}_x \frac{\partial^2 w}{\partial x^2} - 2 \bar{N}_{xy} \frac{\partial^2 w}{\partial x \partial y} \qquad (2.30)$$

$$-\bar{N}_y \frac{\partial^2 w}{\partial y^2} + \gamma \frac{\partial^2 w}{\partial t^2}$$

The higher order terms $\left(N'_x \frac{\partial^2 w}{\partial x^2} , \quad N'_y \frac{\partial^2 w}{\partial y^2} , \text{ and } N'_{xy} \frac{\partial^2 w}{\partial x \partial y} \right)$, have been neglected in equation (2.30).

Defining a stress function F such that:

$$N'_x = \frac{\partial^2 F}{\partial y^2} \qquad (a)$$

$$N'_y = \frac{\partial^2 F}{\partial x^2} \qquad (b) \qquad\qquad (2.31)$$

$$N'_{xy} = -\frac{\partial^2 F}{\partial x \partial y} \qquad (c)$$

then equations (2.28) and (2.29) are satisfied identically by the function. The function F is referred to in the literature (See ref. 26.) as the Airy stress function. Using the definitions of F given by equations (2.31), the definitions of curvature given by equation (2.5), and the expression for the moments given by equation (2.22) in equation (2.30), the following expression is obtained:

$$\frac{\partial^2}{\partial x^2} \left(- B^*_{11} \frac{\partial^2 F}{\partial y^2} - B^*_{21} \frac{\partial^2 F}{\partial x^2} + B^*_{61} \frac{\partial^2 F}{\partial x \partial y} - D^*_{11} \frac{\partial^2 w}{\partial x^2} - D^*_{12} \frac{\partial^2 w}{\partial y^2} \right.$$

$$\left. -2 D^*_{16} \frac{\partial^2 w}{\partial x \partial y} \right) + 2 \frac{\partial^2}{\partial x \partial y} \left(-B^*_{16} \frac{\partial^2 F}{\partial y^2} - B^*_{26} \frac{\partial^2 F}{\partial x^2} + B^*_{66} \frac{\partial^2 F}{\partial x \partial y} \right. \qquad (2.32)$$

$$- D_{16}^{*} \frac{\partial^2 w}{\partial x^2} - D_{26}^{*} \frac{\partial^2 w}{\partial y^2} - 2 D_{66}^{*} \frac{\partial^2 w}{\partial x \partial y} \Bigg) + \frac{\partial^2}{\partial y^2} \Bigg(- B_{12}^{*} \frac{\partial^2 F}{\partial y^2}$$

$$- B_{22}^{*} \frac{\partial^2 F}{\partial x^2} + B_{62}^{*} \frac{\partial^2 F}{\partial x \partial y} - D_{12}^{*} \frac{\partial^2 w}{\partial x^2} - D_{22}^{*} \frac{\partial^2 w}{\partial y^2} - 2 D_{26}^{*} \frac{\partial^2 w}{\partial x \partial y}$$

$$= - p - \bar{N}_{x} \frac{\partial^2 w}{\partial x^2} - \bar{N}_{y} \frac{\partial^2 w}{\partial y^2} - 2 \bar{N}_{xy} \frac{\partial^2 w}{\partial x \partial y} + \frac{\gamma \partial^2 w}{\partial t^2}$$

or

$$B_{21}^{*} \frac{\partial^4 F}{\partial x^4} + (2 B_{26}^{*} - B_{61}^{*}) \frac{\partial^4 F}{\partial x^3 \partial y} + (B_{11}^{*} + B_{22}^{*} - 2 B_{66}^{*}) \frac{\partial^4 F}{\partial x^2 \partial y^2}$$

$$+ (2 B_{16}^{*} - B_{62}^{*}) \frac{\partial^4 F}{\partial x \partial y^3} + B_{12}^{*} \frac{\partial^4 F}{\partial y^4} + D_{11}^{*} \frac{\partial^4 w}{\partial x^4} + 4 D_{16}^{*} \frac{\partial^4 w}{\partial x^3 \partial y}$$

$$+ 2 (D_{12}^{*} + 2 D_{66}^{*}) \frac{\partial^4 w}{\partial x^2 \partial y^2} + 4 D_{26}^{*} \frac{\partial^4 w}{\partial x \partial y^3} + D_{22}^{*} \frac{\partial^4 w}{\partial y^4} + \gamma \frac{\partial^2 w}{\partial t^2} =$$

$$p + \bar{N}_{x} \frac{\partial^2 w}{\partial x^2} + \bar{N}_{y} \frac{\partial^2 w}{\partial y^2} + 2 \bar{N}_{xy} \frac{\partial^2 w}{\partial x \partial y} \qquad (2.33)$$

If p is taken as the aerodynamic loading due to air flow over the
plate surface, then equation (2.33) is one of the equations needed to
solve for the flutter of flat laminated plates. Aerodynamic loads pre-
dicted by piston theory have often been used in the literature (See ref.
28 - 42) to obtain flutter solutions. Piston theory gives a relatively
simple expression for p and has been shown to be applicable for Mach
numbers greater than 1.6 (See ref. 28 and 29.). For supersonic flow
over one side of a flat plate at an angle of Λ with the x-axis as

shown in figure 7, piston theory gives the following expression for the aerodynamic loads.

$$p = \frac{-2q}{\beta} \left(\frac{\partial w}{\partial x} \cos \Lambda + \frac{\partial w}{\partial y} \sin \Lambda \right) \tag{2.34}$$

Substituting the expression for p given by equation (2.34) into equation (2.33), the following governing equation is obtained for flutter of flat laminated plates.

$$B_{21}^* \frac{\partial^4 F}{\partial x^4} + (2 B_{26}^* - B_{61}^*) \frac{\partial^4 F}{\partial x^3 \partial y} + (B_{11}^* + B_{22}^* - 2 B_{66}^*) \frac{\partial^4 F}{\partial x^2 \partial y^2} \tag{2.35}$$

$$+ (2 B_{16}^* - B_{62}^*) \frac{\partial^4 F}{\partial x \partial y^3} + B_{12}^* \frac{\partial^4 F}{\partial y^4} + D_{11}^* \frac{\partial^4 w}{\partial x^4} + 4 D_{16}^* \frac{\partial^4 w}{\partial x^3 \partial y}$$

$$+ 2 (D_{12}^* + 2 D_{66}^*) \frac{\partial^4 w}{\partial x^2 \partial y^2} + 4 D_{26}^* \frac{\partial^4 w}{\partial x \partial y^3} + D_{22}^* \frac{\partial^4 w}{\partial y^4} +$$

$$\frac{2q}{\beta} \left(\frac{\partial w}{\partial x} \cos \Lambda + \frac{\partial w}{\partial y} \sin \Lambda \right) - \bar{N}_x \frac{\partial^2 w}{\partial x^2} - \bar{N}_y \frac{\partial^2 w}{\partial y^2} - 2 \bar{N}_{xy} \frac{\partial^2 w}{\partial x \partial y} + \gamma \frac{\partial^2 w}{\partial t^2} = 0$$

This expression is a 4th order partial differential equation which governs the flutter behavior of flat laminated plates but is in terms of two unknowns w and F. Thus an additional equation relating w and F is needed before solutions to flutter problems may be obtained.

2.3.2 Compatibility Equation

The additional equation needed to solve for the plate flutter behavior is obtained from the compatibility condition that must be satisfied between the midplane strains. The appropriate equation is obtained by eliminating the midplane displacements from the strain-displacement relations given in equation (2.4). Differentiating ε^o_x (eq. 2.4(a)) twice with respect to y and ε^o_y (eq. 2.4(b)) twice with respect to x and adding, the following expression is obtained:

$$\frac{\partial^2 \varepsilon^o_x}{\partial y^2} + \frac{\partial^2 \varepsilon^o_y}{\partial x^2} = \frac{\partial^3 u^o}{\partial x \partial y^2} + \frac{\partial^3 v^o}{\partial x^2 \partial y} \qquad \text{(a)} \tag{2.36}$$

but from eq. (2.4(c)):

$$\frac{\partial^2 \gamma^o_{xy}}{\partial x \partial y} = \frac{\partial^3 u^o}{\partial x \partial y^2} + \frac{\partial^3 v^o}{\partial x^2 \partial y} \qquad \text{(b)}$$

therefore:

$$\frac{\partial^2 \varepsilon^o_x}{\partial y^2} + \frac{\partial^2 \varepsilon^o_y}{\partial x^2} = \frac{\partial^2 \gamma^o_{xy}}{\partial x \partial y} \tag{2.37}$$

Equation (2.37) is referred to as the compatibility equation and will be used to develop the second governing equation in terms of w and F.

Using the expressions for strains given by equation (2.21) and the force resultants given by equations (2.27) and (2.31) and the curvatures given by equation (2.5) in equation (2.37), give rise to the following expression:

$$\frac{\partial^2}{\partial y^2}\left(A_{11}^*\frac{\partial^2 F}{\partial y^2} + A_{12}^*\frac{\partial^2 F}{\partial x^2} - A_{16}^*\frac{\partial^2 F}{\partial x \partial y} - B_{11}^*\frac{\partial^2 w}{\partial x^2}\right. \tag{2.38}$$

$$\left. - B_{12}^*\frac{\partial^2 w}{\partial y^2} - 2 B_{16}^*\frac{\partial^2 w}{\partial x \partial y}\right) + \frac{\partial^2}{\partial x^2}\left(A_{12}^*\frac{\partial^2 F}{\partial y^2} + A_{22}^*\frac{\partial^2 F}{\partial x^2}\right.$$

$$\left. - A_{26}^*\frac{\partial^2 F}{\partial x \partial y} - B_{21}^*\frac{\partial^2 w}{\partial x^2} - B_{22}^*\frac{\partial^2 w}{\partial y^2} - 2 B_{26}^*\frac{\partial^2 w}{\partial x \partial y}\right)$$

$$= \frac{\partial^2}{\partial x \partial y}\left(A_{16}^*\frac{\partial^2 F}{\partial y^2} + A_{26}^*\frac{\partial^2 F}{\partial x^2} - A_{66}^*\frac{\partial^2 F}{\partial x \partial y} - B_{61}^*\frac{\partial^2 w}{\partial x^2} - B_{62}^*\frac{\partial^2 w}{\partial y^2} - 2 B_{66}^*\frac{\partial^2 w}{\partial x \partial y}\right)$$

or

$$A_{22}^*\frac{\partial^4 F}{\partial x^4} - 2 A_{26}^*\frac{\partial^4 F}{\partial x^3 \partial y} + (2 A_{12}^* + A_{66}^*)\frac{\partial^4 F}{\partial x^2 \partial y^2} - 2 A_{16}^*\frac{\partial^4 F}{\partial x \partial y^3}$$

$$+ A_{11}^*\frac{\partial^4 F}{\partial y^4} - B_{21}^*\frac{\partial^4 w}{\partial x^4} - (2 B_{26}^* - B_{61}^*)\frac{\partial^4 w}{\partial x^3 \partial y} - (B_{11}^* + B_{22}^* - 2 B_{66}^*)\frac{\partial^4 w}{\partial x^2 \partial y^2}$$

$$- (2 B_{16}^* - B_{62}^*)\frac{\partial^4 w}{\partial x \partial y^3} - B_{12}^*\frac{\partial^4 w}{\partial y^4} = 0 \tag{2.39}$$

This is the second governing equation needed to solve for the plate behavior. It is also a fourth order partial differential equation in terms

of F and w and for flutter problems must be solved simultaneously with equation (2.35). In order to solve the equations for a specific problem the boundary conditions must be specified.

2.4 Poundary Conditions

Proper boundary conditions which guarantee unique solutions to the two governing equations must be specified. It has been found (See reference 26.) that the necessary boundary conditions are those of classical homogeneous plate theory plus those of an inplane elasticity problem. Thus due to the coupling, the usual deflection, slope, moment, or shear boundary conditions used in classifical plate theory do not give unique solutions but inplane boundary conditions must also be specified. The resulting boundary conditions require one member of each pair of the following quantities to be specified along the boundaries:

$$w \quad \text{or} \quad \frac{\partial M_{nt}}{\partial t} + Q_n + \bar{N}_n \frac{\partial w}{\partial n} + \bar{N}_{ns} \frac{\partial w}{\partial s} \qquad \text{(a)} \qquad (2.40)$$

$$\frac{\partial w}{\partial n} \quad \text{or} \quad M_n \qquad \text{(b)}$$

$$u_n^o \quad \text{or} \quad N_n \qquad \text{(c)}$$

$$u_t^o \quad \text{or} \quad N_{nt} \qquad \text{(d)}$$

where n and t are used to denote coordinates normal and tangential to the plate boundary respectively.

For this analysis, the boundary conditions chosen represent those for a simply supported plate with no inplane edge restraints and are given as follows:

$$w(0,y) = w(a,y) = w(x,0) = w(x,b) = 0 \qquad (a)$$

(2.41)

$$M_x(0,y) = M_x(a,y) = 0 \qquad (b)$$

$$M_y(x,0) = M_y(x,b) = 0 \qquad (c)$$

$$N'_x(0,y) = N'_x(a,y) = 0 \qquad (d)$$

$$N'_y(x,0) = N'_y(x,b) = 0 \qquad (e)$$

$$N'_{xy}(0,y) = N'_{xy}(a,y) = N'_{xy}(x,0) = N'_{xy}(x,b) = 0 \qquad (f)$$

These equations will be rewritten in terms of w and F using the expression for moments given by equation (2.22) and the definitions of strain, curvature, and F given by equations (2.4), (2.5), and (2.31) respectively. Thus the boundary conditions become:

$$w(0,y) = w(a,y) = w(x,0) = w(x,b) = 0$$

(2.42)

$$- B_{11}^* \frac{\partial^2 F}{\partial y^2} - B_{21}^* \frac{\partial^2 F}{\partial x^2} + B_{61}^* \frac{\partial^2 F}{\partial x \partial y} - D_{11}^* \frac{\partial^2 w}{\partial x^2}$$

(2.43)

$$- D_{12}^* \frac{\partial^2 w}{\partial y^2} - 2 D_{16}^* \frac{\partial^2 w}{\partial x \partial y} = 0 \text{ at } x = 0, a$$

$$- B_{12}^* \frac{\partial^2 F}{\partial y^2} - B_{22}^* \frac{\partial^2 F}{\partial x^2} + B_{62}^* \frac{\partial^2 F}{\partial x \partial y} - D_{12}^* \frac{\partial^2 w}{\partial x^2}$$

$$- D_{22}^* \frac{\partial^2 w}{\partial y^2} + 2 D_{26}^* \frac{\partial^2 w}{\partial x \partial y} = 0 \text{ at } y = 0, b$$

(2.44)

$$\frac{\partial^2 F}{\partial y^2} = 0 \quad \text{at} \quad x = 0, a \qquad (2.45)$$

$$\frac{\partial^2 F}{\partial x^2} = 0 \quad \text{at} \quad y = 0, b \qquad (2.46)$$

$$\frac{\partial^2 F}{\partial x \partial y} = 0 \quad \text{at} \quad \begin{aligned} x &= 0, a \\ y &= 0, b \end{aligned} \qquad (2.47)$$

The governing equations (2.35) and (2.39) along with the boundary conditions (2.42) through (2.47) will be solved by using approximate techniques in the next chapter.

Chapter 3

APPROXIMATE SOLUTIONS OF THE FLUTTER EQUATIONS

The two governing fourth order partial differential equations (2.35)
and (2.39) along with boundary conditions given by equations (2.42)
through (2.47) will be used to obtain approximate flutter solutions. The
analysis will be developed for the flutter of general laminated plates where
arbitrary stacking sequence and orientation of the lamina fibers is
permissible. Since certain special classes of plates have been studied
almost exclusively in the literature, the simplifications to the
general solution due to the special constructions will be discussed. The
special classes of plates considered are symmetric laminated plates and
angle-ply plates. Symmetric plates may be composed of any even number of
lamina of arbitrary thickness and orientation of the fiber directions as
long as for every lamina above the plate midplane there is an identical
(in thickness, material properties, and orientation) lamina equal
distance below the plate midplane. Angle-ply plates are less general than
symmetric plates and consist of an even number of laminas all of the same
thickness and elastic properties with the orthotropic axes of symmetry
in each lamina alternately oriented at $+\theta$ and $-\theta$ to the plate axis.
Although the analysis and solution procedure will be developed basically
to study panel flutter, the analysis is general and the resulting computer
program can also be used to determine static buckling loads and natural
vibration frequencies.

31

3.1 General Laminated Plates

An extended Galerkin method will be used to obtain approximate flutter solutions since it provides a straight-forward solution procedure for nonconservative problems (See ref. 42.) using a simple series to describe the assumed displacements. The extended Galerkin method admits solutions only when the assumed deflections satisfy the geometric (deflection and slope) boundary conditions. However, the number of terms required in the solution to obtain converged results are probably reduced if the assumed deflections satisfy some or all of the natural (force or natural constraints) boundary conditions. Since functions are not available which satisfy all the boundary conditions given by equations (2.42) through (2.47), the capability to account for the natural boundary conditions makes the extended Galerkin method particularly suited to this analysis.

The extended Galerkin method of solution is illustrated by the following equation written in terms of the virtual work for displacements w.

$$\int_0^b \int_0^a (\text{governing equation}) \delta w \; dxdy + \int_0^a f_1(w,x,y) \; \delta w \Big|_0^b dx + \int_0^a f_2(w,x,y) \delta \frac{\partial w}{\partial x} \Big|_0^b dx$$

$$+ \int_0^b f_3(w,x,y) \; \delta w \Big|_0^a dy + \int_0^b f_4(w,x,y) \; \delta \frac{\partial w}{\partial y} \Big|_0^a dy = 0 \qquad (3.1)$$

The terms under the double and single integrals are usually individually set equal to zero and referred to as the governing equation and boundary conditions, respectively. For the boundary conditions to be satisfied, either the functions $f_i(w,x,y)$ or the variation of the deflections or the slopes must be zero at the appropriate boundaries. In usual applications of the Galerkin method, a series of functions is chosen which satisfy all the boundary conditions and the coefficients of the functions are determined so that the double integral term is zero or equivalently the coefficients are determined so that each term of the series is orthognal to the exact solution (See ref. 43). When all the natural boundary conditions are not satisfied, the extended Galerkin method requires that the coefficients be determined using the unsatisfied single integral terms as well as the double integral terms in equation 3.1.

For the flutter of general laminated plates, a series of functions for both w and F are needed which exactly satisfy the geometrical boundary conditions given by equation (2.42) and which satisfy as closely as possible the natural boundary conditions given by equations (2.43) through (2.47). The functions assumed for this analysis are given as follows:

$$w = \sum_{m=1}^{M} \sum_{n=1}^{N} C_{mn} \sin \frac{m\pi x}{a} \sin \frac{n\pi y}{b} e^{i\omega t} \tag{3.2}$$

$$F = \sum_{m=1}^{M} \sum_{n=1}^{N} H_{mn} \cos \frac{m\pi x}{a} \cos \frac{n\pi y}{b} e^{i\omega t} \tag{3.3}$$

These functions exactly satisfy the geometrical boundary conditions and the natural boundary conditions given by equation (2.47) but the remaining natural boundary conditions are not completely satisfied. The unsatisfied natural boundary condition terms are given as follows:

For M_x:
$$\left[B_{11}^* \frac{\partial^2 F}{\partial y^2} + B_{21}^* \frac{\partial^2 F}{\partial x^2} + 2 D_{16}^* \frac{\partial^2 w}{\partial x \partial y} \right]_0^a \qquad \text{(a)} \qquad (3.4)$$

M_y:
$$\left[B_{12}^* \frac{\partial^2 F}{\partial y^2} + B_{22}^* \frac{\partial^2 F}{\partial x^2} + 2 D_{26}^* \frac{\partial^2 w}{\partial x \partial y} \right]_0^b \qquad \text{(b)}$$

N_x:
$$\left[\frac{\partial^2 F}{\partial y^2} \right]_0^a \qquad \text{(c)}$$

N_y:
$$\left[\frac{\partial^2 F}{\partial x^2} \right]_0^b \qquad \text{(d)}$$

The boundary condition terms that must be included in the extended Galerkin method written in terms of the virtual work are given as follows:

For M_x:
$$\int_0^b \left(B_{11}^* \frac{\partial^2 F}{\partial y^2} + B_{21}^* \frac{\partial^2 F}{\partial x^2} + 2 D_{16}^* \frac{\partial^2 w}{\partial x \partial y} \right) \delta \frac{\partial w}{\partial x} \Big|_0^a \, dy \qquad (3.5)$$

M_y:
$$\int_0^a \left(B_{12}^* \frac{\partial^2 F}{\partial y^2} + B_{22}^* \frac{\partial^2 F}{\partial x^2} + 2 D_{26}^* \frac{\partial^2 w}{\partial x \partial y} \right) \delta \frac{\partial w}{\partial y} \Big|_0^b \, dx \qquad (3.6)$$

N_x:
$$\int_0^b \frac{\partial^2 F}{\partial y^2} \delta u^o \Big|_0^a \, dy \qquad (3.7)$$

$$\text{Ny}: \quad \int_0^a \frac{\partial^2 F}{\partial x^2} \, \delta \, v^o \, \bigg|_0^b \, dx \tag{3.8}$$

where the displacements u^o and v^o are given as follows and were obtained by substituting the definition of curvature given by equation (2.5) and the expression for strain given by equation (2.22) into equation (2.4) and integrating.

$$u^o = \int \varepsilon_x^o \, dx = A_{12}^* \, \frac{\partial F}{\partial x} + A_{11}^* \int \frac{\partial^2 F}{\partial y^2} \, dx - A_{16}^* \, \frac{\partial F}{\partial y} \tag{3.9}$$

$$- B_{11}^* \, \frac{\partial w}{\partial x} - B_{12}^* \int \frac{\partial^2 w}{\partial y^2} \, dx - 2 \, B_{16}^* \, \frac{\partial w}{\partial y}$$

$$v^o = \int \varepsilon_y^o \, dy = - A_{26}^* \, \frac{\partial F}{\partial x} + A_{22}^* \int \frac{\partial^2 F}{\partial x^2} \, dy + A_{12}^* \, \frac{\partial F}{\partial y} \tag{3.10}$$

$$- 2 \, B_{26}^* \, \frac{\partial w}{\partial x} - B_{21}^* \int \frac{\partial^2 w}{\partial x^2} \, dy - B_{22}^* \, \frac{\partial w}{\partial y}$$

Using the assumed functions given by equations (3.2) and (3.3) and applying the extended Galerkin method, the orthogonality relations for the governing equations (3.35) and (3.39) with the boundary condition terms given by equations (3.5) through (3.10) added may be written as follows:

$$
\int_0^a \int_0^b \sum_{r=1}^{M} \sum_{s=1}^{N} \left\{ C_{rs} \left[(K_1 - \gamma\omega^2) \sin \frac{m\pi x}{a} \sin \frac{n\pi y}{b} \sin \frac{r\pi y}{a} \sin \frac{s\pi y}{b} \right. \right. \qquad (3.11)
$$

$$
- K_3 \cos \frac{m\pi x}{a} \cos \frac{n\pi y}{b} \sin \frac{r\pi y}{a} \sin \frac{s\pi y}{b} + \frac{2a}{\beta} \left(\cos \Lambda \left(\frac{m\pi}{a}\right) \cos \frac{m\pi x}{a} \sin \frac{n\pi y}{b} \right.
$$

$$
+ \sin \Lambda \left(\frac{n\pi}{b}\right) \sin \frac{m\pi x}{a} \cos \frac{n\pi y}{b} \Big) \sin \frac{r\pi x}{a} \sin \frac{s\pi y}{b} \Bigg] + H_{rs} \left[K_4 \cos \frac{m\pi x}{a} \cos \frac{n\pi y}{b} \right.
$$

$$
\sin \frac{s\pi y}{b} \sin \frac{r\pi x}{a}
$$

$$
\left. \left. - K_2 \sin \frac{m\pi x}{a} \sin \frac{n\pi y}{b} \sin \frac{r\pi x}{a} \sin \frac{s\pi y}{b} \right] \right\} dx \, dy
$$

$$
+ \sum_{r=1}^{M} \sum_{s=1}^{N} C_{rs} \left[2 \, D_{16}^{*}\left(\frac{m\pi}{a}\right)\left(\frac{n\pi}{b}\right)\left(\frac{r\pi}{a}\right) \int_0^b \cos \frac{m\pi x}{a} \cos \frac{n\pi y}{b} \cos \frac{r\pi y}{a} \sin \frac{s\pi y}{b} \Bigg|_0^a \, dy \right.
$$

$$
\left. + 2 \, D_{26}^{*} \left(\frac{m\pi}{a}\right)\left(\frac{n\pi}{b}\right)\left(\frac{s\pi}{b}\right) \int_0^a \cos \frac{m\pi x}{a} \cos \frac{n\pi y}{a} \sin \frac{r\pi x}{b} \cos \frac{s\pi y}{b} \Bigg|_0^b \, dx \right]
$$

$$
- \sum_{r=1}^{M} \sum_{s=1}^{N} H_{rs} \left\{ \left[B_{11}^{*} \left(\frac{n\pi}{b}\right)^2 + B_{21}^{*}\left(\frac{m\pi}{a}\right)^2 \right] \int_0^b \frac{r\pi}{a} \cos \frac{m\pi x}{a} \cos \frac{n\pi y}{b} \cos \frac{r\pi x}{a} \sin \frac{s\pi y}{b} \Bigg|_0^a \, dy \right.
$$

$$
\left. + \left[B_{12}^{*} \left(\frac{n\pi}{b}\right)^2 + B_{22}^{*} \left(\frac{m\pi}{a}\right)^2 \right] \int_0^a \frac{s\pi}{b} \cos \frac{m\pi x}{a} \cos \frac{n\pi y}{b} \sin \frac{r\pi x}{a} \cos \frac{s\pi y}{b} \int_0^b \, dx \right\} = 0
$$

and

$$\int_o^a \int_o^b \sum_{r=1}^{M} \sum_{s=1}^{N} \left\{ H_{rs} \left[K_5 \cos \frac{m\pi x}{a} \cos \frac{n\pi y}{b} + K_6 \sin \frac{m\pi x}{a} \sin \frac{n\pi y}{b} \right] \cos \frac{r\pi x}{a} \cos \frac{s\pi y}{b} \right.$$

$$\left. + H_{mn} \left[K_2 \cos \frac{m\pi x}{a} \cos \frac{n\pi y}{b} - K_4 \sin \frac{m\pi x}{a} \sin \frac{n\pi y}{b} \right] \cos \frac{r\pi y}{a} \cos \frac{s\pi y}{b} \right\} dx\, dy \qquad (3.12)$$

$$-\sum_{m=1}^{M} \sum_{n=1}^{N} H_{mn} \left\{ \left(\frac{n\pi}{b}\right)^2 \int_o^b \left[A_{16}^* \left(\frac{s\pi}{b}\right) - B_{11}^* \left(\frac{r\pi}{a}\right) - B_{12}^* \left(\frac{s\pi}{b}\right)^2 \left(\frac{a}{r\pi}\right) \right] \cos \frac{m\pi x}{a} \cos \frac{n\pi y}{b} \right.$$

$$\left. \cos \frac{r\pi x}{a} \sin \frac{s\pi y}{b} \right|_o^a dy$$

$$\left. - \left(\frac{m\pi}{a}\right)^2 \int_o^a \left[A_{26}^* \left(\frac{r\pi}{a}\right) - B_{21}^* \left(\frac{r\pi}{a}\right)^2 \left(\frac{b}{s\pi}\right) - B_{22}^* \left(\frac{s\pi}{b}\right) \right] \cos \frac{m\pi x}{a} \cos \frac{n\pi y}{b} \sin \frac{r\pi x}{a} \cos \frac{s\pi y}{b} \right|_o^b dx \right\} = 0$$

where

$$K_1 = D_{11}^* \left(\frac{m\pi}{a}\right)^4 + 2 (D_{12}^* + 2D_{66}^*) \left(\frac{m\pi}{a}\right)^2 \left(\frac{n\pi}{b}\right)^2 + D_{22}^* \left(\frac{n\pi}{b}\right)^4 + \bar{N}_x \left(\frac{m\pi}{a}\right)^2 + \bar{N}_y \left(\frac{n\pi}{b}\right)^2$$

$$K_2 = (2B_{26}^* - B_{61}^*)\left(\frac{m\pi}{a}\right)^3 \left(\frac{n\pi}{b}\right) + (2B_{16}^* - B_{62}^*) \left(\frac{m\pi}{a}\right)\left(\frac{n\pi}{b}\right)^3$$

$$K_3 = 4 D_{16}^* \left(\frac{m\pi}{a}\right)^3 \left(\frac{n\pi}{b}\right) + 4 D_{26}^* \left(\frac{m\pi}{a}\right)\left(\frac{n\pi}{b}\right)^3 + 2 \left(\frac{m\pi}{a}\right)\left(\frac{n\pi}{b}\right) \bar{N}_{xy} \qquad (3.13)$$

$$K_4 = B_{21}^* \left(\frac{m\pi}{a}\right)^4 + (B_{11}^* + B_{22}^* - 2 B_{66}^*) \left(\frac{m\pi}{a}\right)^2 \left(\frac{n\pi}{b}\right)^2 + B_{12}^* \left(\frac{n\pi}{b}\right)^4$$

$$K_5 = A_{11}^* \left(\frac{n\pi}{b}\right)^4 + (2 A_{12}^* + A_{66}^*)\left(\frac{m\pi}{a}\right)^2 \left(\frac{n\pi}{b}\right)^2 + A_{22}^* \left(\frac{m\pi}{a}\right)^4$$

$$K_6 = 2 A_{16}^* \left(\frac{m\pi}{a}\right)\left(\frac{n\pi}{b}\right)^3 + 2 A_{26}^* \left(\frac{m\pi}{a}\right)^3 \left(\frac{n\pi}{b}\right)$$

Integrating and rearranging the terms, the following equations are obtained:

$$\left[C_{mn}\left(K_1 - \frac{\omega^2}{\omega_r^2}\frac{D_{11}^*\pi^4}{a^4}\right) - H_{mn}K_2\right] + \frac{4}{\pi^2}\sum_{r=1}^{M}\sum_{s=1}^{N}\left[C_{rs}K_3 + H_{rs}K_4\right]\frac{rs\,(1-(-1)^{s+n})(1-(-1)^{r+m})}{(s^2-n^2)(r^2-m^2)}$$

$$+\sum_{r=1}^{M}4\,C_{rn}\frac{\lambda D_{11}^*}{a^4}mr\,\frac{\cos\Lambda}{(r^2-m^2)}(1-(-1)^{r+m}) + \sum_{s=1}^{N}4\,C_{ms}\frac{\lambda D_{11}^*}{a^3b}ns\,\frac{\sin\Lambda}{s^2-n^2}(1-(-1)^{s+n})$$

$$-\sum_{r=1}^{M}\sum_{s=1}^{N}4\frac{\pi^2}{a^4}\left\{\left[2\,C_{rs}D_{16}^*\frac{a}{b}mnrs - B_{11}^*H_{rs}\left(\frac{a}{b}\right)^2n^2\,rs\right.\right. \tag{3.14}$$

$$\left.- B_{21}^*H_{rs}m^2\,rs\right]\frac{(1-(-1)^{s+n})((-1)^{r+m}-1)}{s^2-n^2} + \left[2\,C_{rs}D_{26}^*\left(\frac{a}{b}\right)^3mnrs\right.$$

$$\left.\left.- B_{12}^*H_{rs}\left(\frac{a}{b}\right)^4n^2sr - B_{22}^*H_{rs}\left(\frac{a}{b}\right)^2m^2rs\right]\frac{(1-(-1))((-1)^{s+n}-1)}{(r^2-m^2)}\right\} = 0$$

and

$$H_{mn}K_5 + K_2C_{mn} + \frac{4}{\pi^2}\sum_{r=1}^{M}\sum_{s=1}^{N}\left[H_{rs}K_6 - K_4C_{rs}\right]\frac{rs\,(1-(-1)^{r+n})(1-(-1)^{s+n})}{(r^2-m^2)(s^2-n^2)}$$

$$-\sum_{r=1}^{M}\sum_{s=1}^{N}\frac{4\,m^2\,\pi^2}{a^2b}\,\frac{rH_{rs}}{r^2-m^2}(1-(-1)^{r+m})((-1)^{s+n}-1)\left[B_{21}^*\left(\frac{r}{a}\right)^2\frac{b}{s} + B_{22}^*\left(\frac{s}{b}\right) - A_{26}^*\left(\frac{r}{a}\right)\right]$$

$$\tag{3.15}$$

$$-\sum_{r=1}^{M}\sum_{s=1}^{N}\frac{4\,n^2\pi^2}{ab^2}\,\frac{sH_{rs}}{s^2-n^2}(1-(-1)^{s+n})((-1)^{r+m}-1)\left[B_{11}^*\left(\frac{r}{a}\right) + B_{12}^*\left(\frac{s}{b}\right)^2\left(\frac{a}{r}\right) - A_{16}^*\left(\frac{s}{b}\right)\right] = 0$$

where

$$\lambda = \frac{2qa^3}{\beta D_{11}^*} \tag{3.16}$$

$$\omega_r^2 = \frac{\pi^4 D_{11}^*}{a^4 \gamma} \tag{3.17}$$

Equations (3.14) and (3.15) results in 2(MxN) equations in terms of the two unknowns C_{rs} and H_{rs}. In order to get the equations in a form that can be solved, H_{rs} must be solved for in terms of C_{rs}. This can be done using equation (3.15) and writing it in the following matrix form:

$$[b_{mnrs}] \ [H_{rs}] = [a_{mnrs}] \ [C_{rs}] \tag{3.18}$$

where r and s are summed from 1 to M and N respectively and b_{mnrs} and a_{mnrs} are the coefficient matrices for H_{mn} and C_{mn} respectively. To obtain H_{rs} as a function of C_{rs}, premultiply each side of equation (3.18) by the inverse of $[b_{mnrs}]$ as follows:

$$[b_{mnrs}]^{-1} \ [b_{mnrs}] \ [H_{rs}] = [b_{mnrs}]^{-1} \ [a_{mnrs}] \ [C_{rs}] \tag{3.19}$$

since $[b_{mnrs}]^{-1} \ [b_{mnrs}] = 1$

$$[H_{mn}] = [b_{mnrs}]^{-1} \ [a_{mnrs}] \ [C_{rs}] \tag{3.20}$$

Equation (3.20) results in a series solution for H_{mn} in terms of the unknown coefficients C_{rs}.

Using equation (3.20) to eliminate H_{mn} from equation (3.14), MxN

homogenous equations are obtained in terms of the unknown C_{rs}. The

resulting equations may be written in the following form:

$$
\begin{pmatrix}
(c_{11} - \omega_{11}) & c_{12} & \cdots & & C_{1N} \\
c_{21} & (c_{22} - \omega_{22}) & \cdot & & \\
& & \cdot & & \\
\cdot & \cdot & \cdot & \cdot & \\
\cdot & \cdot & \cdot & \cdot & \\
c_{M1} & \cdot & \cdot & \cdot & (c_{MN} - \omega_{MN})
\end{pmatrix}
C_{mn} = 0
\qquad (3.21)
$$

where the c_{mn} are the coefficients of C_{mn}. Equation (3.21) is recog-

nized as the well known characteristic equation and has a non-trivial

solution obtained by setting the determinant of the coefficient matrix

to zero. This results in an algebraic equation of order MxN in terms

of w. The roots of the algebraic equation are the characteristic values

or eigenvalves and represent the plate nondimensional vibration fre-

quencies.

Flutter solutions have been obtained using a digital computer to

solve equation (3.21) for its eigenvalves. Since the coefficients,

c_{ij}, are a function of the flutter parameter, λ, the plate vibration

frequencies are also a function of λ. The criteria used to define the

point of flutter is the lowest value of λ which results in two of the

frequencies (ω_{ij}) coalescing and thus having a negative imaginary

value. This criteria was selected because a negative imaginary fre-

quency results in the assumed deflection function (See equation (3.2).)

becoming unbounded since it is multiplied by $e^{i\omega t}$. Similar criteria has been used extensively in the literature (See ref. 39.) to define the point of flutter.

3.2 Symmetric Laminated Plates

Plates that are lami_ated such that they are symmetric about the midplane represent the largest class of laminated plates of practical use. Their symmetric construction results in warp-free structural elements which are desirable in most applications. Also, the governing differential equations and the boundary conditions are considerably simpler than for general laminated plates. Thus, symmetric plates have been investigated more than any other class of laminated plates.

As was pointed out in section (2.2) and as shown by equation (2.18(b)), B_{mn} is an even function of the lamina thickness and for symmetric plates all the B_{mn} terms vanish. Thus, the flutter equations (equations (2.35) and (2.39)) are considerably shortened and more importantly become uncoupled. Then only equation (2.35) needs to be solved to obtain a flutter solution. For a symmetrically laminated plate, the governing flutter equation becomes:

$$D_{11} \frac{\partial^4 w}{\partial x^4} + 4 D_{16} \frac{\partial^4 w}{\partial x^3 \partial y} + 2 (D_{12} + 2 D_{66}) \frac{\partial^4 w}{\partial x^2 \partial y^2} + 4 D_{26} \frac{\partial^4 w}{\partial x \partial y^3}$$

$$+ D_{22} \frac{\partial^4 w}{\partial y^4} + \frac{2q}{\beta} \left(\frac{\partial w}{\partial x} \cos \Lambda + \frac{\partial w}{\partial y} \sin \Lambda \right) - \bar{N}_x \frac{\partial^2 w}{\partial x^2} \qquad (3.22)$$

$$- \bar{N}_y \frac{\partial^2 w}{\partial y^2} - 2 \bar{N}_{xy} \frac{\partial^2 w}{\partial x \partial y} + \gamma \frac{\partial^2 w}{\partial t^2} = 0$$

where the asterisks have been left off the D_{mn} terms since $D_{mn} = D^*_{mn}$ for symmetric laminated plates.

Although equation (3.22) is considerably simpler than the flutter equations for general laminated plates, it differs from the governing equation for flutter of an orthotropic plate by the additional D_{16} and D_{26} terms. These terms appear in the governing equation as a result of the fibers not being aligned with the plate axes.

Since for symmetric plates the governing equations become uncoupled, the boundary conditions that must be satisfied for a flutter solution are given by equations (2.42) through (2.44) and are rewritten as follows with the B_{mn} terms removed:

$$w(0,y) = w(a,y) = w(x,0) = w(x,b) = 0 \tag{2.23}$$

$$-D_{11} \frac{\partial^2 w}{\partial x^2} - D_{12} \frac{\partial^2 w}{\partial y^2} - 2 D_{16} \frac{\partial^2 w}{\partial x \partial y} = 0 \text{ at } x = 0, a \tag{2.24}$$

$$- D_{12} \frac{\partial^2 w}{\partial x^2} - D_{22} \frac{\partial^2 w}{\partial y^2} - 2 D_{26} \frac{\partial^2 w}{\partial x \partial y} = 0 \text{ at } y = 0, b \tag{2.25}$$

These equations differ from the boundary conditions for a simply supported orthotropic plate by the D_{16} and D_{26} terms.

To obtain a standard Galerkin solution for symmetric plates, it is necessary to assume a function for w that satisfies all the boundary conditions (3.23) through (3.25). However, the D_{16} and D_{26} terms make it difficult to find satisfactory functions. Therefore, the same deflection function used in section (3.1) for general laminated plates and given by equation (3.2) will be assumed and the extended Galerkin

method used to account for the unsatisfied natural boundary conditions. The boundary condition terms that must be accounted for by the extended Galerkin method are given as follows:

$$\int_0^b 2 D_{16} \frac{\partial^2 w}{\partial x \partial y} \delta \frac{\partial w}{\partial x} \Big|_0^a dy \tag{3.26}$$

$$\int_0^a 2 D_{26} \frac{\partial^2 w}{\partial x \partial y} \delta \frac{\partial w}{\partial y} \Big|_0^b dx \tag{3.27}$$

Using the assumed functions given by equation (3.2) and applying the extended Galerkin method to the governing equation (3.22) with the D_{16} and D_{26} boundary condition terms included, results in the following equation:

$$C_{mn}\left[m^4 + 2 \frac{(D_{12} + 2D_{66})}{D_{11}} \left(\frac{mna}{b}\right)^2 + \frac{D_{22}}{D_{11}}\left(\frac{na}{b}\right)^4 - \frac{\omega^2}{\omega_r^2} + \frac{\bar{N}_x}{D_{11}}\left(\frac{ma}{\pi}\right)^2 + \frac{\bar{N}_y}{D_{11}}\left(\frac{na}{\pi b}\right)^2 \right]$$

$$- \sum_{r=1}^M \sum_{s=1}^N \frac{16 C_{rs}}{\pi^2} \left[\frac{D_{16}}{D_{11}} m^3 \left(\frac{an}{b}\right) + \frac{D_{26}}{D_{11}} m\left(\frac{an}{b}\right)^3 + \frac{\bar{N}_{xy}}{2} \frac{mna^3}{b\pi^2} \right] \frac{rs\,(1-(-1)^{r+m})(1-(-1)^{s+n})}{(r^2-m^2)(s^2-n^2)}$$

$$+ \sum_{r=1}^M C_{rn} \frac{4\lambda}{\pi^4} \frac{mr\,(1-(-1)^{r+m})}{r^2-m^2} \cos\Lambda + \sum_{s=1}^N C_{ms} \frac{4\lambda}{\pi^4} \frac{nsa}{b} \sin\Lambda \frac{(1-(-1)^{s+n})}{s^2-n^2}$$

$$+ \sum_{r=1}^M \sum_{s=1}^N \frac{8}{\pi^2} C_{rs} \frac{D_{16}}{D_{11}} \left(\frac{a}{b}\right) \frac{mnrs}{s^2-n^2} (1-(-1)^{s+n})((-1)^{r+m}-1) \tag{3.29}$$

$$+ \sum_{r=1}^M \sum_{s=1}^N \frac{8}{\pi^2} C_{rs} \frac{D_{26}}{D_{11}} \left(\frac{a}{b}\right)^3 \frac{mnrs}{(r^2-m^2)} (1-(-1)^{r+m})((-1)^{s+n}-1) = 0$$

Equation (3.29) represents a system of (MxN) linear homogenous equations in terms of the unknown C_{mn} and is recognized as the eigenvalue equation. Flutter solutions are obtained for equation (3.29) in the same manner as discussed in section (3.1) for general laminated plates.

3.3 Angle-ply Plates

Angle-ply plates by definition are constructed so as to have an even number of layers all of the same thickness and elastic properties and with the orthotropic axis of symmetry in each ply alternately oriented at $+\theta$ and $-\theta$ to the plate axis (See Fig. 2.). Although angle-ply plates do not represent as large or as important a group as the symmetric plates, they are important from an analytic viewpoint for obtaining a better understanding of general laminated plates. Because of the special geometry of angle-ply plates, the governing equations are considerably simplified but are still coupled. Thus, angle-ply plates retain many of the characteristics of general laminated plates but relatively simple solutions can be obtained. These characteristics have resulted in the angle-ply plates being studied extensively in the literature to obtain a better understanding of general laminated plates.

For angle-ply plates, it can be shown (See ref. 5.) that this special construction results in some of the coefficients being zero as follows:
$$A^{*}_{16} = A^{*}_{26} = D^{*}_{16} = D^{*}_{26} = 0$$

$$B^{*}_{21} = B^{*}_{11} = B^{*}_{22} = B^{*}_{66} = B^{*}_{12} = 0 \tag{3.30}$$

Setting these terms to zero in the flutter equations (2.35) and (2.39), results in the following governing equations.

$$(2 B_{26}^* - B_{61}^*) \frac{\partial^4 F}{\partial x^3 \partial y} + (2 B_{16}^* - B_{62}^*) \frac{\partial^4 F}{\partial x \partial y^3} + D_{11}^* \frac{\partial^4 w}{\partial x^4} \qquad (3.31)$$

$$+ 2 (D_{12}^* + 2 D_{66}^*) \frac{\partial^4 w}{\partial x^2 \partial y^2} + D_{22}^* \frac{\partial^4 w}{\partial y^4} + \frac{2q}{\beta} \left(\frac{\partial w}{\partial x} \cos \Lambda + \frac{\partial w}{\partial y} \sin \Lambda \right)$$

$$- \bar{N}_x \frac{\partial^2 w}{\partial x^2} - \bar{N}_y \frac{\partial^2 w}{\partial y^2} - 2 \bar{N}_{xy} \frac{\partial^2 w}{\partial x \partial y} + \gamma \frac{\partial^2 w}{\partial \pi^2} = 0$$

and

$$A_{22}^* \frac{\partial^4 F}{\partial x^4} + (2 A_{12}^* + A_{66}^*) \frac{\partial^4 F}{\partial x^2 \partial y^2} + A_{11}^* \frac{\partial^4 F}{\partial y^4} \qquad (3.32)$$

$$- (2 B_{26}^* - B_{61}^*) \frac{\partial^4 w}{\partial x^3 \partial y} - (2 B_{16}^* - B_{62}^*) \frac{\partial^4 w}{\partial x \partial y^3} = 0$$

These equations are coupled and must be solved simultaneously.

Since the governing equations for angle-ply plates are coupled, all the boundary conditions given by equations (2.42) through (2.47) must be satisfied. However with some of the coefficients being zero as indicated by equations (3.29), the boundary conditions are simplified as follows:

$$w(0,y) = w(a,y) = w(x,0) = w(x,b) = 0 \qquad (3.33)$$

$$- B_{61}^* \frac{\partial^2 F}{\partial x \partial y} + D_{11}^* \frac{\partial^2 w}{\partial x^2} + D_{12}^* \frac{\partial^2 w}{\partial y^2} = 0 \text{ at } x = 0, a \qquad (3.34)$$

$$- B_{62}^* \frac{\partial^2 F}{\partial x \partial y} + D_{12}^* \frac{\partial^2 w}{\partial x^2} + D_{22}^* \frac{\partial^2 w}{\partial y^2} = 0 \text{ at } y = 0, b \qquad (3.35)$$

$$\frac{\partial^2 F}{\partial y^2} = 0 \qquad \text{at} \quad x = 0, \text{ a} \tag{3.36}$$

$$\frac{\partial F}{\partial x^2} = 0 \qquad \text{at} \quad y = 0, \text{ b} \tag{3.37}$$

$$\frac{\partial^2 F}{\partial x \partial y} = 0 \qquad \text{at} \quad x = 0, \text{ a} \tag{3.38}$$
$$\qquad\qquad\qquad\qquad y = 0, \text{ b}$$

If the functions for w and F used for the general laminated plates (section 3.1) and given by equations (3.2) and (3.3) are used, then boundary conditions (3.33), (3.34), (3.35), and (3.38) are satisfied. Boundary conditions (3.36) and (3.37) are not satisfied directly but will be shown to be satisfied indirectly by the following development. Since equations (3.36) and (3.37) are not satisfied, the terms that must be included in the extended Galerkin method are given by equations (3.7) and (3.8) and are repeated as follows:

$$\int_0^b \frac{\partial^2 F}{\partial y^2} \, \delta u^o \left. \int_0^a \right| \, dy \tag{3.7}$$

$$\int_0^a \frac{\partial^2 F}{\partial x^2} \, \delta v^o \left. \int_0^b \right| \, dx \tag{3.8}$$

Using equations (3.9), (3.10), (3.29) and (3.30), the displacements u^o and v^o are given as follows:

$$u^o = A_{11}^* \frac{\partial F}{\partial x} + A_{12}^* \int \frac{\partial^2 F}{\partial y^2} \, dx - 2 B_{16}^* \frac{\partial w}{\partial y} \tag{3.39}$$

$$v^o = A_{22}^* \int \frac{\partial^2 F}{\partial x^2} \, dy + A_{12}^* \frac{\partial F}{\partial y} - 2 B_{26}^* \frac{\partial w}{\partial x} \tag{3.40}$$

Using the assumed functions given by equations (3.2) and (3.3) in equations (3.39) and (3.40) results in zero values for u^o and v^o on the boundaries $x = 0$ and a, and $y = 0$ and b, respectively. Thus, all the boundary conditions are satisfied without using the extended Galerkin method.

Substituting the expressions for F and w given by equations (3.2) and (3.3) into equations (3.31) and (3.32) results in the following equations:

$$\sum_{m=1}^{M} \sum_{n=1}^{N} \left\{ \left[D_{11}^* \left(\frac{m\pi}{a}\right)^4 + 2 (D_{12}^* + 2 D_{66}^*) \left(\frac{m\pi}{a}\right)^2 \left(\frac{n\pi}{b}\right)^2 + D_{22}^* \left(\frac{n\pi}{b}\right)^4 \right] C_{mn} \sin\frac{m\pi x}{a}\sin\frac{n\pi y}{b} \right.$$

$$- \left[(2 B_{26}^* - B_{61}^*)\left(\frac{m\pi}{a}\right)^3\left(\frac{n\pi}{b}\right) + (2 B_{16}^* - B_{62}^*)\left(\frac{m\pi}{a}\right)\left(\frac{n\pi}{b}\right)^3 \right] H_{mn} \sin\frac{m\pi x}{a} \sin\frac{n\pi y}{b}$$

$$+ \left[\bar{N}_x \left(\frac{m\pi}{a}\right)^2 + \bar{N}_y \left(\frac{n\pi}{b}\right)^2 - \gamma\omega^2 \right] C_{mn} \sin\frac{m\pi x}{a} \sin\frac{n\pi y}{b} \tag{3.41}$$

$$- 2 C_{rs} \bar{N}_{xy} \left(\frac{m\pi}{a}\right)\left(\frac{n\pi}{b}\right) \cos\frac{n\pi y}{b} \cos\frac{m\pi x}{a} + C_{rs} \frac{2q}{\beta}\left[\left(\frac{m\pi}{a}\right) \cos\Lambda \cos\frac{m\pi x}{a} \sin\frac{n\pi y}{b} \right.$$

$$\left. + \left(\frac{n\pi}{b}\right) \sin\Lambda \sin\frac{m\pi x}{a} \cos\frac{n\pi y}{b} \right] \bigg\} = 0$$

and

$$\sum_{m=1}^{M} \sum_{n=1}^{N} \left\{ \left[A_{22}^{*} \left(\frac{m\pi}{a}\right)^{4} + (2 A_{12}^{*} + A_{66}^{*}) \left(\frac{m\pi}{a}\right)^{2} \left(\frac{n\pi}{b}\right)^{2} + A_{11}^{*} \left(\frac{n\pi}{b}\right)^{4} \right] H_{mn} \quad (3.42) \right.$$

$$\left. + \left[(2 B_{26}^{*} - B_{61}^{*}) \left(\frac{m\pi}{a}\right)^{3} \left(\frac{n\pi}{b}\right) + (2 B_{16}^{*} - B_{62}^{*}) \left(\frac{m\pi}{a}\right)\left(\frac{n\pi}{b}\right)^{3} \right] C_{mn} \right\} = 0$$

Eliminating H_{mn} between the two equations, the following expression is obtained:

$$\sum_{m=1}^{M} \sum_{n=1}^{N} C_{mn} \left\{ \left[K_{1} + \frac{K_{2}^{2}}{K_{3}} + \bar{N}_{x} \left(\frac{m\pi}{a}\right)^{2} + \bar{N}_{y} \left(\frac{n\pi}{b}\right)^{2} - \gamma\omega^{2} \right] \sin\frac{m\pi x}{a} \sin\frac{n\pi y}{b} \right.$$

$$- 2\bar{N}_{xy} \left(\frac{m\pi}{a}\right)\left(\frac{n\pi}{b}\right) \cos\frac{m\pi x}{a} \cos\frac{n\pi y}{b} + \frac{2q}{\beta} \left[\cos \Lambda\left(\frac{m\pi}{a}\right) \cos\frac{m\pi x}{a} \sin\frac{n\pi y}{b} \right. \qquad (3.43)$$

$$\left. \left. + \sin \Lambda \left(\frac{n\pi}{b}\right)\sin\frac{m\pi x}{a} \cos\frac{n\pi y}{b} \right] \right\} = 0$$

where

$$K_{1} = D_{11}^{*} \left(\frac{m\pi}{a}\right)^{4} + 2 (D_{12}^{*} + 2 D_{66}^{*}) \left(\frac{m\pi}{a}\right)^{2} \left(\frac{n\pi}{b}\right)^{2} + D_{22}^{*} \left(\frac{n\pi}{b}\right)^{4}$$

$$K_{2} = (2 B_{26}^{*} - B_{61}^{*}) \left(\frac{m\pi}{a}\right)^{3}\left(\frac{n\pi}{b}\right) + (2 B_{16}^{*} - B_{62}^{*}) \left(\frac{m\pi}{a}\right) \left(\frac{n\pi}{b}\right)^{3} \qquad (3.44)$$

$$K_{3} = A_{22}^{*} \left(\frac{m\pi}{a}\right)^{4} + (2 A_{12}^{*} + A_{66}^{*}) \left(\frac{m\pi}{a}\right)^{2}\left(\frac{n\pi}{b}\right)^{2} + A_{11}^{*} \left(\frac{m\pi}{b}\right)^{4}$$

Applying the Galerkin procedure to equation (3.43) and rearranging the terms, the following equation is obtained:

$$C_{mn}\left[\left(K_1 + \frac{K_2^2}{K_3} + \bar{N}_x \left(\frac{m\pi}{a}\right)^2 + N_y \left(\frac{n\pi}{b}\right)^2 \frac{a^4}{\pi^4 D_{11}^*} - \frac{\omega^2}{\omega_r^2}\right)\right.$$

$$+ 8 \bar{N}_{xy} \sum_{m=1}^{M} \sum_{n=1}^{N} C_{rs} \frac{mnrs}{\pi^4 D_{11}^*} \frac{a^3}{b} \frac{(1-(-1)^{r+m})(1-(-1)^{n+s})}{(r^2-m^2)(n^2-s^2)} \qquad (3.45)$$

$$\left. + \frac{2\lambda}{\pi^4}\left[\sum_{r=1}^{M} C_{rn} \cos \Lambda \frac{mr}{r^2-m^2} (1-(-1)^{r+m}) + \sum_{s=1}^{N} C_{ms} \left(\frac{a}{b}\right) \sin \Lambda \frac{ns}{(s^2-n^2)} (1-(-1)^{s+n})\right]\right] = 0$$

Equation (3.45) results in MxN homogenous equations in terms of C_{mn} and is recognized as the eigenvalue equation. Flutter solutions are obtained for equation (3.45) in the same manner as discussed in section 3.1 for general and symmetric laminated plates.

3.4 Approximate Solutions

An approximate theory (See ref. 20.) referred to as the reduced bending stiffness theory will be compared with the present analysis. In the approximate theory, the plate bending stiffness is reduced by an amount depending on the coupling between the governing equations and then the coupling is neglected when solving the equations. The reduced bending stiffness is the same as that defined by equation (2.18(c)). Thus, the governing equation for the reduced bending stiffness theory is obtained from equation (2.35) by neglecting the coupling $[B_{mn}]$ and is given as follows: ·

$$D_{11}^* \frac{\partial^4 w}{\partial x^4} + 4 D_{16}^* \frac{\partial^4 w}{\partial x^3 \partial y} + 2 (D_{12}^* + 2 D_{66}^*) \frac{\partial^4 w}{\partial x^2 \partial y^2} + 4 D_{26}^* \frac{\partial^4 w}{\partial x \partial y^3}$$

$$+ D_{22}^* \frac{\partial^4 w}{\partial y^4} - \bar{N}_x \frac{\partial^2 w}{\partial x^2} - \bar{N}_y \frac{\partial^2 w}{\partial y^2} - 2 \bar{N}_{xy} \frac{\partial^2 w}{\partial x \partial y} + \gamma \frac{\partial^2 w}{\partial t^2} = 0 \quad (3.46)$$

Since the coupling is neglected, only boundary conditions given by equations (2.42) through (2.44) with $[B_{mn}] = 0$ need to be satisfied. The boundary conditions are given as follows:

$$w(0,y) = w(a,y) = w(x,0) = w(x,b) = 0 \quad (3.47)$$

$$- D_{11}^* \frac{\partial^2 w}{\partial x^2} - D_{12}^* \frac{\partial^2 w}{\partial y^2} - 2 D_{16}^* \frac{\partial^2 w}{\partial x \partial y} = 0 \text{ at } x = 0, a \quad (3.48)$$

$$- D_{12}^* \frac{\partial^2 w}{\partial x^2} - D_{22}^* \frac{\partial^2 w}{\partial y^2} - 2 D_{26}^* \frac{\partial^2 w}{\partial x \partial y} = 0 \text{ at } y = 0,b \quad (3.49)$$

The resulting governing equation (3.46) and boundary conditions (3.47) through (3.49) are identical to those used for symmetric laminated plates (See equations (2.22) through (2.25).) except that $[D^*]$ is used instead of $[D]$. Thus, the approximate theory reduces the solution for general laminated plates to that of a symmetric plate with the bending stiffness reduced. For angle-ply plates; the D^*_{16} and D^*_{26} terms (See equation (3.29).) are zero and the approximate governing equation (3.46) and boundary conditions (3.47) through (3.49) are identical to those for classical plate theory. Thus, the reduced bending stiffness theory can be used to obtain solutions for angle-ply plates from

published classical plate theory results. Since for symmetric plates $[B_{mn}] = 0$ and $[D^*] = [D]$, the reduced bending stiffness theory and the present analysis are identical.

The advantages of using the approximate theory are evident for angle-ply plates since results can be obtained using well known published solutions. For symmetric and general laminated plates, the advantages are not so clear since a symmetric analysis similar to the one discussed in section 3.2 is necessary even to obtain approximate solutions. However, prior to the present analysis the reduced bending stiffness theory was the only solution procedure available for general laminated plates.

Chapter 4

RESULTS AND DISCUSSIONS

The equations governing the behavior of general laminated plates
have been programed for approximate solution on a digital computer.
Although the computer programs were developed largely to obtain flutter
results, natural vibration frequencies and static buckling loads may
readily be obtained using the programs. Special analysis and programs
were developed to obtain solutions for symmetric and angle-ply plates.
However, the advantages of using the special programs over the one
developed for the general laminated plates were minimal and in all cases
gave identical results.

Flutter boundaries have been calculated for symmetric, angle-ply,
and general laminated plates. The plate nomenclature and geometry are
shown in figure 8 for symmetric plates, in figure 9 for angle-ply plates,
and in figure 10 for general laminated plates. Flutter boundaries were
also obtained for an aluminum plate with one, two and four layers of
composite material applied to one or both sides of the plate as shown in
figure 11. The material properties of the individual lamina used in
making the calculations are typical of those for boron-epoxy and glass-
epoxy materials. These material properties are given in table I.
Material properties for the composite stiffened aluminum plate are given
in table II.

4.1 Convergence of Results

When using a series solution, it is important to determine that sufficient terms are used in the analysis to obtain converged results. However, using more terms than necessary results in considerably longer computation times. The usual procedure for determining convergence is to start with a small number of terms and increase the number until the solution does not change as more terms are included. For solutions obtained herein, a converged result is one which changes no more than 1 percent when more terms are included in the flutter determinant. This method of determining convergence is demonstrated in figure 12 for a four-ply, symmetric, square panel where the flutter parameter is shown as a function of the number of terms in the x-direction. Curves are shown for $\theta = 0^\circ$ and 60°, and the symbols represent the different numbers of terms used in the y-direction. For $\theta = 0^\circ$, four terms in the x-direction and only one term in the y-direction are sufficient for converged results. For $\theta = 60^\circ$, approximately six terms in both the x- and y-directions are needed to obtain results converged within 1 percent. Note that for $\theta = 60^\circ$, the converged solution is approached from higher values of λ for $m > 4$ and $n > 2$. This suggests that the cross-stiffness terms have an adverse effect on the flutter solution, a phenomena that will be discussed in a later section.

The modes that coalesce to produce flutter for $\theta = 0^\circ$ and $\theta = 60^\circ$ are shown in figures 13(a) and 13(b), respectively, where λ is shown as a function of the non-dimensional frequency squared. For both cases,

the (1,1) and (2,1) modes coalesce and result in flutter. The different numbers of terms required to obtain converged results for the two cases are due to the D_{16} and D_{26} cross-stiffness terms. For $\theta = 0^{\circ}$, the cross-stiffness terms are zero, and the plate is an orthotropic plate for which it has been shown (See ref. 40.) that only the first mode in the cross-stream direction has an effect on the flutter solutions. For $\theta = 60^{\circ}$, the cross-stiffness terms couple the modes in the x- and y-directions, and consequently, all modes effect the flutter solutions. An attempt has been made throughout the remainder of this study to insure that the values presented are converged within approximately 1 percent.

4.2 Comparison with Literature

In order to verify, as well as possible, the accuracy of the present analysis, the analysis will be used to obtain flutter data comparable with that presented in reference 19 for square symmetric plates. The material properties for the plate considered in reference 19 are given in table III. A comparison of the flutter boundaries is shown in figure 14 where λ is shown as a function of the orientation angle of the outside lamina. The dashed curves were obtained from reference 19, and the solid curves were obtained using the present analysis. Both sets of curves were calculated using only two terms in the x- and y-directions. The agreement between the two analyses is very good except for $\theta' = 0^{\circ}$ and $\theta' = 90^{\circ}$ and for θ near 90° where large discrepancies do exist. Since the present analysis uses a Galerkin method of solution and the

analysis of reference 19 uses a Rayleigh-Ritz method, the discrepancy is attributed to the difference between the two methods when an insufficient number of terms are used in the analysis to obtain converged results. For converged results, both analyses should give the same values. Converged flutter boundaries obtained using the present analysis are shown in figure 15. Although it is evident that the two-term solutions are not converged, there is still good agreement between the trends shown by the two-term and the converged analysis. For $\theta = 0^{\circ}$ or $\theta = 90^{\circ}$ and for $\theta' = 0^{\circ}$ or $\theta' = 90^{\circ}$, the present analysis should give the same results as an orthotropic analysis since the cross-stiffness terms are zero. This is shown in figure 15 where the symbols represent orthotropic results obtained from reference 31.

Although no flutter solutions were found in the literature for angle-ply or general laminated plates, some comparisons of natural frequencies for angle-ply and cross-ply plates are possible. The four lowest natural frequencies calculated using the present analysis are compared in tables IV and V with those calculated in reference 15 using a Rayleigh-Ritz method for square angle-ply and cross-ply plates, respectively. The natural frequencies calculated by the present analysis for simple supports should compare directly with those referred to in reference 15 as having hinge-free-tangential and hinge-free-normal boundary conditions, respectively, for the angle-ply and cross-ply plates. For angle-ply plates, natural frequencies are given for the principal material directions rotated at 0°, 10°, 20°, 30°, and 40° with respect to the plate axes. The agreement between the two analyses

is excellent.

For cross-ply plates, natural frequencies calculated using the two analyses are compared (See table V.), for values of E_{11}/E_{22} = 1, 10, 20, 30, and 40. The agreement between the two analyses is excellent except for the higher frequencies and high values of the ratio E_{11}/E_{22}. However, the differences are too small to be of practical significance. Since a special analysis was not made for cross-ply plates, the analysis for general laminated plates was used to obtain the natural frequencies. Thus, the assumed mode shape functions do not satisfy the boundary conditions exactly, but they are satisfied through the extended Galerkin procedure as discussed in section (3.1). The good agreement between the natural frequencies indicates the validity of using the Galerkin method to account for the boundary conditions not satisfied by the assumed mode functions.

4.3 Symmetric Plates

Flutter boundaries for symmetric plates with lamina properties typical of boron-epoxy material or a glass-epoxy material are presented in this section where λ is shown as a function of the angle that the fibers make with the x-axis. The effects of inplane norm__ and shear loads and cross-flow on the flutter of a square boron-epoxy plate composed of 4 laminas are also shown. The values of λ in each case are based on $\bar{D}_{11}$ which is the value of D_{11} with all the fibers aligned with the x-axis.

4.3.1 Flutter Boundaries

Flutter boundaries for square, symmetric, glass-epoxy and boron-epoxy plates are presented in figure 16(a), and 16(b), respectively, for plates composed of two, four, and six laminas. For square symmetric plates, the highest flutter stability is obtained with the fibers aligned with the x-axis; rotating the fibers away from the x-axis results in a continuous reduction in flutter stability for values of θ up to 90°. Flutter boundaries calculated using classical orthotropic plate theory which neglects the cross-stiffness terms D_{16} and D_{26} are seen to be inaccurate and nonconservative. Thus, inclusion of the cross-stiffness terms in the analysis has a destabilizing effect on flutter. Increasing the number of laminas composing the plate results in improved flutter stability and flutter boundaries that are closer to those given by classical plate theory. A comparison of the flutter boundaries for the glass-epoxy (See fig. 16(a).) and boron-epoxy (See fig. 16(b).) plates shows that increasing the orthotropy (for glass-epoxy material E_{11}/E_{22} = 3, and for boron-epoxy material E_{11}/E_{22} = 10) of the laminas causes the discrepancy between classical plate theory and the present analysis to be more pronounced. Also, for the more highly orthotropic material properties, orienting the fibers transverse to the flow has a larger destabilizing effect on flutter.

Flutter boundaries similar to those presented in figure 16 for a square plate are presented in figure 17 for a boron-epoxy plate with a length-width ratio of 2.0. These flutter boundaries show the solutions based upon classical plate theory to be highly nonconservative due to

the neglect of the cross-stiffness terms. For the a/b = 2.0 plate, rotation of the fibers away from the x-axis results in an increase in the flutter stability to maximum values of λ for θ of approximately 30° and 40°, respectively, for plates composed of two and four laminas. Thus, in designing composite laminated plates, proper fiber orientation is important to improved flutter stability for the plate.

4.3.2 Effect of Inplane Normal and Shear Loads

The effect of the flutter boundaries of inplane normal and shear loads for a square, symmetric, boron-epoxy panel composed of four laminas is shown in figures 18 and 19 where λ is presented as a function of the inplane load. Flutter boundaries are shown for values of $\theta = 0^\circ$, 15°, and 30°. The circle symbols indicate the point of buckling with air flow.

Inplane normal loads (See fig. 18.) result in approximately a linear reduction in flutter stability for loads up to the point of buckling. The effects of the cross-stiffness terms and rotation of the fibers away from the x-axis both result in a reduction in the flutter stability and buckling loads. Thus, classical plate theory, which neglects the cross-stiffness terms, is nonconservative in its predictions of both flutter stability and buckling loads.

Small inplane shear loads (See fig. 19.) have a stabilizing effect on flutter for $\theta = 15^\circ$ and $\theta = 30^\circ$, but larger loads decrease the flutter stability. The increase in flutter stability with small inplane shear loads is contrary to results obtained for isotropic plates (See

ref. 41.) and is due to a change in the modes that coalesce to produce
flutter. This is shown in figure 20 where coalescence of the frequencies
for $\theta = 15^O$ are shown for values of inplane shear loads $\overline{K}_{xy} = 0., .5,$
and 1.0. For $\overline{K}_{xy} = 0$ (See fig. 20(a).) and $\overline{K}_{xy} = 1.0$ (See fig. 20(c).),
the two lowest frequencies which correspond to the (1,1) and (1,2) modes
coalesce and result in flutter. However, for a small inplane shear load
$\widetilde{K}_{xy}$ of 0.5 (See fig. 20(b).), the lowest frequency and one of the higher
frequencies, which correspond to the (1,1) and (2,1) modes, coalesce to
produce flutter. For $\overline{K}_{xy}$ greater than 1.0, the (1,1) and (1,2) mode
continue to coalesce to produce flutter but at lower values of λ (See
fig. 19.). The cross-stiffness terms and rotating the fibers away from
the x-axis both result in increased buckling loads and in improved
flutter stability for most values of inplane shear loads. This is con-
trary to results noted for inplane normal loads. It should be noted
that at the point of buckling, the flutter values of λ for inplane
shear loads (See fig. 19.) are considerably lower than those of inplane
normal loads (See fig. 18.). This is in contrast with results presented
in reference 41 for isotropic plates.

4.3.3 Effect of Cross-flow

The effects of cross-flow on the flutter boundaries for a square,
symmetric, boron-epoxy plate composed of four laminas are shown in
figure 21. Flutter boundaries are presented for $\theta = 0^O$, 15° and 30°
where λ is shown as a function of the cross-flow angle. For $\theta = 15^O$
and $\theta = 30^O$, flow at small cross-flow angles may have a substantial

stabilizing effect on flutter. For $\theta = 15^{\circ}$, a 30 percent increase in λ may be obtained for a 10° cross-flow angle whereas larger cross-flow angles result in a reduction in flutter stability. Similar results are obtained for $\theta = 30^{\circ}$ where a 45 percent increase in λ is obtained for a cross-flow angle of 20°. This increase in the flutter stability with cross-flow angle can be explained as follows: Cross-flow is destabilizing for an orthotropic plate (See ref. 40.). Orienting the fibers at an angle with the plate axis results in the maximum bending stiffness and thus the maximum flutter resistance occurring in that direction. These factors tend to counteract each other and result in the maximum flutter stability occurring at an angle between the x-axis and the fiber directions. Note that the maximum value of λ for the cases shown are obtained at an angle approximately two-thirds of the angle Λ the fibers make with the x-axis.

For plates with the fibers aligned with the x-axis ($\theta = 0^{\circ}$), cross-flow is destabilizing, but at small cross-flow angles they have higher values of λ than plates with the fibers rotated at $\theta = 15^{\circ}$ and $\theta = 30^{\circ}$. Classical plate theory does not show any beneficial effects of cross-flow and thus, underpredicts the flutter stability for large cross-flow angles. For laminated composite plates, cross-flow may be either stabilizing or destabilizing depending on the flow angle and the orientation of the fibers. Thus, in designing composite plates that will experience cross-flow, an optimum orientation of the fibers may considerably improve the flutter stability of the plate.

4.4 Angle-ply Plates

Flutter boundaries calculated using the present analysis, classical plate theory, and reduced bending stiffness theory are presented in this section for typical angle-ply plates. The effects of inplane normal and shear loads and cross-flow on the flutter of a square boron-epoxy plate composed of four laminas are also shown. There is a bending-extensional coupling between the governing equations for an angle-ply plate which is neglected by classical plate theory. Since the cross-stiffness terms discussed in section 4.3 for symmetric plates are zero for angle-ply plates, the only difference between classical plate theory and the present analysis is due to bending-extensional coupling. The reduced bending stiffness theory accounts for the coupling in an approximate way by reducing the bending stiffness of the plate by an amount determined from the coupling terms and then neglecting the coupling in solving the equations. For $\theta = 0^{\circ}$ or $\theta = 90^{\circ}$, the coupling terms are zero, and the present analysis and the reduced bending stiffness theory become identical with classical plate theory.

4.4.1 Flutter Boundaries

Flutter boundaries for square, angle-ply plates with properties typical of a glass-epoxy and a boron-epoxy material are presented in figure 22(a) and 22(b), respectively, where λ is shown as a function of θ. Bending-extensional coupling has a large destabilizing effect on the plate composed of only two laminas, but as the number of laminas increase, the coupling effect becomes smaller, and the boundaries

approach those given by classical plate theory. The reduced bending stiffness theory gives flutter boundaries that are in good agreement with the actual boundaries even for the plate composed of only two laminas. The small errors associated with using the reduced bending stiffness theory, however, are not always conservative. Comparing the flutter boundaries for the glass-epoxy (See fig. 22(a).) and the boron-epoxy (See fig. 22(b).) plates shows that increasing the orthotropy of the laminas increases the destabilizing effect of bending-extensional coupling. The good agreement between the present analysis and the reduced bending stiffness analysis does not deteriorate as the lamina orthotropy is increased.

Flutter boundaries similar to those presented in figure 22 for a square plate are presented in figure 23 for a boron-epoxy plate with a length-width ratio of 2.0. The flutter boundaries show larger destabilizing effects due to bending-extensional coupling than found for the square plates, but increasing the number of laminas composing the plate reduces the destabilizing effects. For plates with four or more laminas, orienting the fibers at an angle with the x-axis may result in large improvements in the flutter stability with the highest flutter values being obtained at $\theta \cong 45^{\circ}$. For plates with two laminas, rotating the fibers away from the x-axis results in little or no improvement in the flutter stability. In each case, orienting the fibers transverse to the x-axis results in the most unstable condition. Good agreement is obtained between the present analysis and the reduced bending stiffness theory for all plates, but the largest discrepancy is obtained for the plate

composed of two laminas.

4.4.2 Effect of Inplane Normal and Shear Loads

The effects of inplane normal and shear loads on the flutter of square angle-ply plates are shown in figure 24(a) and 24(b), respectively. Flutter boundaries are shown for values of $\theta = 0^\circ$, 15°, and 30°. The circle symbols indicate the point of buckling with air flow. Inplane normal and shear loads result in a sharp drop in the flutter stability for loads up to the point of buckling. Bending-extensional coupling has a destabilizing effect on flutter and reduces the panel buckling loads. For plates with inplane normal loads (See fig. 24(a).), rotating the fibers away from the x-axis generally has a destabilizing effect on the flutter and reduces the buckling loads, but for plates with large inplane shear loads (See fig. 24(b).), the opposite effect occurs. However, for small values of inplane shear, rotating the fibers away from the x-axis may also be destabilizing. The reduced bending stiffness theory gives flutter boundaries that are in good agreement with the present analysis for each case shown. It should be noted that at the point of buckling, the flutter values of λ for inplane shear loads are considerably lower than those for inplane normal loads. This is in agreement with results shown for symmetric laminated plates.

4.4.3 Effect of Cross-Flow

The effect of cross-flow on the flutter boundaries for a square, angle-ply, boron-epoxy plate composed of four laminas is shown in figure

25. Flutter boundaries are presented for $\theta = 0°$, $15°$, and $30°$ where λ is shown as a function of the cross-flow angle. In each case, cross-flow and bending-extensional coupling have a large destabilizing effect on the flutter boundary. However, rotating the fibers away from the x-axis results in cross-flow having a less destabilizing effect on the flutter boundary. Thus, for angle-ply plates, aligning the plate axis with the flow results in the most stable condition, but if cross-flow is unavoidable, proper orientation of the fiber directions may reduce its destabilizing effects. For each condition shown, the reduced bending stiffness theory shows good agreement with the present analysis.

4.5 General Laminated Plates

The term "general laminated plates" as used in this study encompasses plates composed of any number of laminas, with arbitrary thickness, stacking sequence, and material properties, that satisfy the linear small deflection theory assumptions. This definition covers an infinite number of plates including the symmetric and angle-ply plates discussed in sections 4.3 and 4.4.

Flutter boundaries will be shown for two square, boron-epoxy panels that are composed of four laminas stacked in the sequence shown in figure 10 and designated as P-1 and P-2. In addition, flutter boundaries will be calculated for six square, composite-stiffened aluminum plates configured as shown in figure 11. The flutter boundaries calculated for plates P- and P-2 using the present analysis will be compared with those calculated using classical plate theory, and reduced bending

stiffness theory and with those presented for the symmetric and angle-ply plates in sections 4.3 and 4.4. The difference between the present analysis and classical plate theory for general laminated plates is due to both cross-stiffness terms and bending-extensional coupling.

4.5.1 Flutter Boundaries

Flutter boundaries calculated using the present analysis are compared with those calculated using classical plate theory and reduced bending stiffness theory in figure 26(a) and 26(b), respectively, for plates P-1 and P-2. The bending-extensional coupling and cross-stiffness terms have a large influence on the flutter boundary for both plates and render the classical plate theory highly nonconservative. For these cases, neglecting the coupling and cross-stiffness terms may result in flutter values that are close to 100 percent too high. However, flutter boundaries calculated using the reduced bending stiffness theory show good agreement with the present analysis. The agreement is slightly better for plate P-1 than for P-2. This is expected since plate P-1 is more nearly symmetric and thus, the coupling effect is smaller than for plate P-2.

4.5.2 Effect of Plate Construction

Flutter boundaries for plates P-1 and P-2 are compared in figure 27 with those obtained for the symmetric and angle-ply plates. The curves shown represent flutter boundaries for six plates, all of which are composed of the same material and have the same thickness but which have different flutter characteristics as a result of the number of layers

and the sequence in which they are laminated. Although the flutter boundaries for all the plates follow the same basic trends with θ, the angle-ply plate with $K = 4$ shows considerably more resistance to flutter than any of the other plate constructions. The symmetric plate with $K = 4$ shows the next best resistance to flutter followed by the general laminated plates P-1 and P-2 which have similar flutter boundaries. The symmetric and angle-ply plates with $K = 2$ show the lowest values of λ, which are as much as 40 percent lower than the maximum values obtained for the angle-ply plate with $K = 4$. Thus, improvements in the flutter stability are obtained by increasing the number of laminas and stacking them in an angle-ply sequence.

The effects of cross-flow on the flutter boundaries for the general laminated plates may be seen in figure 28 where λ is plotted as a function of the cross-flow angle. The flutter boundaries for the symmetric and angle-ply plates with $K = 4$ are also shown for comparison. For the general laminated plates, cross-flow at small angles slightly improve the flutter stability. For plate P-1, cross-flow at angles greater than 20° and for plate P-2, cross-flow at angles greater than 5° each results in a steady decrease in flutter stability. Similar results are obtained for the symmetric plate where large improvements in the flutter stability are obtained for cross-flow angles up to 10°. However, for the angle-ply plate, even a small amount of cross-flow results in a reduction in flutter stability. Although it was pointed out previously that for no cross-flow, the angle-ply construction is the most resistant to flutter, the presence of cross-flow may result in the symmetric construction giving better

flutter stability. Thus, in designing laminated plates, the stacking sequence may have a significant effect on the flutter stability.

4.5.3 Composite Stiffened Aluminum Plates

Flutter boundaries are presented in figure 29 for six square, composite stiffened aluminum plates constructed as shown in figure 11 and with material properties as given in table II. Two of the plates are of symmetric construction witn one or two layers of composite material applied to each side of the aluminum. The other four plates are of unsymmetric construction with one and two layers of composite material applied to one or both sides of the aluminum. In each case, 50 percent of the plate mass is composed of composite materials, and the only difference between the plates is the way in which the composite material is applied. The flutter boundaries for the composite stiffened plate are compared with the flutter boundary for an equal mass aluminum plate. The values of λ shown in figure 29 are based on D_{11} of the aluminum plate so that the relative advantages of the various constructions may be seen.

The composite stiffened aluminum plates have considerably higher flutter stability than the aluminum plate. For small values of θ, aluminum plates with laminas on both sides of the plate have values of λ that are 50 percent higher than those obtained for plates with the laminas only on one side and over three times those for the aluminum plate. However, for increasing values of θ, the values of λ decrease until little or no improvement in stability is obtained by using the

composite material. For values of θ between 0° and 90°, increasing the number of layers of composite material also increases the flutter stability.

These results show that composite materials may be used very effectively to increase the flutter stability of an isotropic plate. For square plates, aligning the fibers with the plate axis and applying the composite material symmetrically about the midplane of the plate both result in improved flutter stability. If the fibers are rotated with respect to the plate axis, increasing the number of laminas also increases the flutter stability.

Chapter 5

CONCLUDING REMARKS AND RECOMMENDATIONS

For general laminated plates, the bending and extensional governing equations are coupled and have cross-stiffness terms which are not included in classical orthotropic plate theory. The coupling and cross-stiffness terms occur as a result of the lamina principal directions not coinciding with the plate axis. These additional terms and the coupling increase the difficulty of obtaining solutions. However, a solution procedure has been developed using linear small deflection theory for the flutter of arbitrarily laminated simply supported plates. The extended Galerkin method is used to obtain solutions to the governing equations, and the aerodynamic pressure loading used in the analysis is that given by linear piston theory with flow at arbitrary cross-flow angles.

Flutter solutions were obtained for typical symmetric, angle-ply, and general laminated composite plates, and a limited parametric study was conducted. The parameters studied include the number, orientation, and orthotropy of the lamina; the plate length-width ratio; the inplane normal and shear loads; and the cross-flow angle. In addition, flutter solutions for several composite stiffened aluminum plate designs were obtained to determine the most flutter resistant design.

The bending-extensional coupling and the cross-stiffness terms both have a large destabilizing effect on the flutter of unstressed laminated plates, but increasing the number of laminas, reducing the lamina

69

orthotropy, and stacking the laminas in the "best" order reduce the de-
stabilizing effect. For a square plate, aligning the fibers with the
x-axis results in the highest flutter stability, but for a plate with a
length-width ratio of 2.0, large improvements in flutter stability may
be obtained by rotating the fibers away from the x-axis. For angle-ply
plates, inplane normal and shear loads and cross-flow have a destabiliz-
ing effect on flutter similar to that obtained for orthotropic plates.
However, for symmetric plates with the fibers not aligned with the
x-axis, the cross-stiffness terms result in small inplane shear loads
and cross-flow angles improving the flutter stability. Flutter calcula-
tions for equivalent symmetric, angle-ply, and general unsymmetric
plates indicate that for no cross-flow and no inplane shear loads,
plates with an angle-ply construction will have the highest flutter
stability. If cross-flow or inplane shear loads are present, symmetric-
ally constructed plates may have higher flutter stability.

Since classical plate theory does not consider bending-extensional
coupling and cross-stiffness terms, it gives inaccurate and usually non-
conservative flutter boundaries for laminated plates. Reduced bending
stiffness theory, an approximate flutter theory which accounts for the
coupling by reducing the plate bending stiffness as determined by the
coupling terms and then neglects the coupling in solving the equations,
gives flutter solutions that are adequate for all plates for which numer-
ical results were obtained. For angle-ply plates, reduced bending stiff-
ness theory results are obtained using published classical orthotropic
plate theory solutions. However, for symmetric or general laminated

plates, a solution procedure similar to the present one for symmetric
plates is necessary to obtain even approximate solutions.

The flutter stability of composite stiffened aluminum plates was
considerably better than the flutter stability for an equal mass aluminum
plate. Applying the composite material to both sides of the aluminum
plate results in better flutter stability than by applying all the
material to one side of the plate. Also, if the fiber directions do not
coincide with the plate axis, increasing the number of layers of material
improves the flutter stability.

Since only a limited parametric study was conducted in this investi-
gation, it would be beneficial to use the present analysis to conduct a
paramet.ic study in greater depth. Specifically, a wider variety of
lamina material properties should be considered and additional plates
with general unsymmetric construction should be investigated. Also, the
possible benefits of using composite materials to stiffen conventional
orthotropic and isotropic plates should be studied for several additional
plates. For all results presented, the fiber directions of the laminas
were rotated by the same absolute angle about the plate axis. Thus,
further investigations should be made into the flutter characteri ics
for laminated plates in which the fiber directions of the individual
lamina are rotated independently. This becomes of special significance
for laminated plates with inplane shear or cross-flow where significant
improvements in flutter stability may be obtained by rotating the fibers
away from the plate axis.

The flutter results presented in the present analysis were obtained

for simply supported plates with free normal and tangential inplane dis-
placements. Other boundary conditions, which restrict the inplane dis-
placements have been considered in the literature for simply supported
plates and have resulted in large changes in natural frequencies. Since
changes in flutter characteristics are usually associated with changes
in the natural frequencies, the inplane boundary conditions may have a
significant effect on the flutter characteristics. Thus, an extension
of the present analysis to consider other inplane boundary conditions
would be a worthwhile endeavor.

Although the reduced bending stiffness theory adequately predicted
the flutter characteristics for all the plates studied, it was shown in
the literature not to give natural frequencies and deflections as
accurately as desired for certain plates. Thus, additional comparisons
between reduced bending stiffness theory and the present analysis are
needed for a wider range of plates. Also, since the reduced bending
stiffness theory does not account for the inplane boundary conditions,
any change in the flutter characteristics due to the changes in boundary
conditions suggested in the above paragraph would not be shown with the
reduced bending stiffness theory. These additional studies are needed
before the reduced bending stiffness theory can be used with confidence.

Since the literature survey revealed no numerical results available
for general laminated plates, a significant contribution to the litera-
ture could be made by using the present analysis to calculate the natural
vibration frequencies and the inplane normal and shear static buckling
loads for general laminated plates. Although this study has been

concerned primarily with flutter characteristics, the analysis and re-
sulting computer program can be used without modifications to perform
the indicated calculations.

REFERENCES

1. Reissner, E.; Stavsky, Y.: Bending and Stretching of Certain Types of Heterogeneous Aeolotropic Elastic Plates, Journal of Applied Mechanics, Vol. 28, No. 3, Trans. ASME, Vol. 83, Series E, September 1961, pp. 402-408.

2. Stravsky, Yehuda: Bending and Stretching of Laminated Aeolotropic Plates, Proc. ASCE, Vol. 87, No. EM6, December 1961.

3. Stravsky, Y.: Finite Deformations of a Class of Aeolotropic Plates with Material Heterogenity, Israel J. Technol. 1, 69-74 (1963).

4. Tsai, Stephen W.; Azzi, Victor D.: Strength of Laminated Composite Materials, AIAA Journal, Vol. 4, No. 2, 1965.

5. Whitney, J. M.; Leissa, A. W.: Analysis of Heterogeneous Anisotropic Plates, Journal of Applied Mechanics, Vol. 36, 1969, pp. 261-266.

6. Yang, P. Constance, Norris, Charles H.; Stavsky, Yehuda: Elastic Wave Propagation in Heterogeneous Plates, International Journal of Solids and Structures, Vol. 2, 1966, pp. 665-683.

7. Ashton, J. E.; Waddoups, M E.: Analysis of Anisotropic Plates, Journal of Composite Materials, Vol. 3, 1969, pp. 148-165.

8. Ashton, J. E.: Analysis of Anistropic Plates II, Journal of Composite Materials, Vol. 3, 1969, pp. 470-478.

9. Ashton, J. E.: Anisotropic Plate Analysis - Boundary Conditions, Journal of Composite Materials, Vol. 4, 1970, pp. 162-171.

10. Srinives, S.; Rao, A. K.: Bending, Vibration and Buckling of Simply Supported Thick Orthotropic Rectangular Plates and Laminates, International Journal of Solids and Structures, Vol. 6, 1970, pp. 1463-1481.

11. Whitney, J. M.: The Effect of Transverse Shear Deformation on the Bending of Laminated Plates, Journal of Composite Materials, Vol. 3, 1969, pp. 534-547.

12. Whitney, J. M: Bending-Extensional Coupling in Laminated Plates under Tranverse Loading, Journal of Composite Materials, Vol. 3, 1969, pp. 20-29.

13. Bert, Charles W.; Mayberry, Byron L.: Free Vibrations of Unsymmetrically Laminated Anisotropic Plates with Clamped Edges, Journal of Composite Materials, Vol. 3, 1969, pp. 282-293.

14. Whitney, J. M.: Shear Buckling of Unsymmetrical Cross-ply Plates, Journal of Composite Materials, Vol. 3, April 1969, pp. 359-363.

15. Fortier, Richard Camille: A Study into the Behavior of Unsymmetrically Layered Anisotropic Plates, Doctor's Thesis, Northeastern University, Boston, Mass. 1972.

16. Whitney, J. M.: Stress Analysis of Thick Laminated Composite and Sandwich Plates, Journal of Composite Materials, Vol. 6, 1972, pp. 426-440.

17. Smirnov, A. I.· Laminated Panel Flutter in Supersonic Flow, Izvestiya Vuz. Aviatsionnaya Tekhnika, Vol. 11, No. 2, 1968, pp. 33-38.

18. Smirnov, A. I.: Dynamic Stability and Vibrations of Sandwich Panels in a Supersonic Gas Flow, Soviet Physics-Doklady, vol. 13, No. 6, December 1968, pp. 609-612.

19. Librescu, L.; Badoiu, Tr.: Supersonic Flutter of Plane, Rectangular, Anisotropic Heterogeneous Structures, NASA TT F-15, 890, Aug. 1974.

20. Ashton, J. E.: Approximate Solutions for Unsymmetrically Laminated Plates, Journal of Composite Materials, Vol. 3, 1969, pp. 189-191.

21. Whitney, J. M.: The Effect of Boundary Conditions on the Response of Laminated Composites, Journal of Composite Materials, Vol. 4, April 1970, pp. 192-203.

22. Srinivas, S.: A Refined Analysis of Composite Laminates, Journal of Sound and Vibration, Vol. 30, No. 4, 1973, pp. 495-507.

23. Ramkumar, R. L.: Flutter Analysis of Flat Rectangular Anisotropic P ls in a High Mach Number Supersonic Flow, Master's Thesis, Virginia Polytechnic Institute and State University, Blacksburg, VA., 1974.

24. Dietz, Albert G. H.: Composite Engineering Laminates, The MIT Press, 1969.

25. Ashton, H. E.; Halpin, J. C.; Petit, P. H.: Primer on Composite Materials Analysis, Technomic Publishing Co., Inc., 1969.

26. Ashton, J. E.; Whitney, J. M.: Theory of Laminated Plates, Technomic Publishing Co., Inc., 1970.

27. Cunningham, Herbert J.: Flutter Analysis of Flat Rectangular Panels Based on Three-Dimensional Supersonic Unsteady Flow, NASA TR-256, 1967.

28. Dixon, Sidney C.: Comparison of Panel Flutter Results from Approximate Aerodynamic Theory with Results from Exact Inviscid Theory and Experiment, NASA TN D-3649, 1966.

29. Dowell, E. H.; Voss, H. M.: Theoretical and Experimental Panel Flutter Studies in the Mach Number Range 1.0 to 5.0, AIAA Journal, Vol. 3, No. 12, pp. 2292-2304.

30. Bohon, Herman L.: Flutter of Flat Rectangular Orthotropic Panels with Biaxial Loading and Arbitrary Flow Direction, NASA TN D-1949, 1963.

31. Erickson, Larry L.: Supersonic Flutter of Flat Rectangular Orthotropic Panels Elastically Restrained Against Edge Rotation, NASA TN D-3500, 1966.

32. Bohon, Herman L.; Anderson, Melvin S.: Role of Boundary Conditions on Flutter of Orthotropic Panels. AIAA Symposium on Structural Dynamics and Aeroelasticity, Aug. - Sept. 1965, pp. 59-69.

33. Dowell, E. H.: Panel Flutter: A Review of the Aeroelastic Stability of Plates and Shells, AIAA Journal, Vol. 8, No. 3, pp. 385-398.

34. Ashley, Holt; Zartarian, Garabed: Piston Theory - A New Aerodynamic Tool for the Aeroelastician, Presented at the Aeroelasticity Session, Twenty-fourth Annual Meeting, IAS, New York, Jan. 23-26, 1956.

35. Bohon, Herman L.; Anderson, Melvin S.; Heard, Walter L., Jr.: Flutter Design of Stiffened-Skin Panel for Hypersonic Aircraft, NASA TN D-5555, 1969.

36. Shore, C. P.: Effects of Structural Damping on Flutter of Stressed Panels, NASA TN D-4990, 1969.

37. Heard, Walter L., Jr.; Bohon, Herman L.: Natural Vibration and Flutter of Elastically Supported Corrugation-Stiffened Panels - Experiment and Theory, NASA TN D-5986, 1970.

38. Eisley, J. G.; Luessen, G.: Flutter of Thin Plates Under Combined Shear and Normal Edge Forces, AIAA Journal, Vol. 1, No. 2, March 1963.

39. Fung, Y. C.: Some Recent Contributions to Panel Flutter Research, Paper No. 63-26, Inst. Aerospace Sci., Jan. 1963.

40. Sawyer, James Wayne: Flutter of Elastically Supported Orthotropic Panels Including the Effects of Flow Angle, NASA TN D-7491, 1974.

41. Sawyer, James Wayne: Supersonic Flutter of Panels Loaded with
    Inplane Shear, NASA TN D-7888, 1975.

42. Dixon, Sidney C.; Hudson, M. Latrelle: Flutter, Vibration, and
    Buckling of Truncated Orthotropic Conical Shells with Generalized
    Edge Restraint, NASA TN D-5759, 1970.

43. Fung, Y. C.: Foundations of Solid Mechanics. Prentice-Hall, Inc.
    1965, pp. 338-339.

TABLE I

LAMINA MATERIAL PROPERTIES USED IN ANALYSIS

Properties	Material	
	Boron-epoxy	Glass-epoxy
E_{11}	30,000,000 psi	7,500,000 psi
E_{22}	3,000,000 psi	2,500,000 psi
G_{12}	1,000,000 psi	1,000,000 psi
ν_{12}	.30	.30

TABLE II

MATERIAL PROPERTIES FOR COMPOSITE STIFFENED

ALUMINUM PLATE

Properties	Material	
	Aluminum	Composite
E_{11}	10,000,000 psi	29,600,000 psi
E_{22}	10,000,000 psi	4,130,000 psi
G_{12}	3,850,000 psi	2,020,000 psi
ν_{12}	.30	.21

TABLE III

MATERIAL PROPERTIES OF REFERENCE PLATE

	Material	
Properties	Outside layers	Middle layers
E_{11}	E	10E
E_{22}	10E	E
G_{12}	.5E	.5E
ν_{12}	.0349	.349

TABLE IV

COMPARISON OF FOUR LOWEST NATURAL FREQUENCIES

FOR A SQUARE ANGLE-PLY PLATE ($E_{11}/E_{22} = 40$, $G_{12}/E_{22} = 1$, $\nu_{12} = .25$)

θ	$\omega a^2 \sqrt{Y/E_{22}h^3}$			
	Extended Galerkin Method			
0	19.232	24.524	36.229	54.691
10	16.615	23.584	36.471	56.045
20	14.610	24.567	40.984	46.414
30	14.377	28.170	40.452	49.336
40	14.592	32.275	36.235	58.369
	Rayleigh-Ritz Method, ref. 15			
0	19.232	24.524	36.229	54.691
10	16.615	23.584	36.471	56.045
20	14.610	24.567	40.984	46.414
30	14.377	28.170	40.452	49.336
40	14.592	32.278	36.235	58.369

TABLE V

COMPARISON OF FOUR LOWEST NATURAL FREQUENCIES

FOR A SQUARE CROSS-PLY PLATE $(G_{12}/E_{22} = .5, \nu_{12} = .25)$

E_{11}/E_{22}	$\omega a^2 \sqrt{\gamma/E_{22}h^3}$			
	Extended Galerkin Method			
1	6.155	15.148	15.148	24.619
10	7.932	21.274	21.274	31.727
20	9.152	25.136	25.136	36.608
30	10.210	28.403	28.403	40.840
40	11.164	31.312	31.312	44.656
	Rayleigh-Ritz Method, ref. 15			
1	6.155	15.148	15.148	24.619
10	7.931	21.275	21.275	31.721
20	9.152	25.135	25.135	36.601
30	10.210	28.400	28.400	40.831
40	11.163	31.308	31.308	44.646
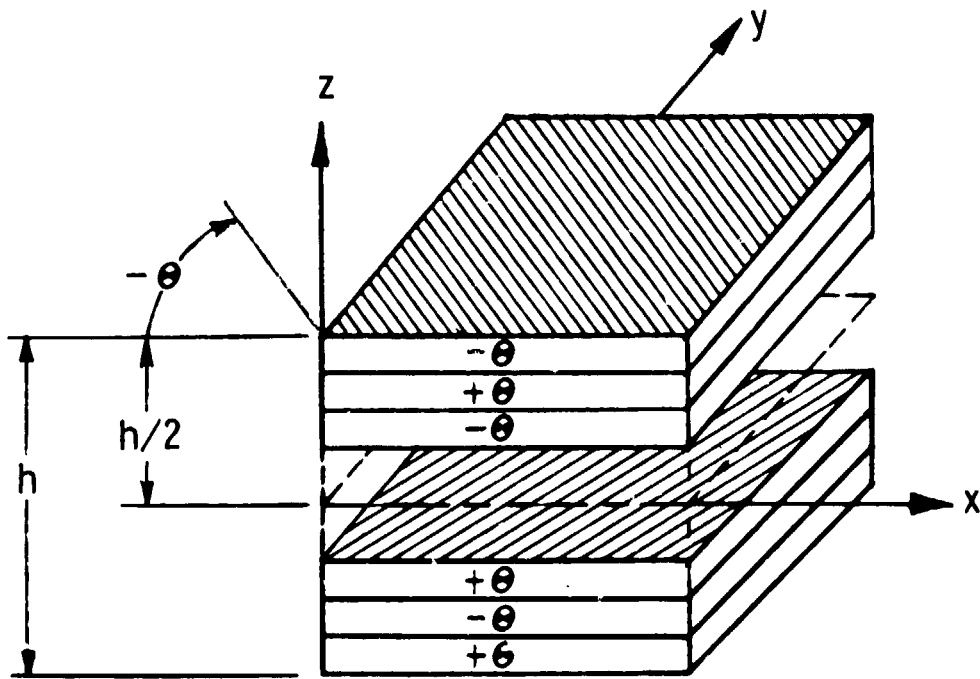
Figure 1.- Geometry of angle-ply plates.
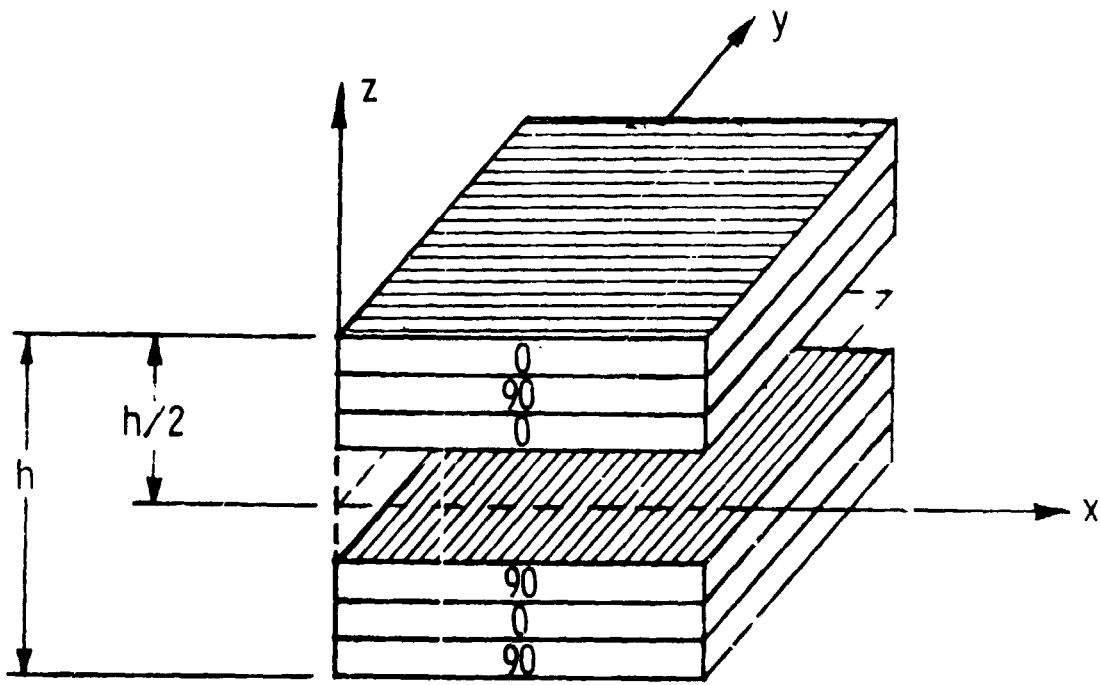
Figure ⌐ - Geometry of cross-ply plates.
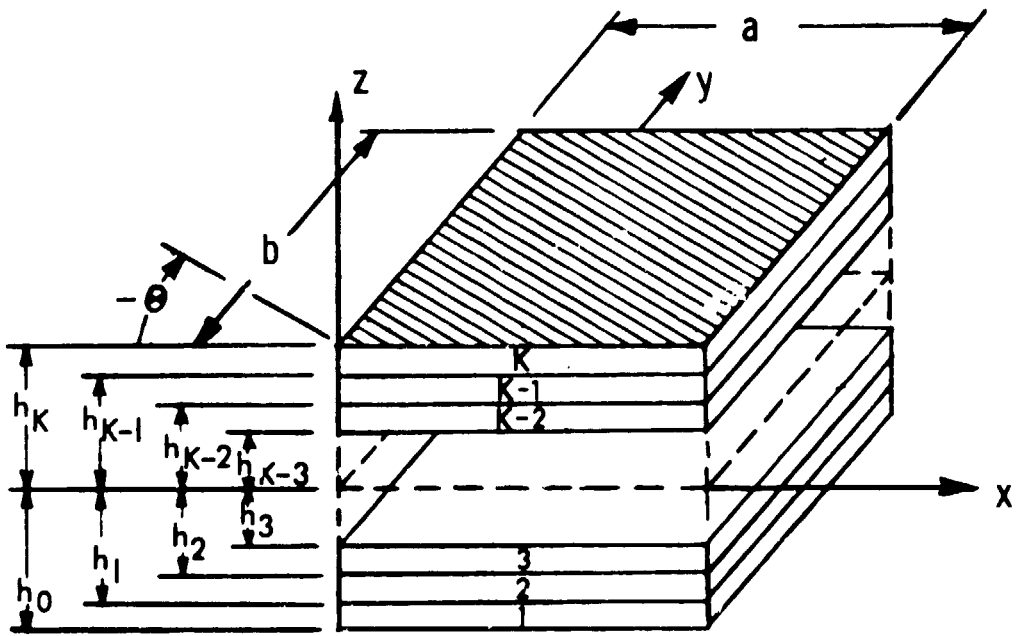
Figure 3.- Lamina coordinate system.
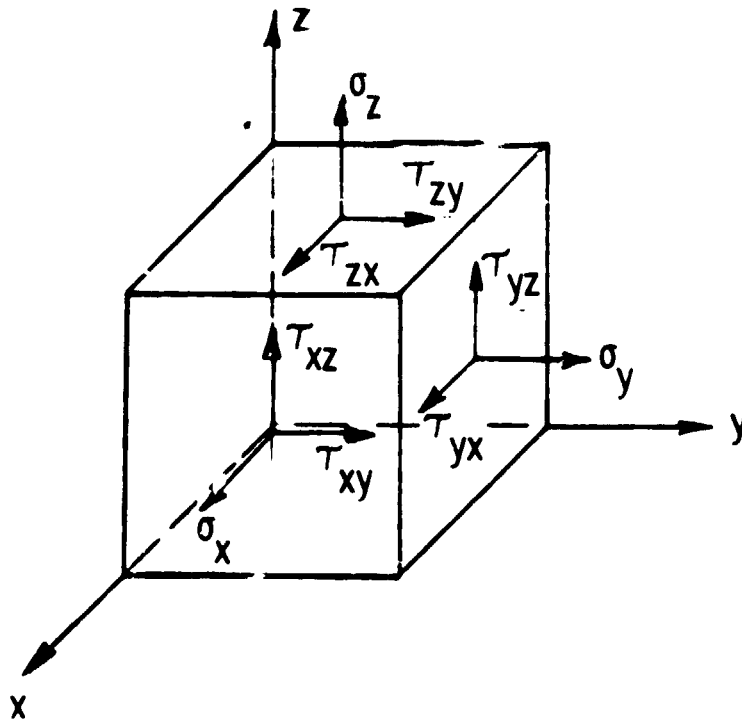
Figure 4.- Lamina notation and positive direction of stress.
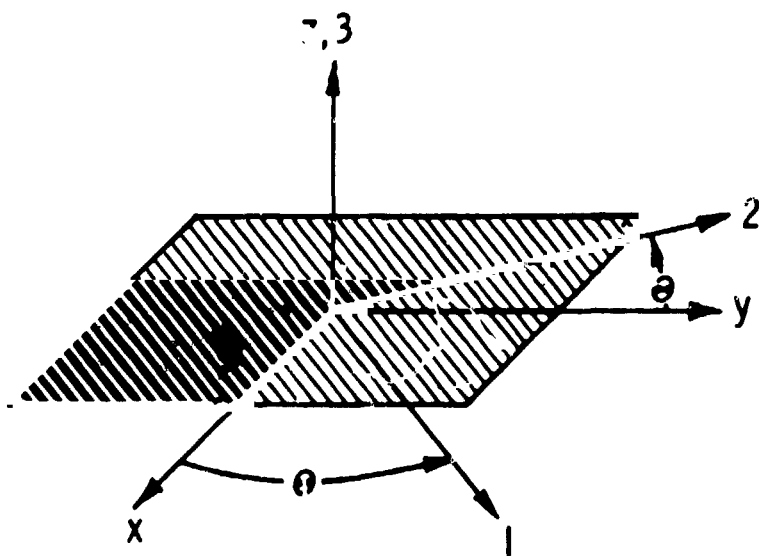
Figure 5.- Rotation of lamina axes.
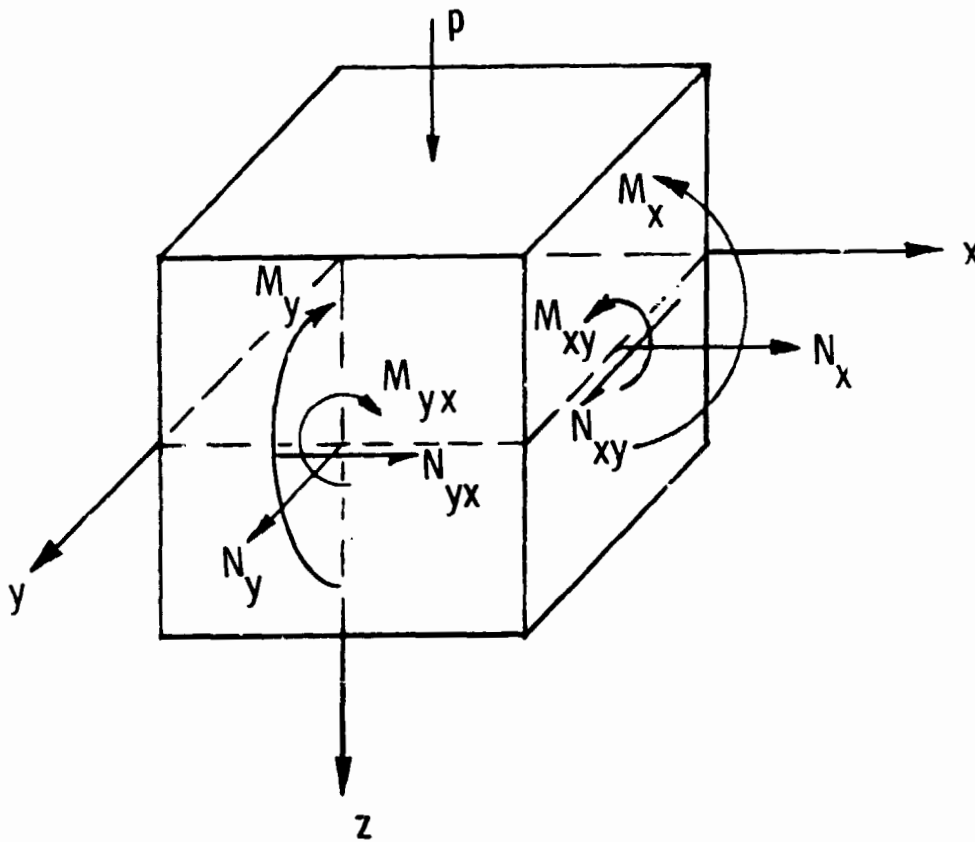
Figure 6.- Positive direction of stress and moment resultants.

C.2
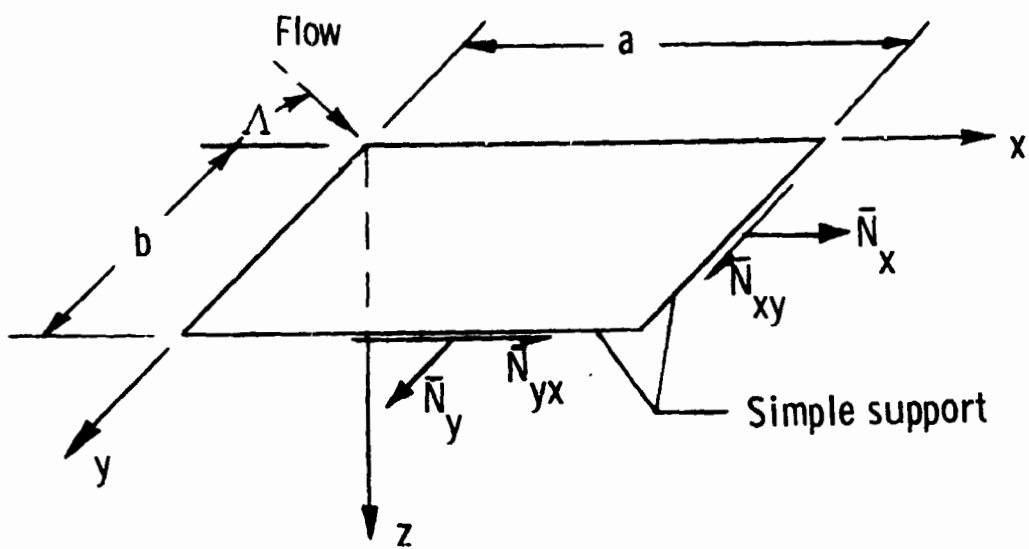
Figure 7.- Plate geometry and coordinate system.
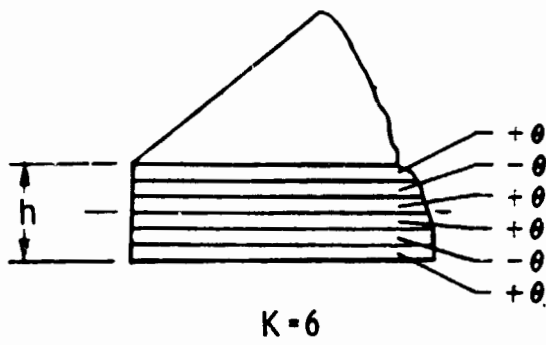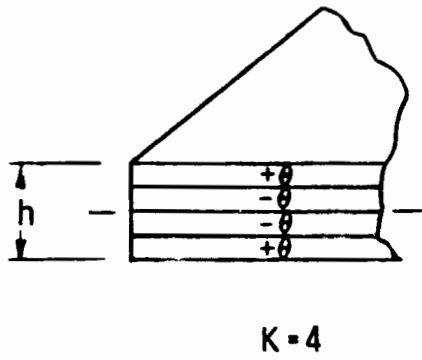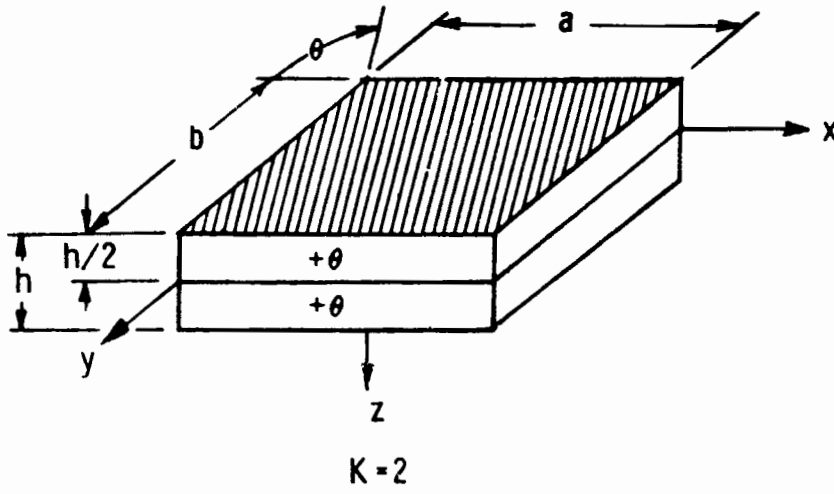
Figure 8.- Nomenclature and geometry of symmetric plates.
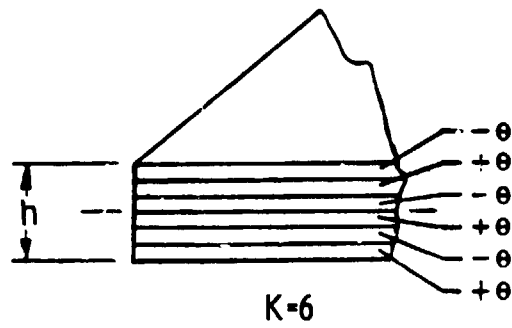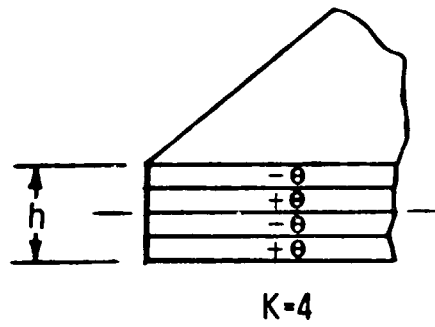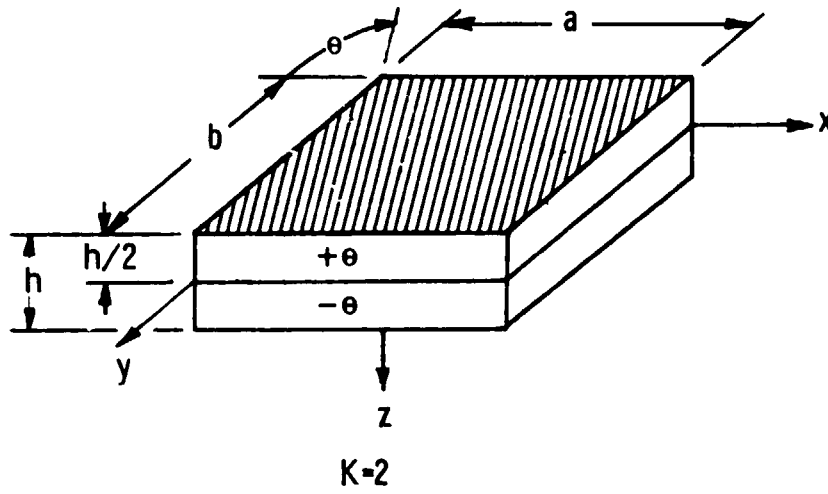
Figure 9.— Nomenclature and geometry of angle-ply plates.
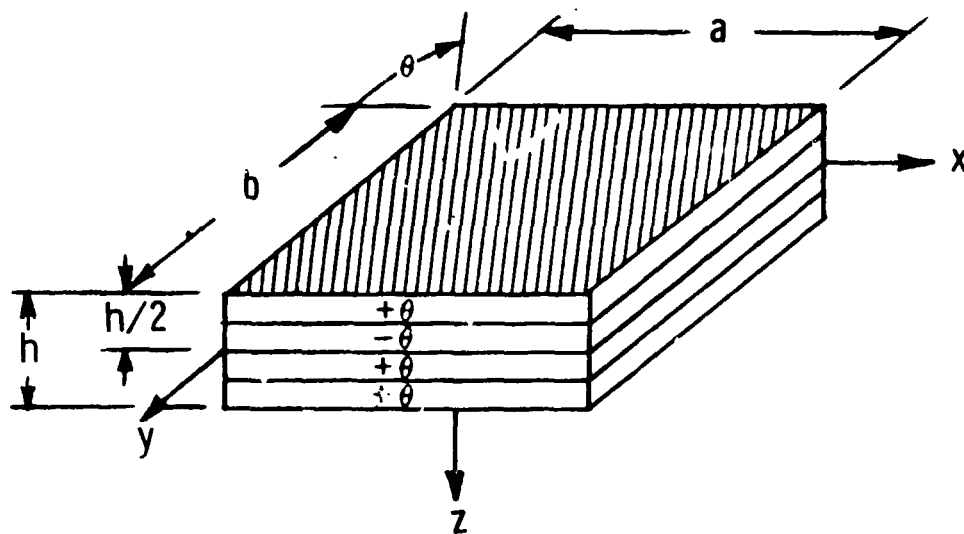
Plate P—2
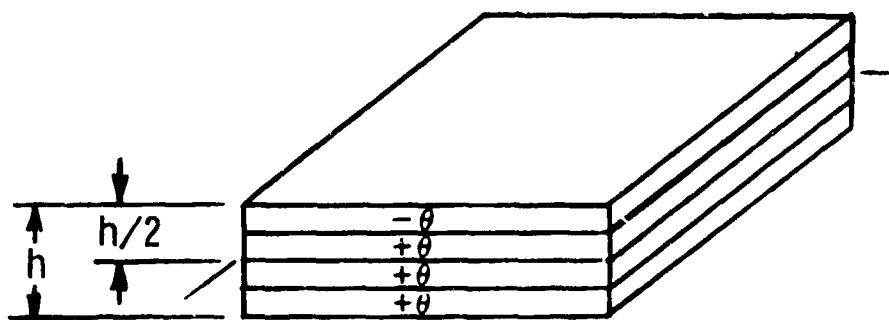
Plate P—I

Figure 10.- Nomenclature and geometry of general laminated plates.
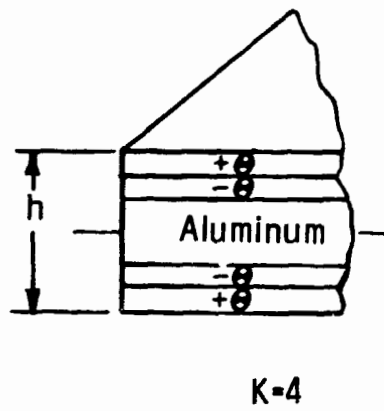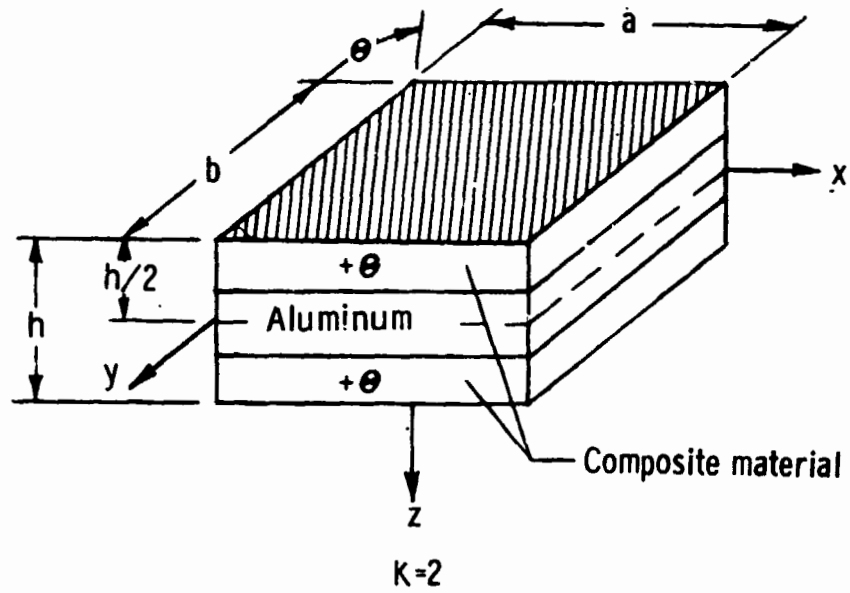
(a) Symmetric plates.

Figure 11.- Nomenclature and geometry of composite stiffened aluminum plate.
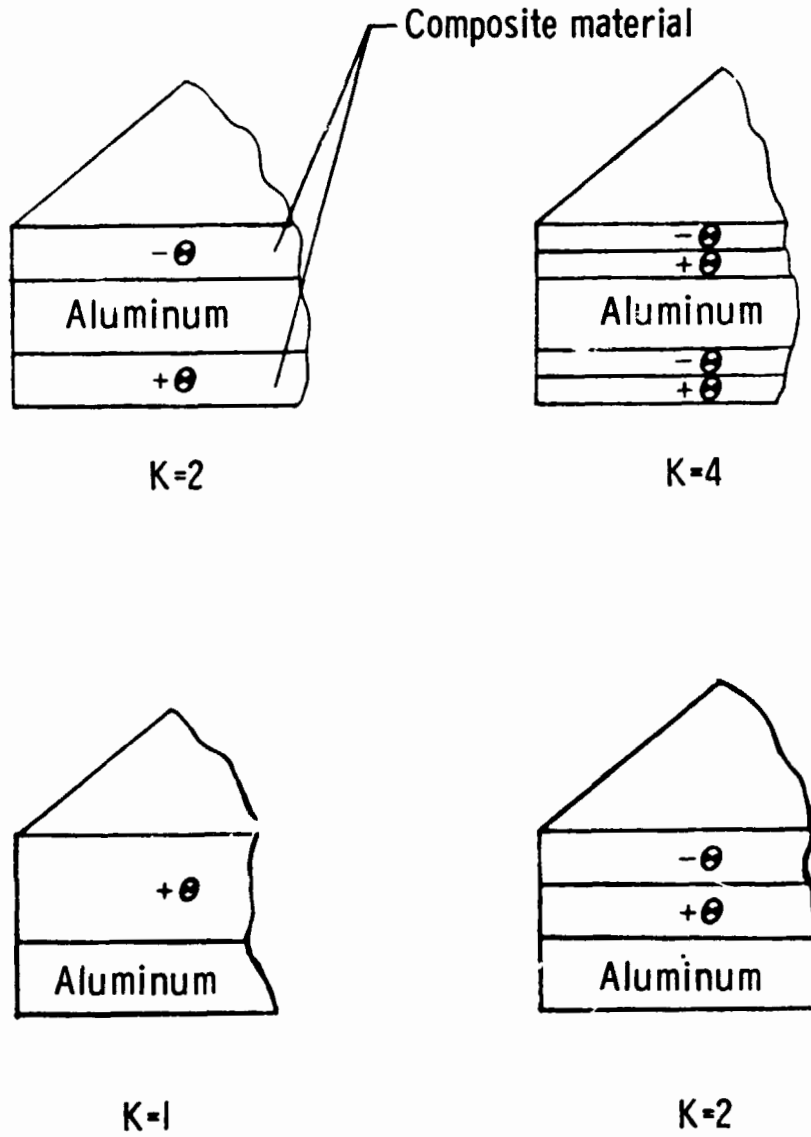
(b) Unsymmetric plates.

Figure 11.- Concluded.
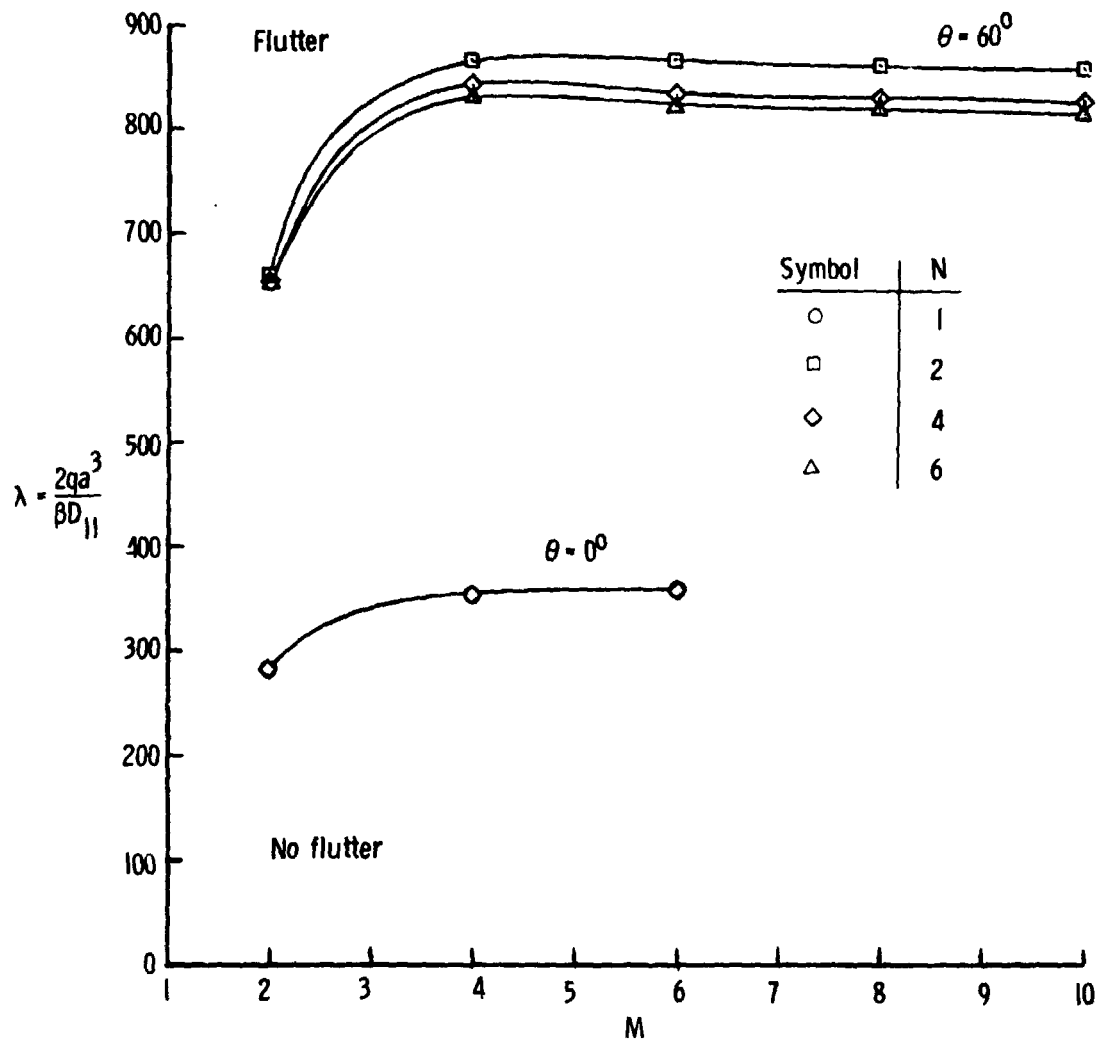
Figure 12.- Convergence of solution for a symmetric, boron-epoxy, square
plate with K = 4.
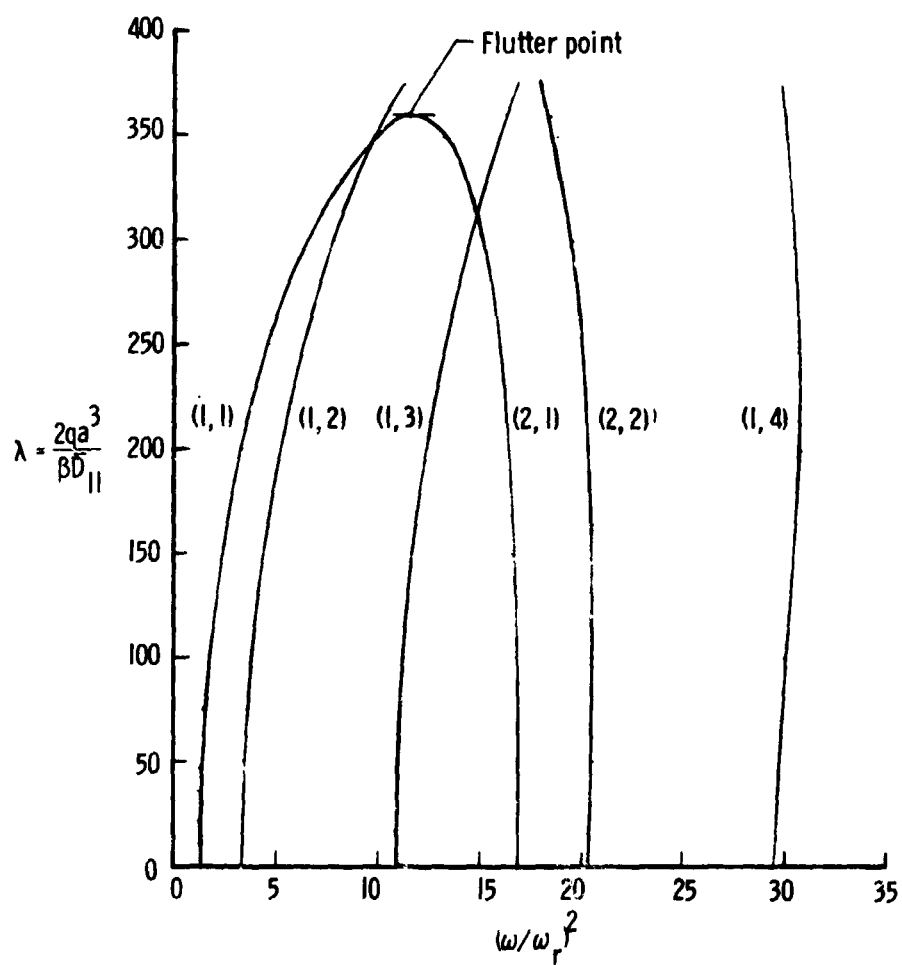
(a) $\theta = 0^\circ$.

Figure 13.- Coalescence of frequencies for a symmetric, boron-epoxy, square plate with $K = 4$.
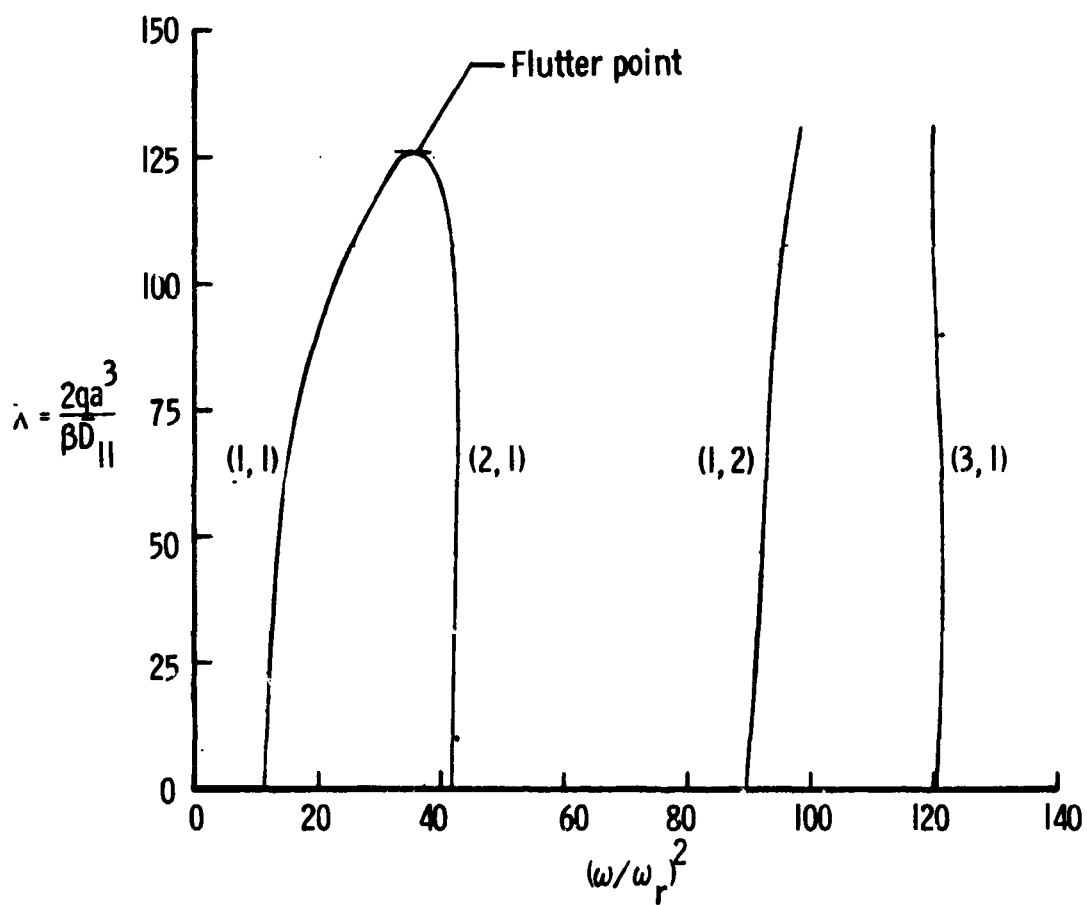
(b) $\theta = 60°$.

Figure 13.- Concluded.
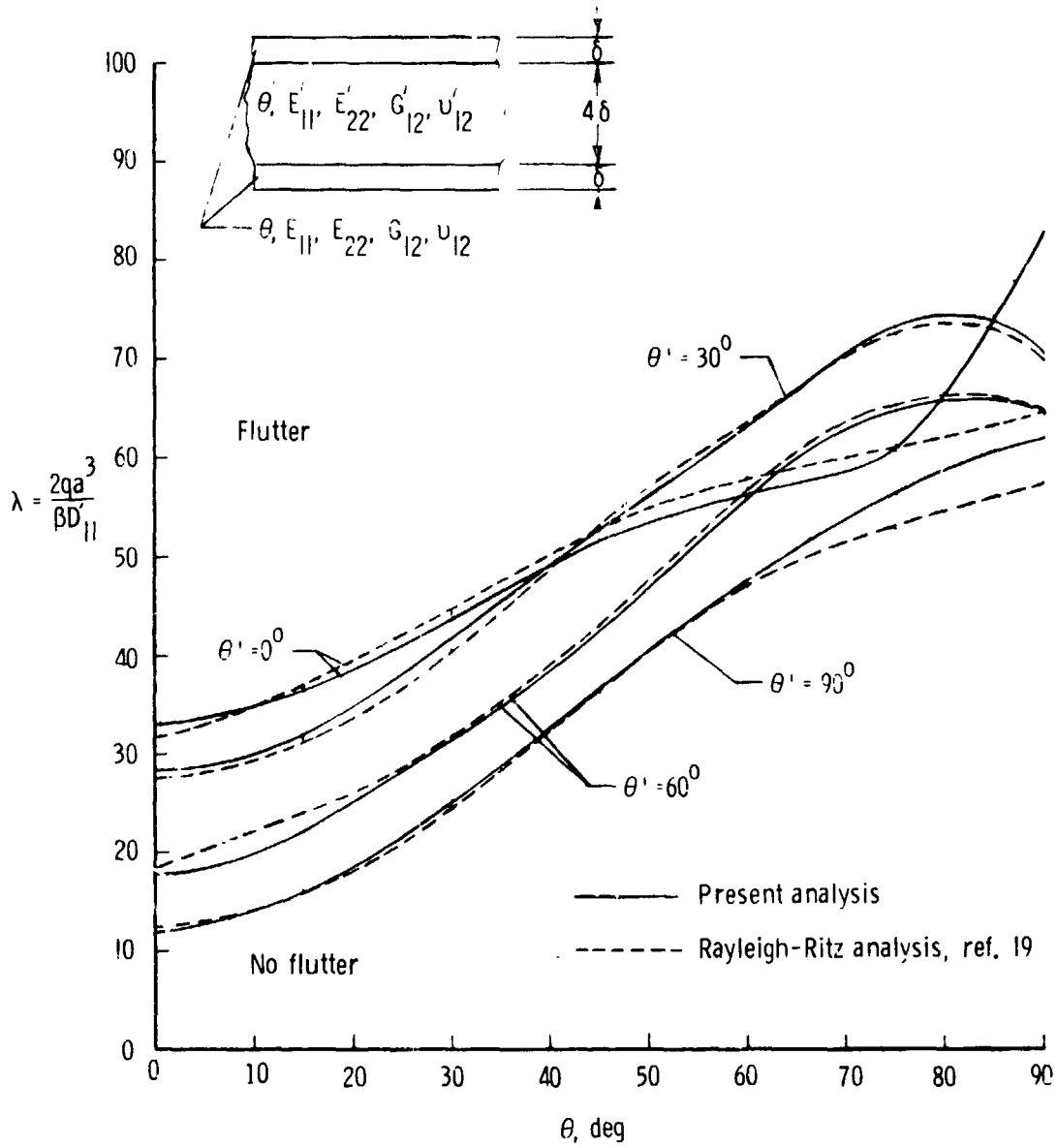
Figure 14.- Comparison of flutter solutions for square reference plate. N = M = 2.
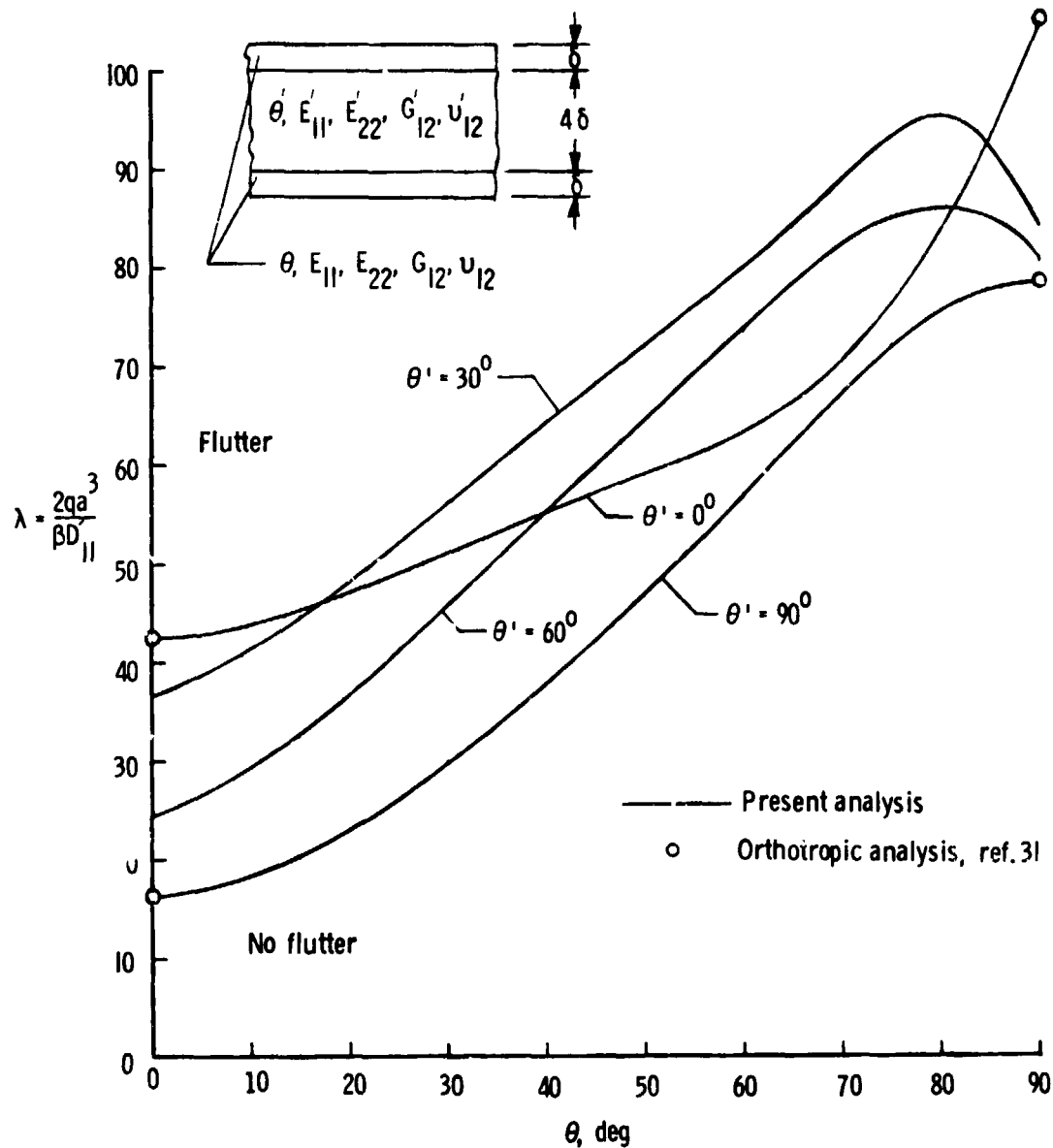
Figure 15.- Converged flutter boundaries for square reference plate.
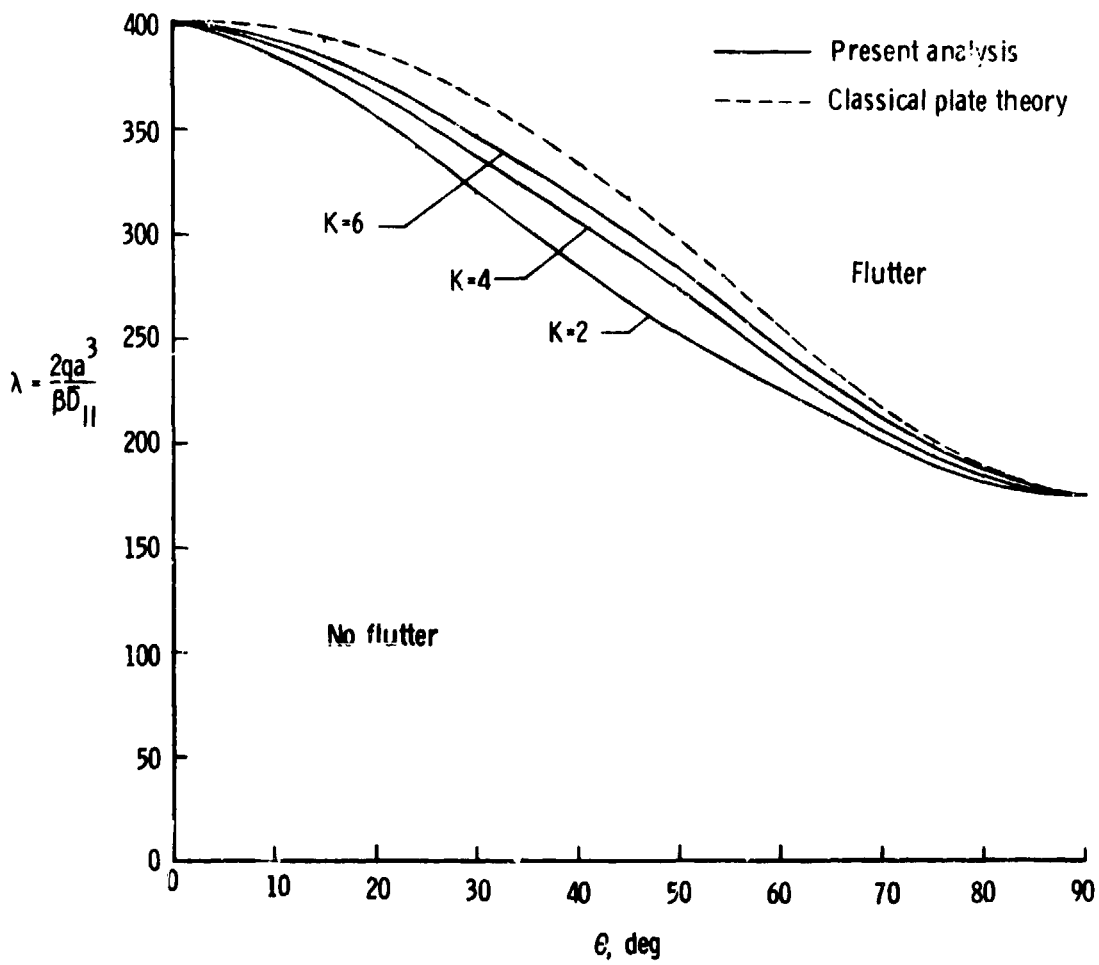
(a) Glass-epoxy plate.

Figure 16.- Flutter boundaries for square, symmetric plates.
$$\bar{N}_x = \bar{N}_y = \bar{N}_{xy} = 0.$$

The chart shows $\lambda = \frac{2qa^3}{\beta D_{11}}$ on the vertical axis (ranging from 0 to 400) versus θ, deg on the horizontal axis (0 to 90). Curves are labeled K=6, K=4, K=2. Legend: Present analysis (solid line), Classical plate theory (dashed line). Regions labeled "Flutter" and "No flutter".
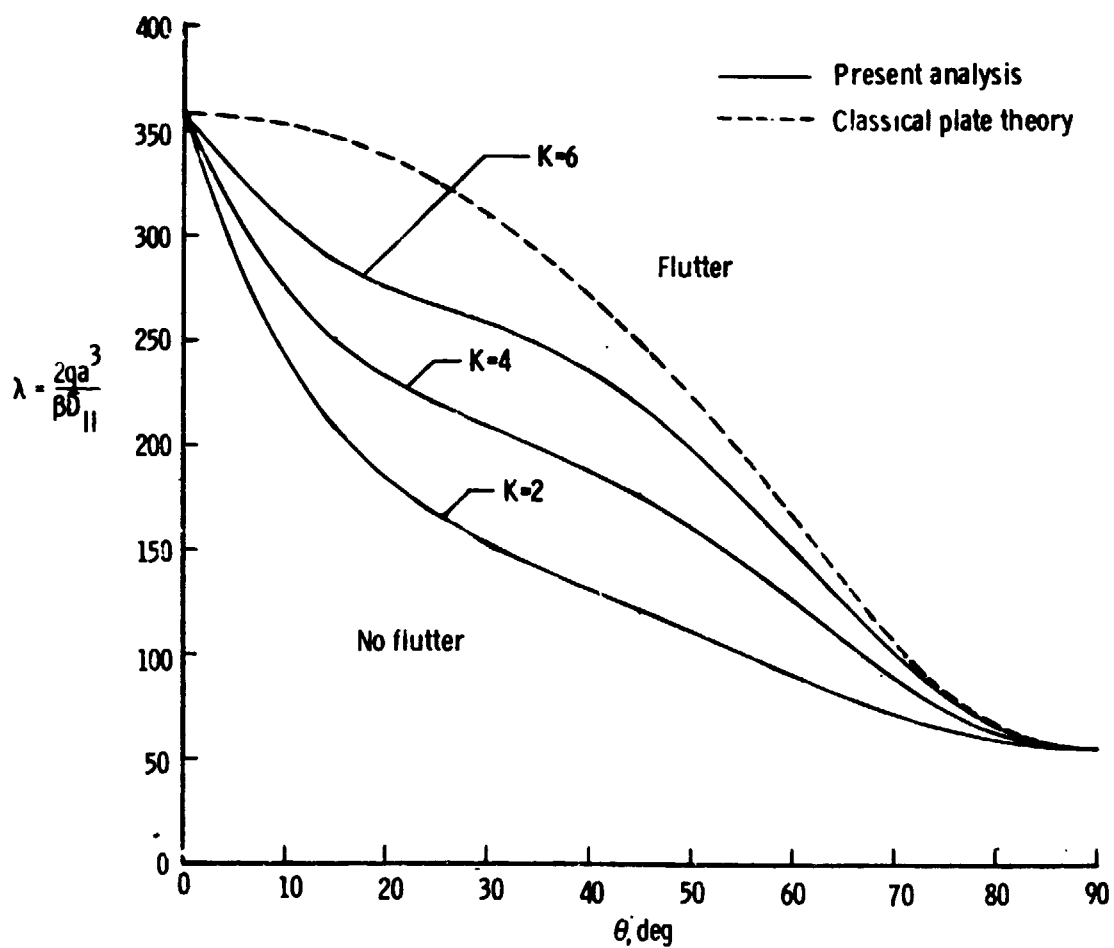
(b) Boron-epoxy plate.

Figure 16.- Concluded.
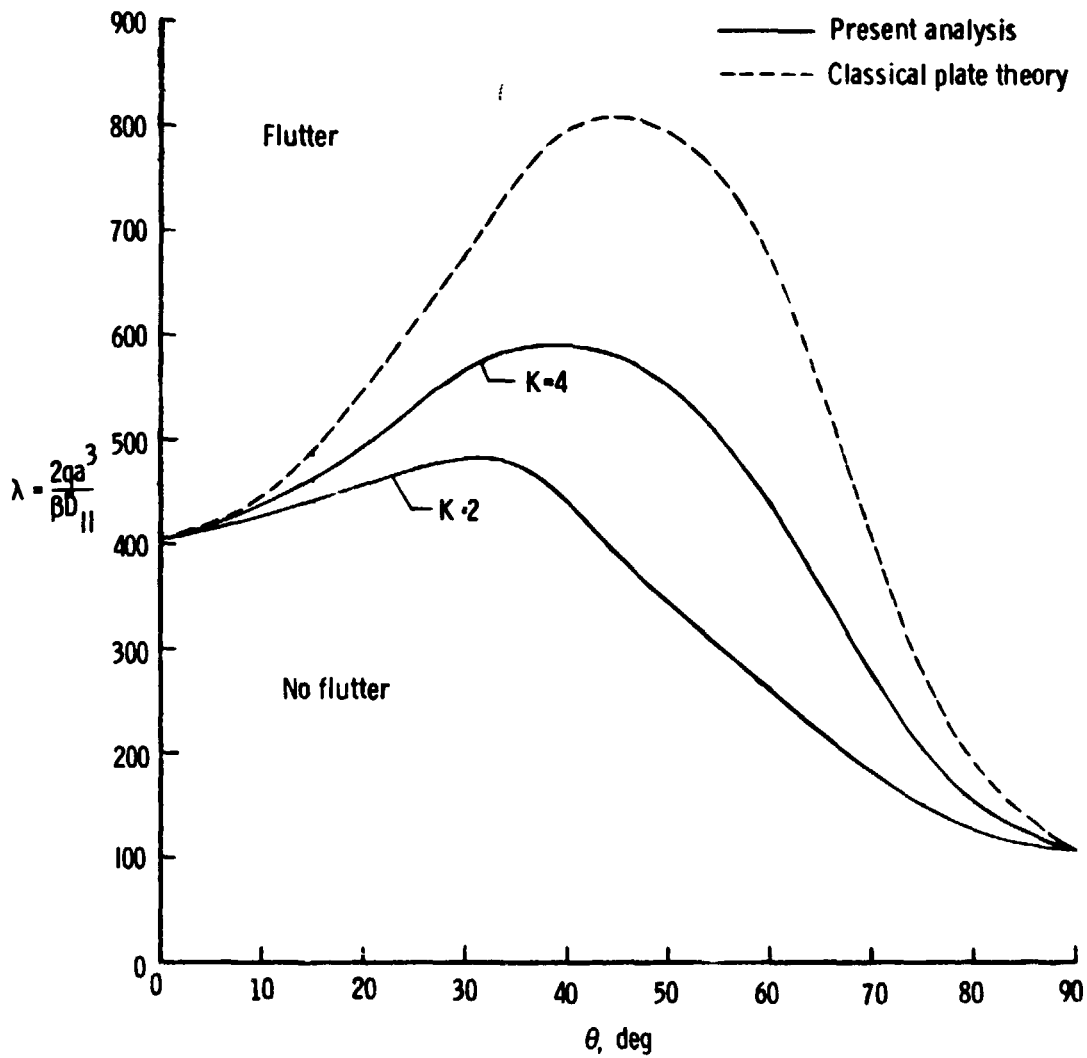
Figure 17.- Flutter boundaries for boron-epoxy, symmetric plate with
a/b = 2.0. $\bar{N}_x = \bar{N}_y = \bar{N}_{xy} = 0.$
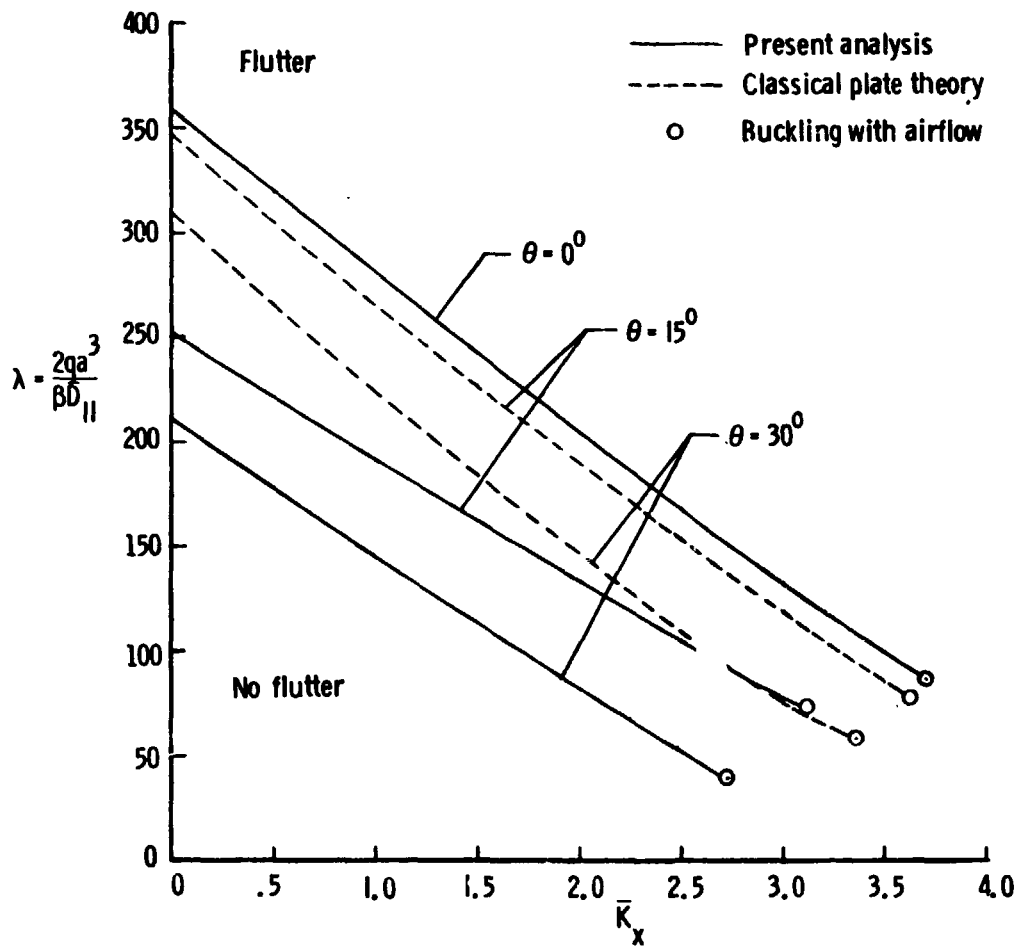
Figure 18.- Flutter boundaries for square, boron-epoxy, symmetric plate with inplane normal loads. $\bar{N}_y = \bar{N}_{xy} = 0$; $\bar{K} = 4$.
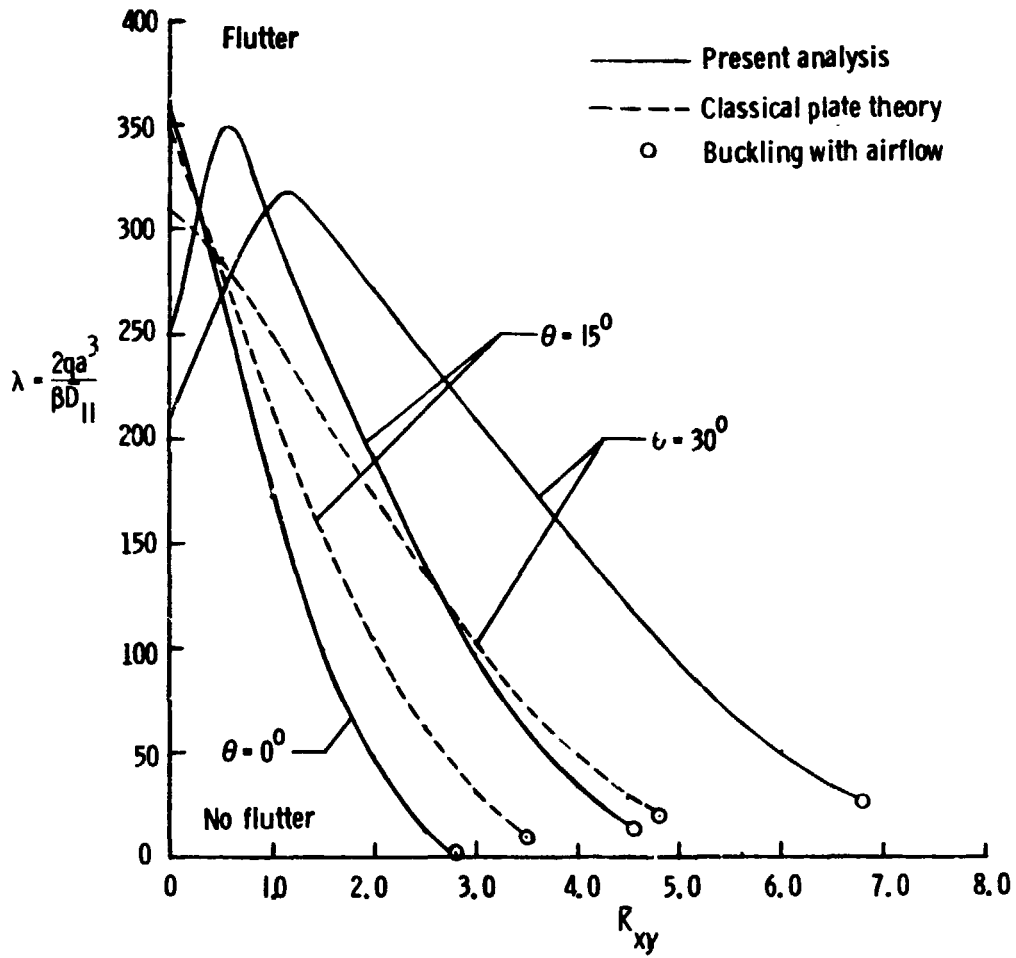
Figure 19.- Flutter boundaries for square, boron-epoxy, symmetric plate with inplane shear loads. $\bar{N}_y = \bar{N}_x = 0$; $K = 4$.
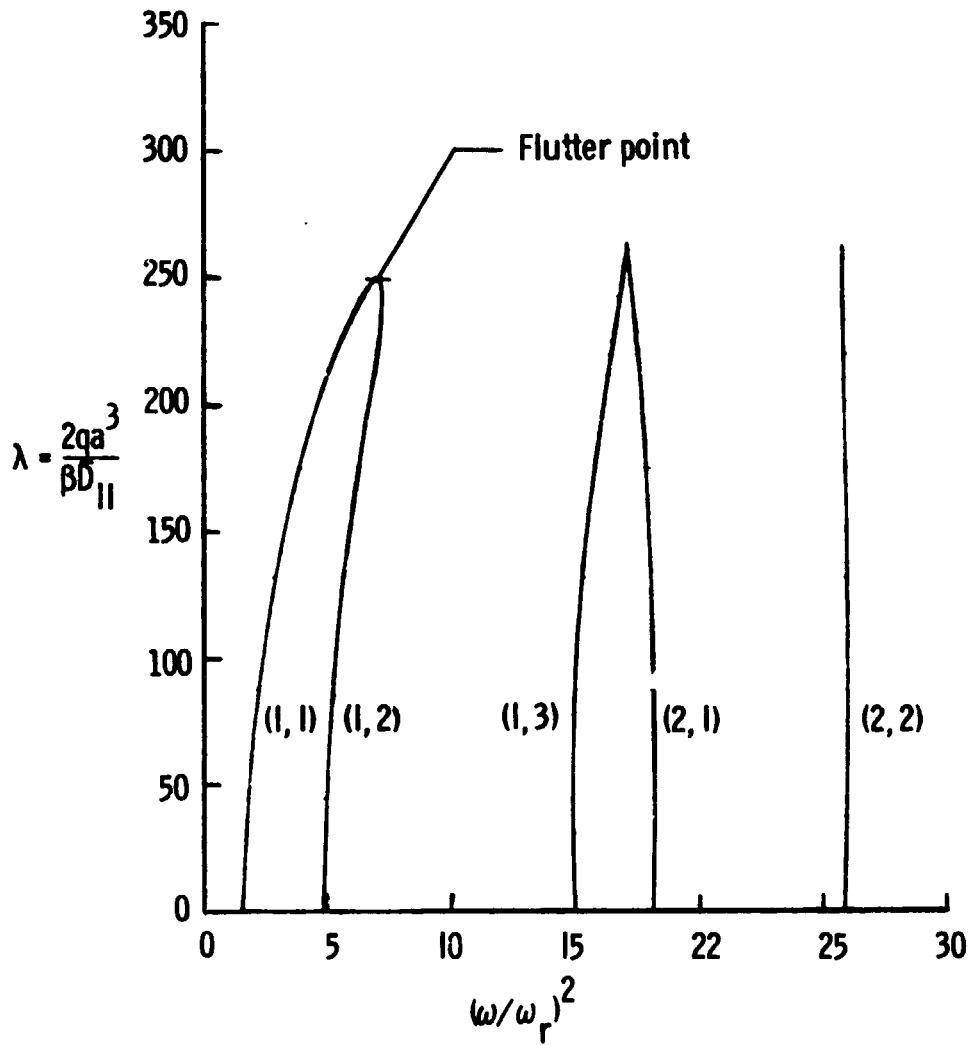
(a) $\bar{K}_{xy} = 0$.

Figure 20.- Coalescence of frequencies for a symmetric, boron-epoxy, square plate with inplane shear loads. $\bar{N}_y = \bar{N}_x = 0$; $K = 4$; and $\theta = 15^\circ$.
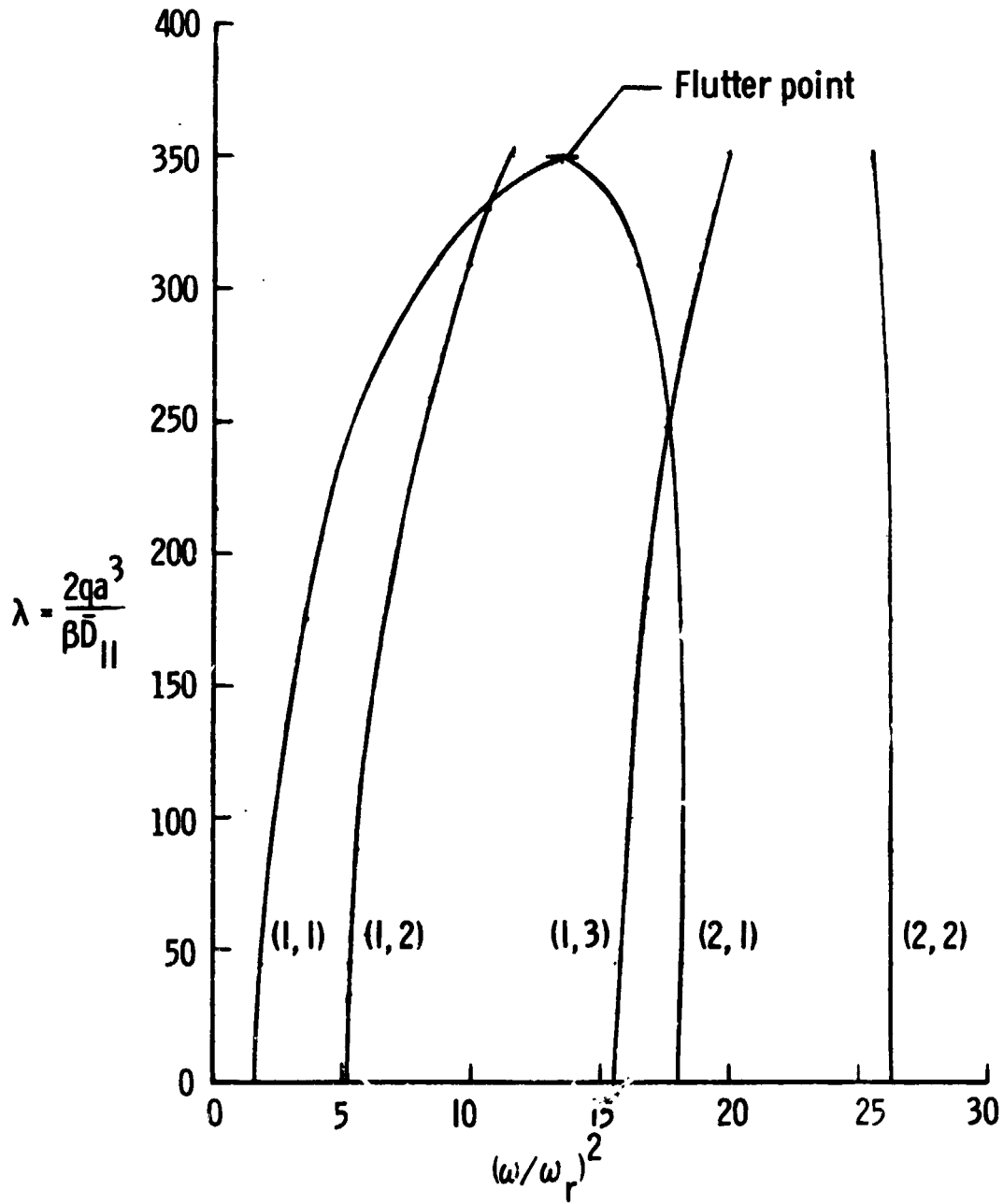
(b) $\bar{R}_{xy} = 0.5$.

Figure 20.- Continued.
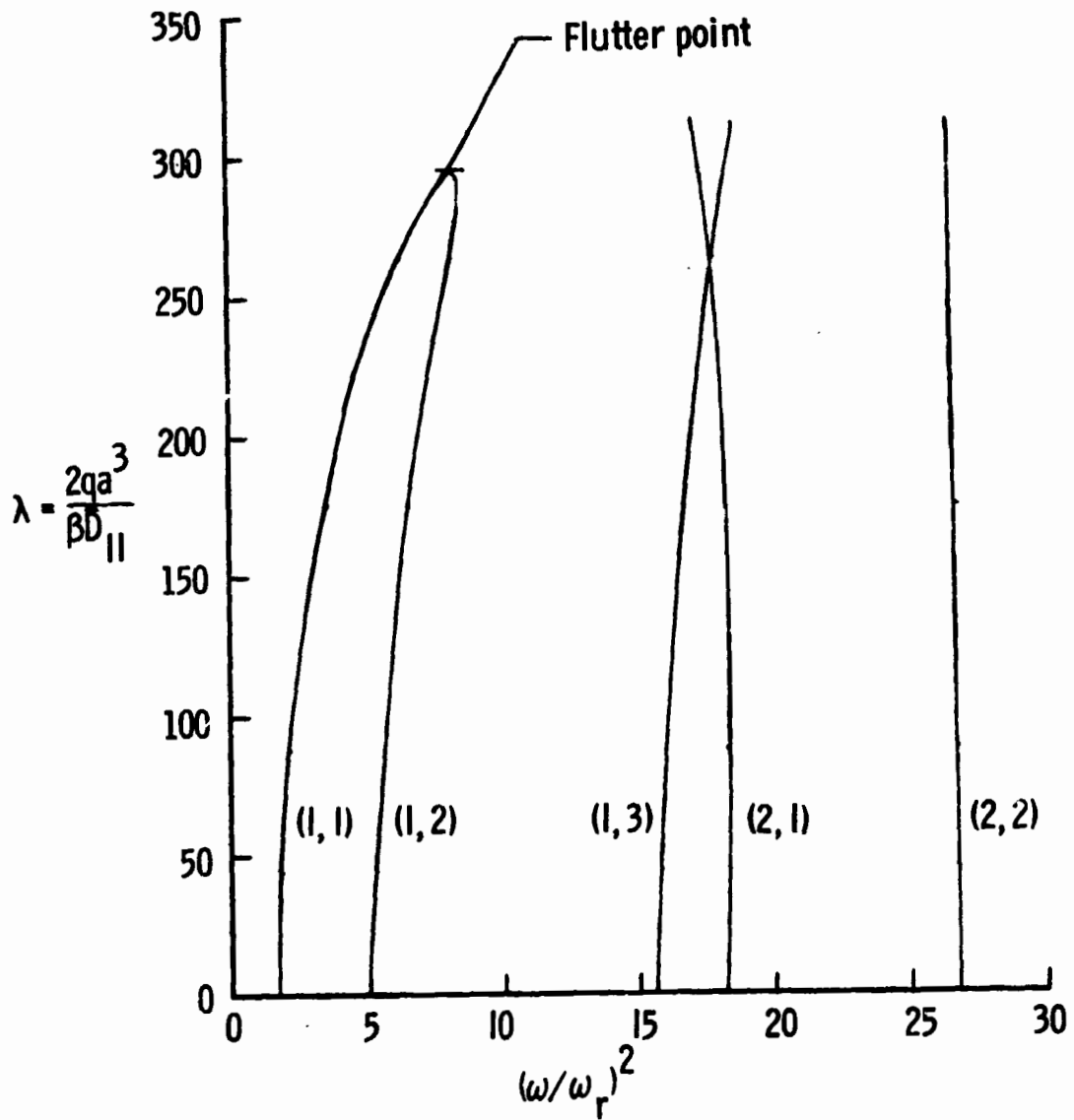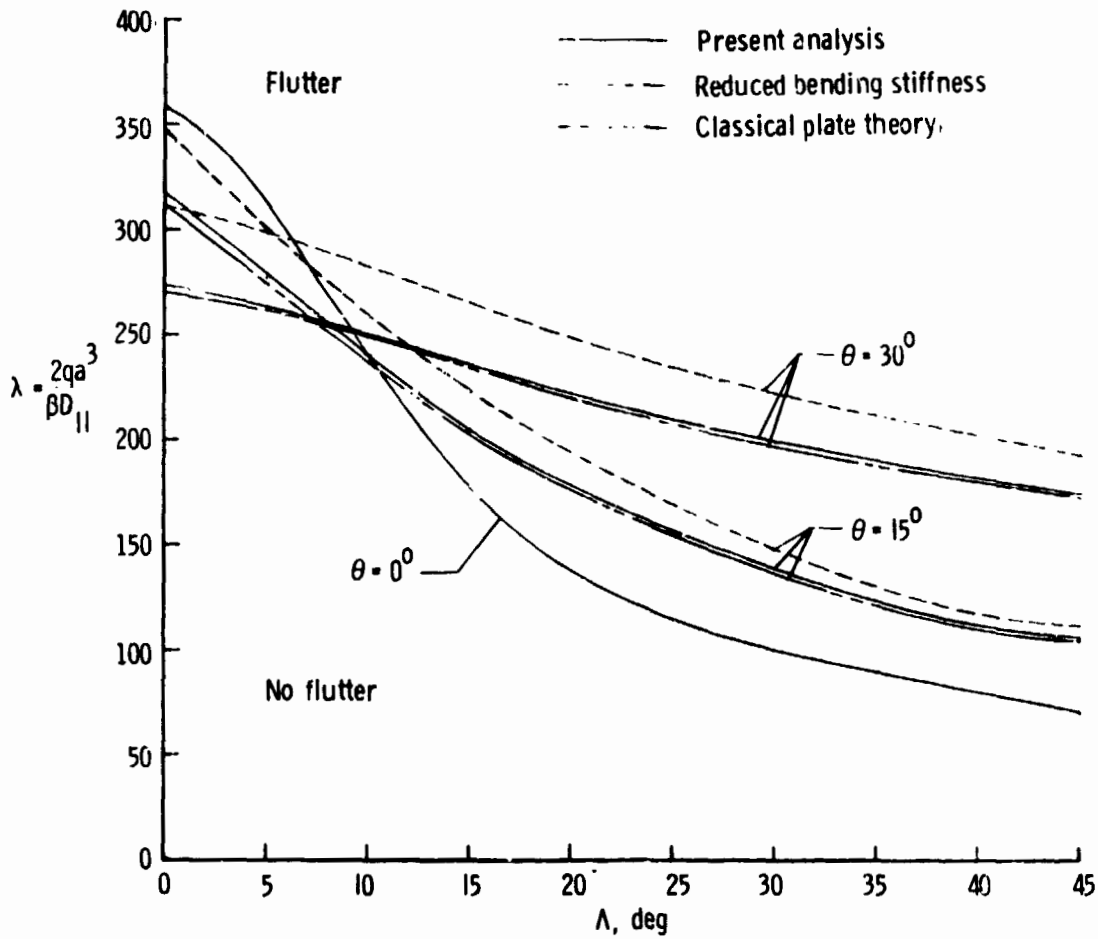
(c) $\bar{R}_{xy} = 1.0$.

Figure 20.- Concluded.
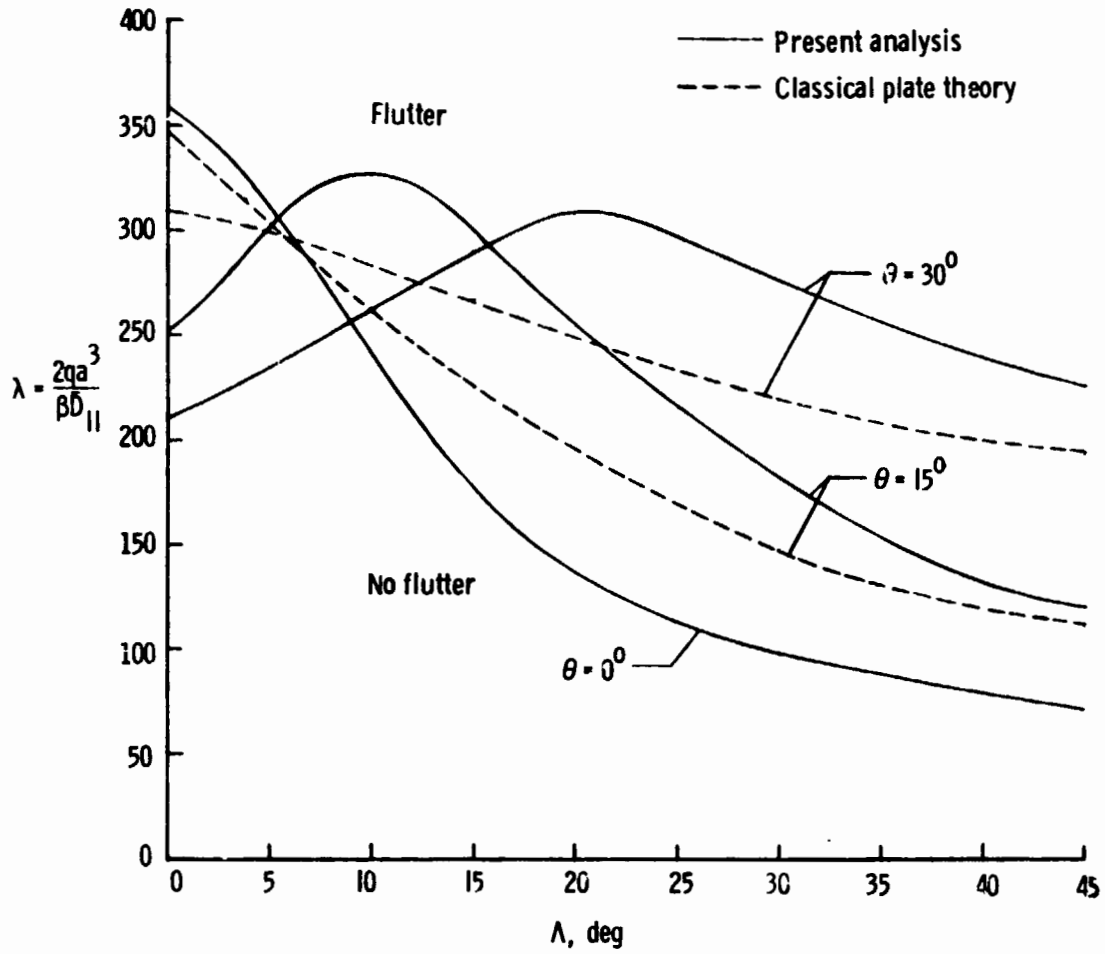
Figure 21.- Flutter boundaries for square, boron-epoxy, symmetric plate with cross flow. $\bar{N}_x = \bar{N}_y = \bar{N}_{xy} = 0$; $K = 4$.
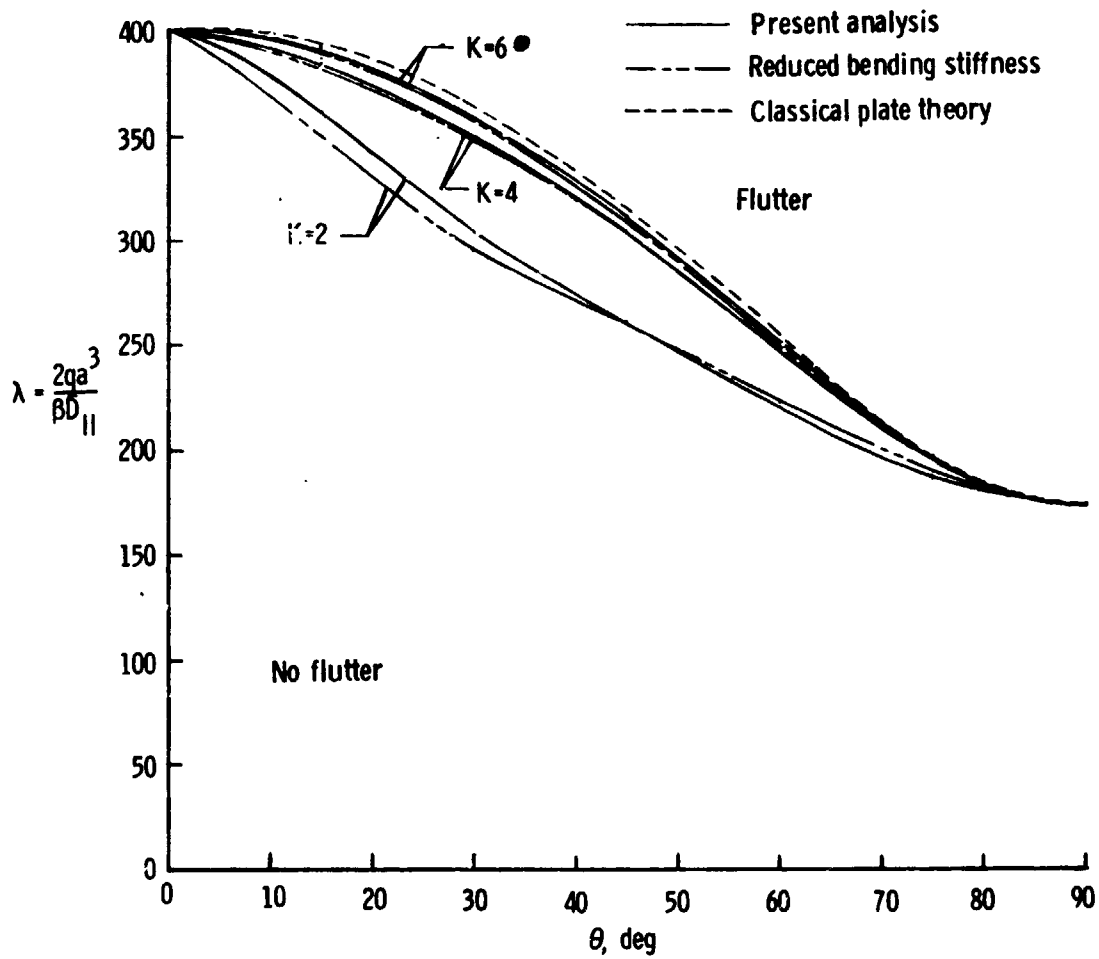
(a) Glass-epoxy plate.

Figure 22.- Flutter boundaries for square, angle-ply plate.
$$\bar{N}_x = \bar{N}_y = \bar{N}_{xy} = 0.$$
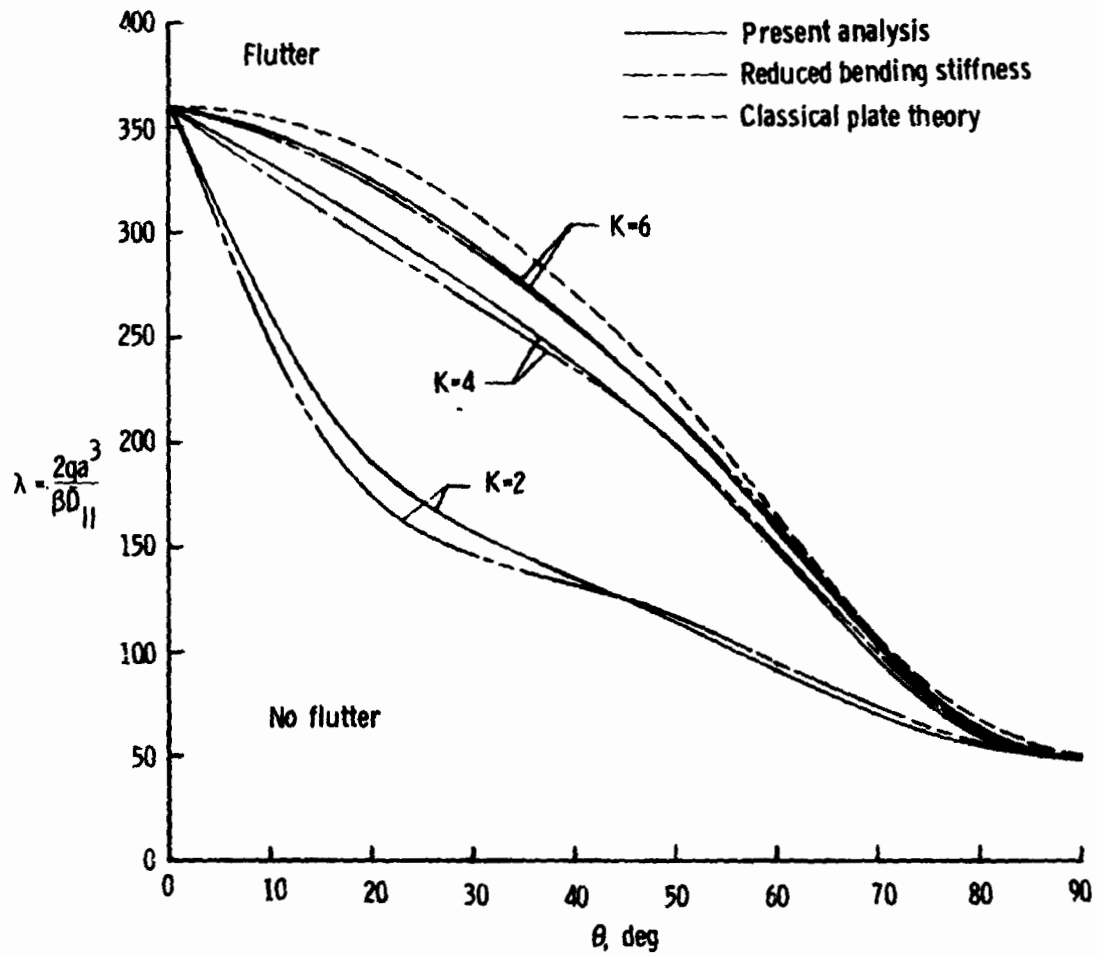
(b) Boron-epoxy plate.

Figure 22.- Concluded.

$$\lambda = \frac{2qa^3}{\beta D_{11}}$$
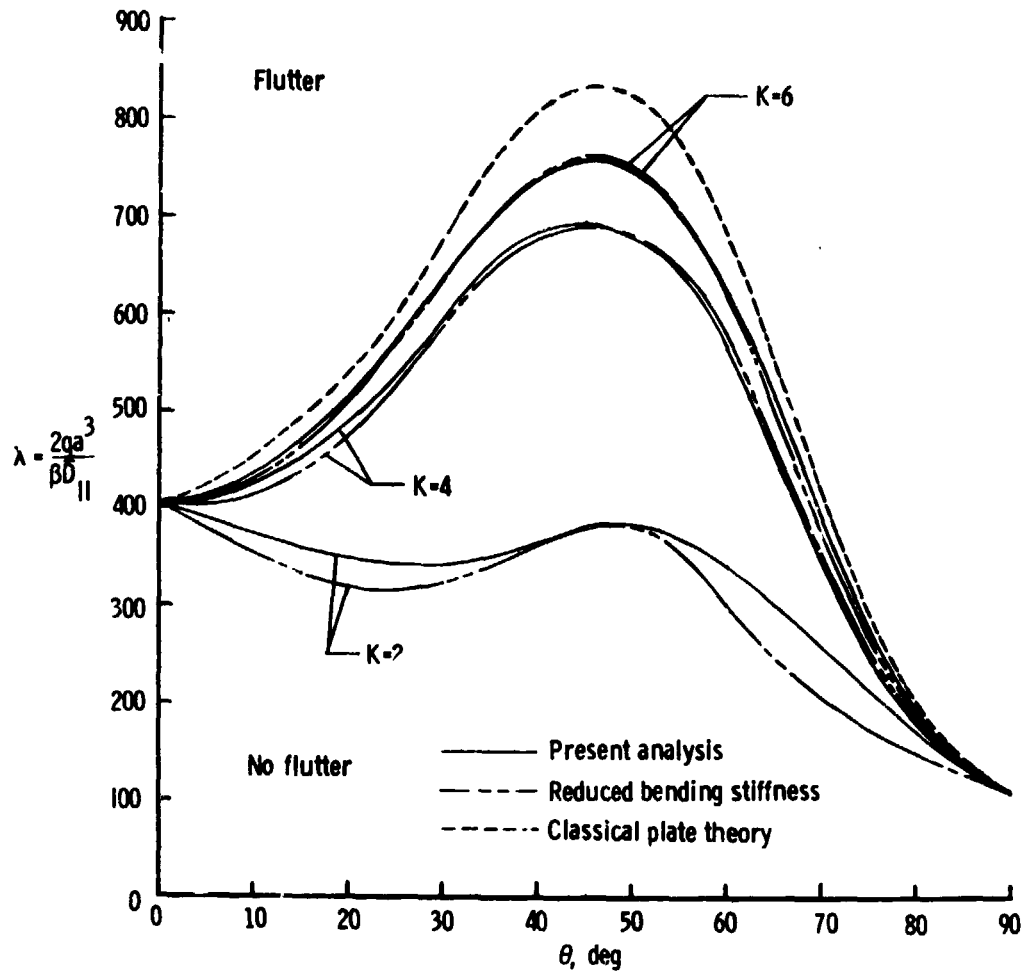
Figure 23.— Flutter boundaries for boron-epoxy, angle-ply plate with a/b = 2.0. $\bar{N}_x = \bar{N}_y = \bar{N}_{xy} = 0$.
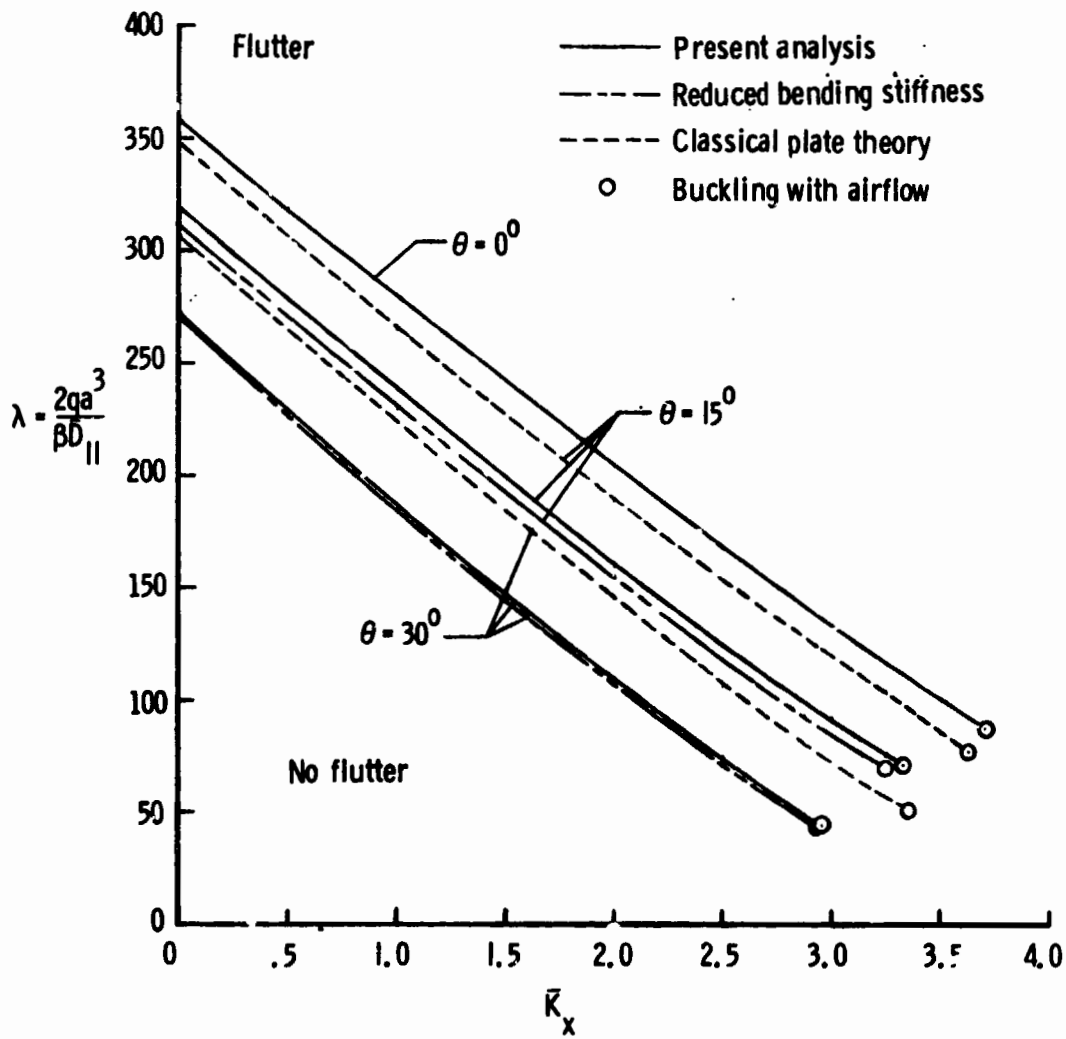
(a) Inplane normal loads, $\bar{\bar{N}}_y = \bar{N}_{xy} = 0$.

Figure 24.- Flutter boundaries for square, boron-epoxy, angle-ply plate with inplane loads. $K = 4$.
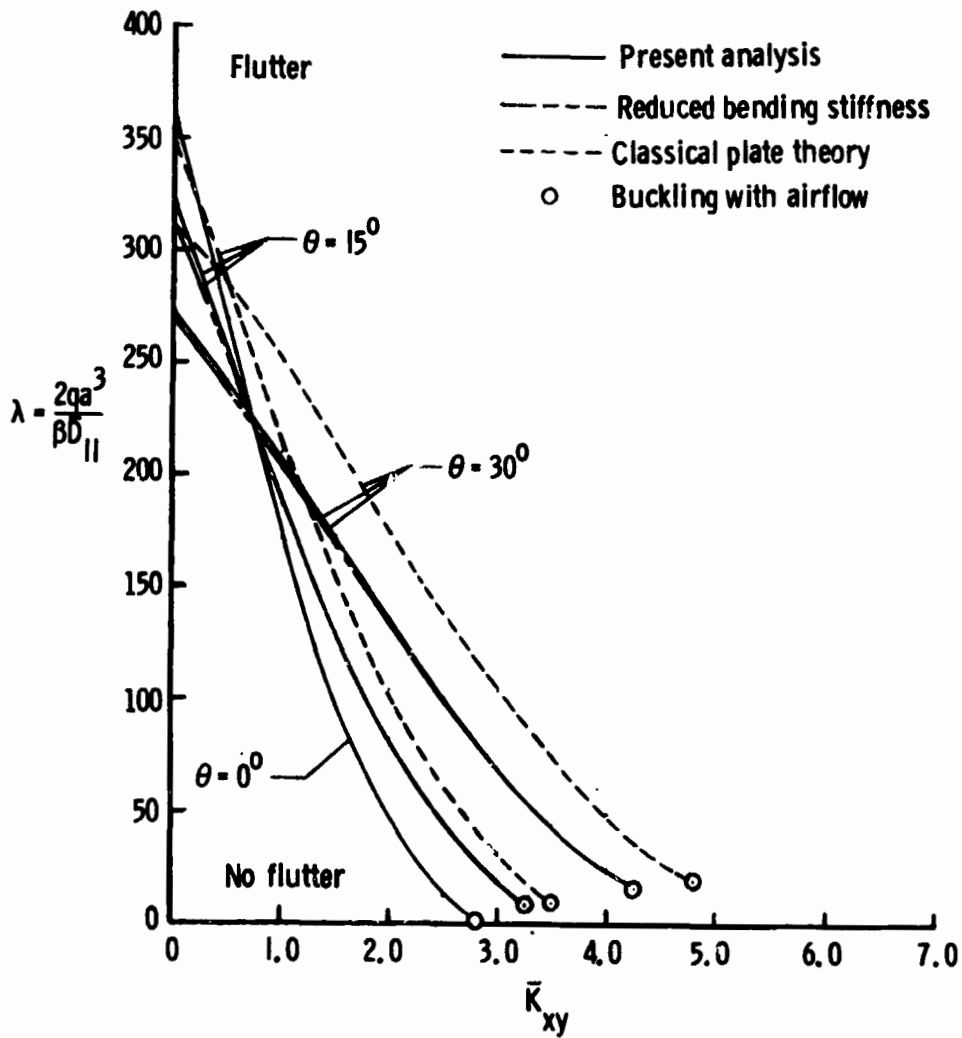
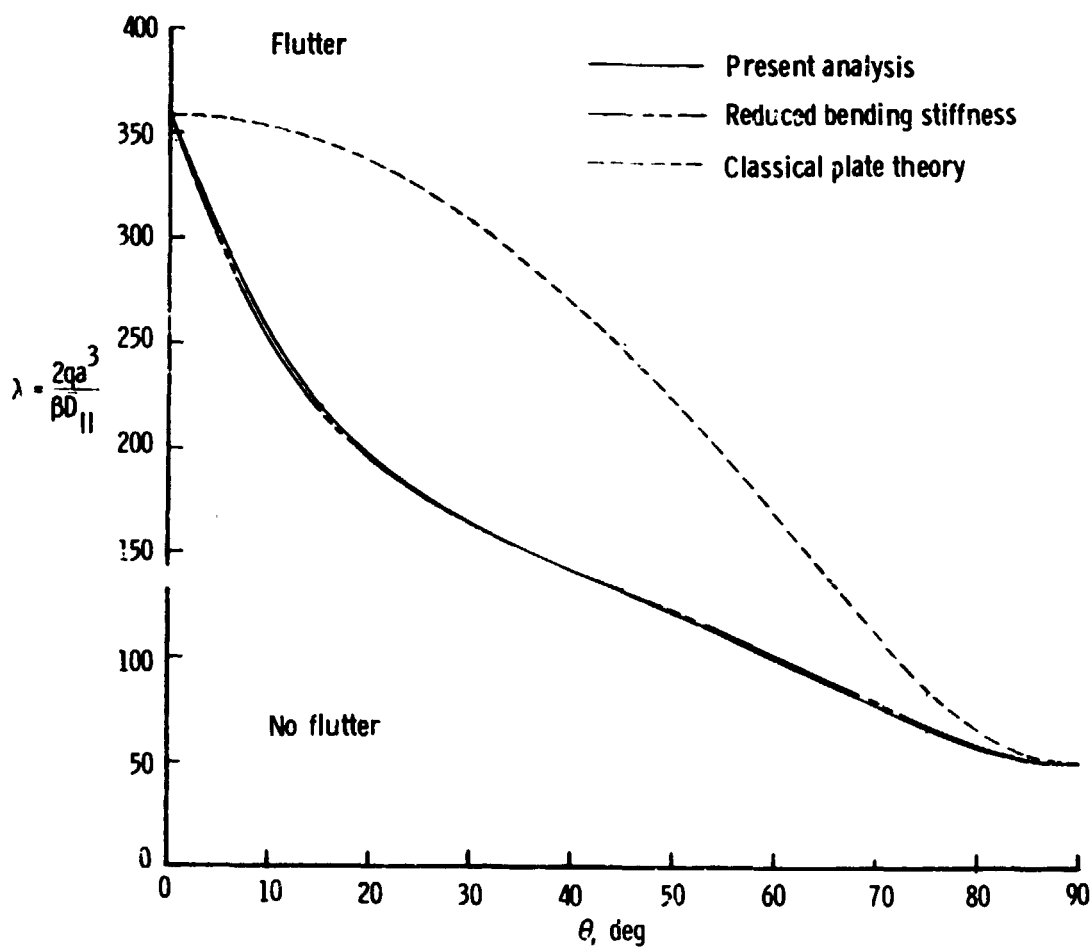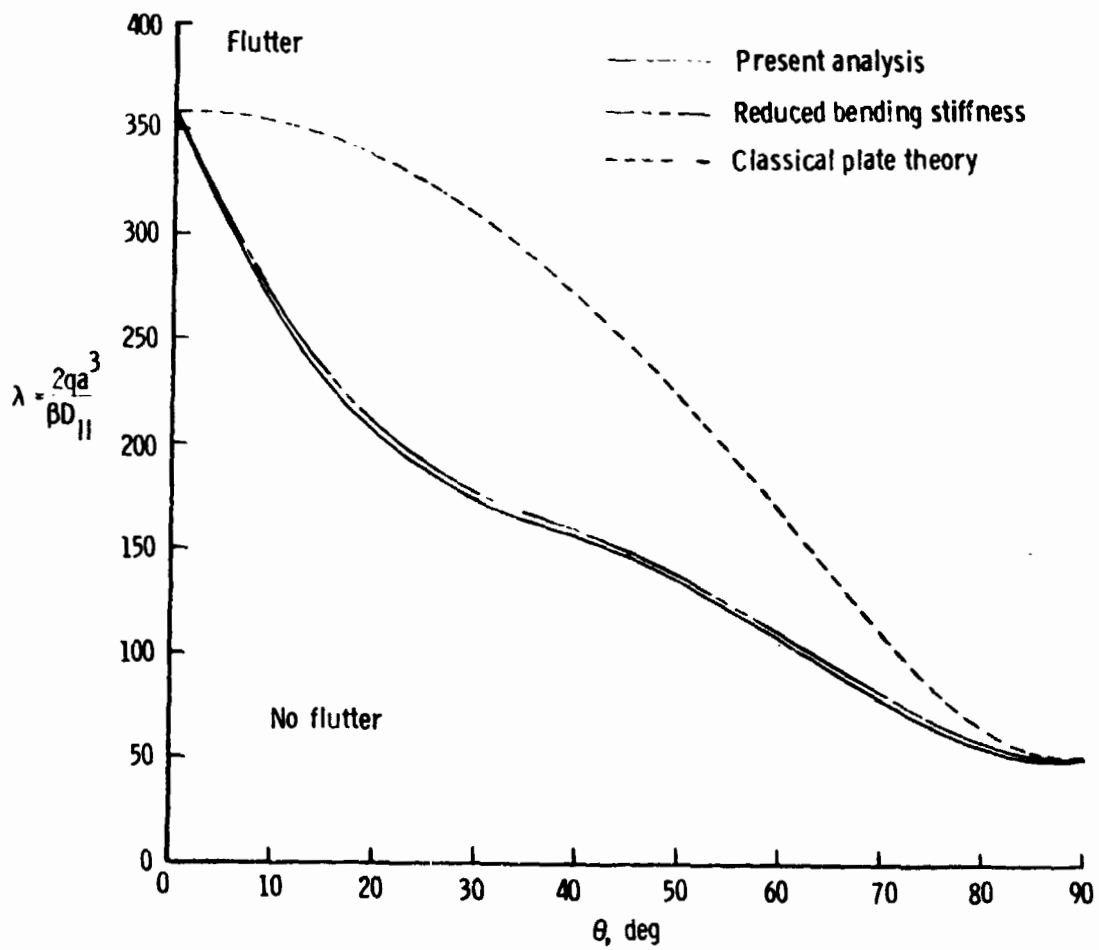(b) Inplane shear loads, $\bar{N}_y = \bar{N}_x = 0$.

Figure 24.- Concluded.

Figure 25.- Flutter boundaries for square, boron-epoxy, angle-ply plate with cross-flow. $\bar{N}_x = \bar{N}_y = \bar{N}_{xy} = 0$; $K = 4$.

(a) Plate P-1.

Figure 26.- Flutter boundaries for square, boron-epoxy, general laminated plates. $\bar{N}_x = \bar{N}_y = \bar{N}_{xy} = 0$.
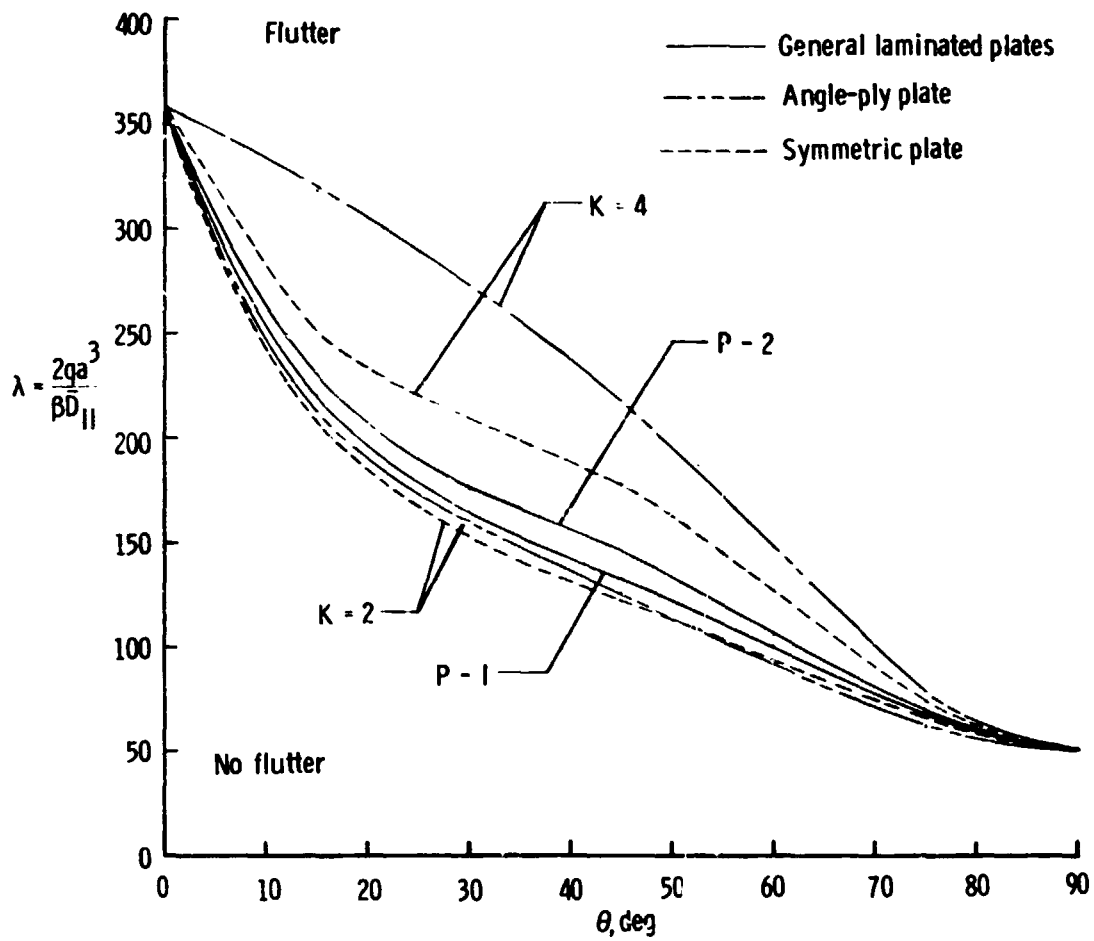
116

$$\lambda = \frac{2qa^3}{\beta D_{11}}$$

Legend:
- ————————— Present analysis
- —— · —— · Reduced bending stiffness
- — — — — Classical plate theory

Flutter

No flutter

θ, deg

(b) Plate P-2.

Figure 26.- Concluded.

Figure 27.- Comparison of flutter boundaries for square, symmetric, angle-ply, and general laminated plates. $\bar{\bar{N}}_x = \bar{\bar{N}}_y = \bar{\bar{N}}_{xy} = 0$.
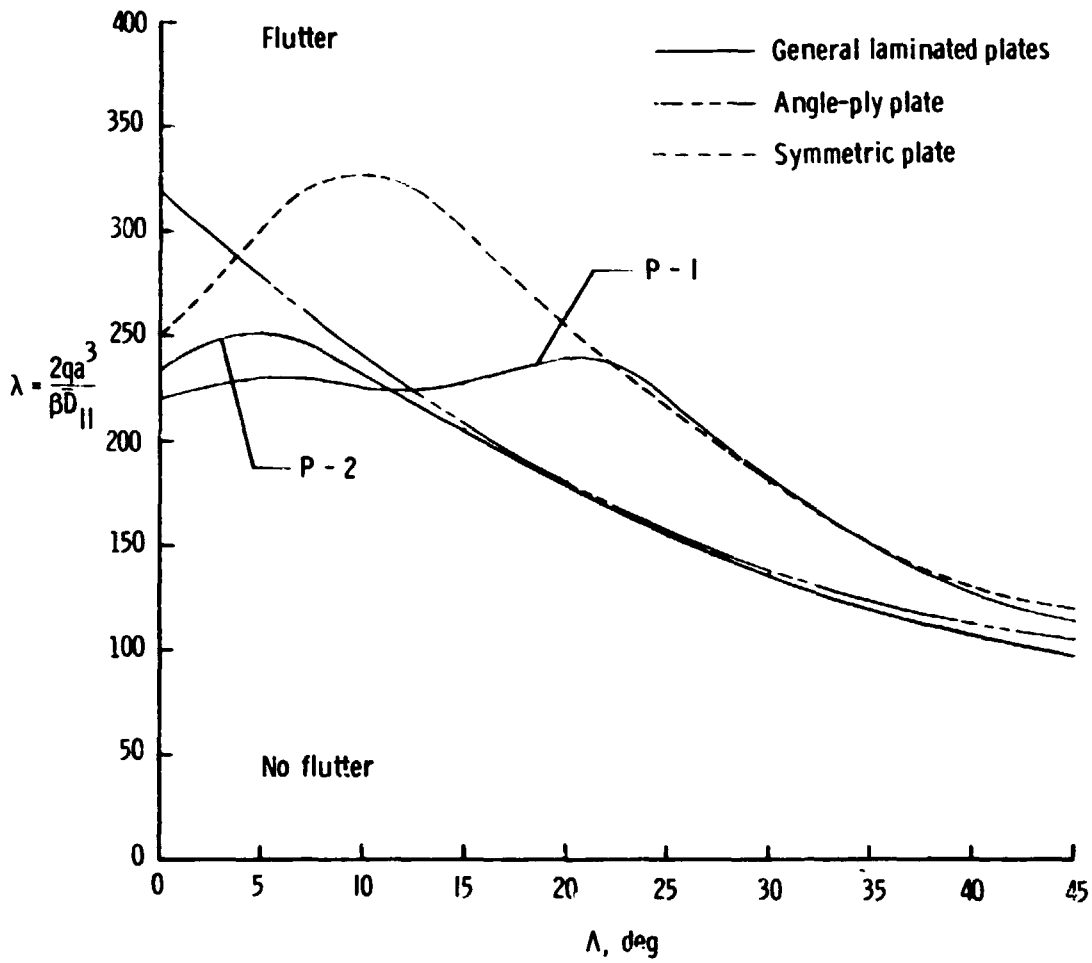
Figure 28.- Effect of cross-flow on flutter of square, symmetric, angle-ply and general laminated plates. $\bar{N}_x = \bar{N}_y = \bar{N}_{xy} = 0$.
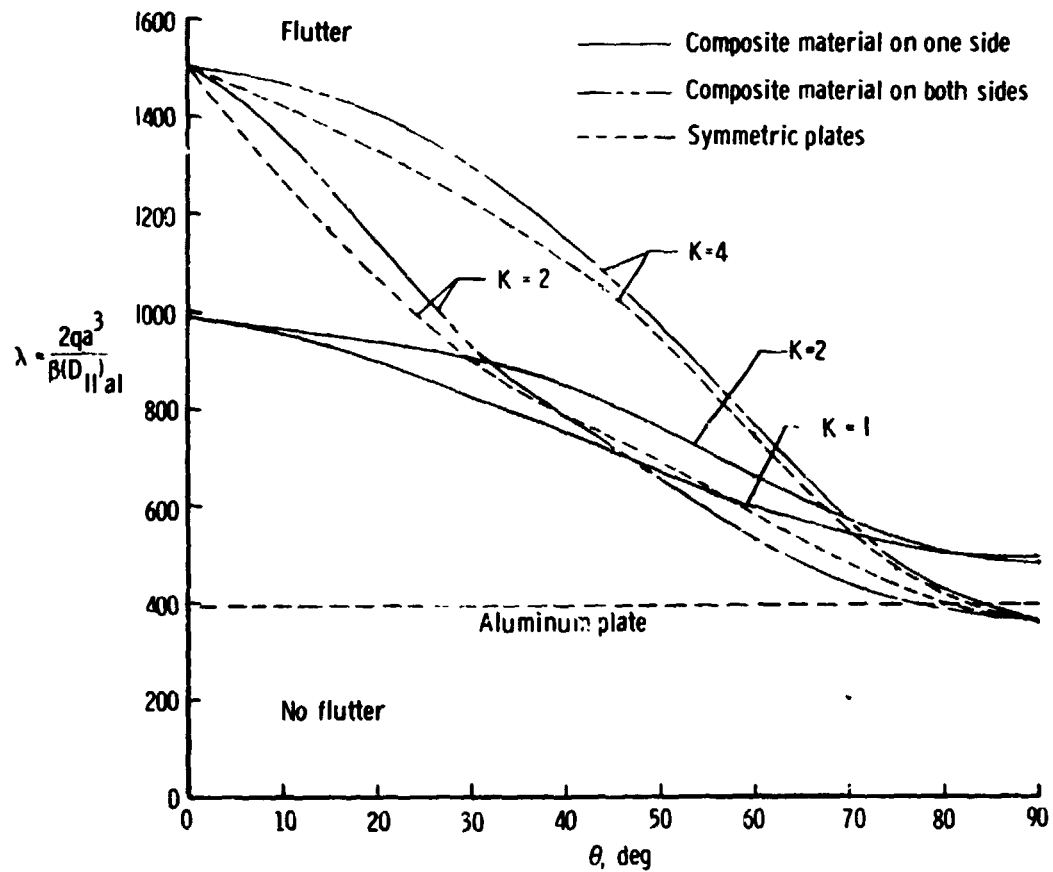
Figure 29.- Flutter boundaries for square, composite-stiffened aluminum plates. $\bar{N}_x = \bar{N}_y = \bar{N}_{xy} = 0$; mass$_{aluminum}$/mass$_{composite}$ = 1.0.